

10
I29A
342
cy. 3



W J Hall

CIVIL ENGINEERING STUDIES
STRUCTURAL RESEARCH SERIES NO. 342



FINAL REPORT

LOW CYCLE FATIGUE OF HY-130(T) BUTT WELDS

Metz Reference Room
Civil Engineering Department
B106 C. E. Building
University of Illinois
Urbana, Illinois 61801

By

J. B. Radziminski
F. V. Lawrence
S. Mukai
P. N. Panjwani
R. Johnson
R. Mah
and
W. H. Munse

A REPORT OF AN INVESTIGATION CONDUCTED
by
THE CIVIL ENGINEERING DEPARTMENT
UNIVERSITY OF ILLINOIS, URBANA
in cooperation with
The Naval Ship Systems Command, U.S. Navy
Contract N00024-68-C-5125
Project Serial No. SF020-01-01, Task 729

UNIVERSITY OF ILLINOIS
URBANA, ILLINOIS

DECEMBER, 1968



Final Report

LOW CYCLE FATIGUE OF HY-130(T) BUTT WELDS

by

J. B. Radziminski

F. V. Lawrence

S. Mukai

P. N. Panjwani

R. Johnson

R. Mah

and

W. H. Munse

A Report of an Investigation Conducted

by

THE CIVIL ENGINEERING DEPARTMENT
UNIVERSITY OF ILLINOIS, URBANA

in cooperation with

The Naval Ship Systems Command, U. S. Navy
Contract N00024-68-C-5125
Project Serial No. SF020-01-01, Task 729

University of Illinois

Urbana, Illinois

December 1968

ABSTRACT

A preliminary evaluation of the axial fatigue behavior of plates and transverse butt-welded joints in HY-130(T) steel is presented. The weldments were prepared using each of two experimental "second-generation" GMA welding wires and a coated electrode. Fatigue tests were conducted using both sound weldments and weldments containing various internal defects, including porosity, slag, lack of fusion, and lack of penetration. Radiographic and ultrasonic testing techniques were used to study the initiation and propagation of fatigue cracks originating at internal weld flaws.

The fatigue studies have indicated that although the highest standards of quality may be used in the fabrication of HY-130(T) welded joints, it has not been possible to guarantee the elimination of all defects which have proven to be critical sites for internal fatigue crack nucleation under axial loading. Internal failures were as likely to occur in specimens rated as sound weldments under radiographic inspection as in weldments having regions containing readily detected flaws.

Fatigue cracks originating at internal defects were found to initiate at approximately twenty to eighty percent of the total cyclic lifetime of a butt-welded joint, for tests conducted at a stress cycle of zero-to-tension. Within the normal limits of scatter for fatigue data, however, the number of cycles of crack propagation to failure beyond the point of internal initiation was found to be reasonably consistent at a specific test stress level, for weldments containing various types and percentages of weld defect area.

TABLE OF CONTENTS

	<u>Page</u>
I INTRODUCTION	1
1.1 Object of Study.	1
1.2 Scope of Investigation	2
1.3 Acknowledgments.	3
II DESCRIPTION OF TEST PROGRAM.	4
2.1 Material	4
2.2 Fabrication of Specimens	4
2.3 Fatigue Testing Equipment and Procedure.	5
2.4 Non-Destructive Testing Equipment and Procedures	6
2.5 Metallurgical Studies.	8
III STUDIES OF HY-130(T) PLATES AND BUTT WELDS	10
3.1 Fatigue Tests of Plain Plates.	10
3.2 Tests of Transverse Butt Welds	11
3.2.1 Welding Procedures, Qualification Tests.	11
3.2.2 Fatigue Tests of As-Welded Joints.	13
3.2.3 Fatigue Tests of Joints with Reinforcement Removed.	16
3.2.4 Metallurgical Examination of Fracture Surfaces	19
3.2.4.1 Introductory Remarks	19
3.2.4.2 Specimens Failing at Toe of Weld	20
3.2.4.3 Specimens Exhibiting Internal Failure.	21
3.3 Fatigue Crack Initiation and Propagation	22
3.3.1 Results of Radiographic Crack Detection Studies.	22
3.3.2 Results of Ultrasonic Crack Detection Studies.	27
3.4 Concluding Remarks	30
IV ANALYSIS OF FATIGUE DATA	32
4.1 Effect of Removal of Reinforcement	32
4.2 Effect of Filler Wire	33
4.3 Concluding Remarks	34
V SUMMARY AND CONCLUSIONS	35
LIST OF REFERENCES	39
TABLES	41
FIGURES	50
DISTRIBUTION	

LIST OF TABLES

<u>Number</u>		<u>Page</u>
2.1	Chemical Composition of HY-130(T) Base Metal	41
2.2	Mechanical Properties of HY-130(T) Base Metal	42
2.3	Chemical Composition of Electrodes for Welding HY-130(T) Plates	43
3.1	Results of Fatigue Tests of HY-130(T) Plain Plate Specimens	44
3.2	Results of Qualification Tests of HY-130(T) Weldments .	45
3.3	Results of Defect Examination and Fatigue Tests of HY-130(T) Transverse Butt Welds in the As-Welded Condition	46
3.4	Results of Defect Examination and Fatigue Tests of HY-130(T) Transverse Butt Welds with Reinforcement Removed	47
3.5	Results of Fatigue Crack Initiation and Propagation Study of HY-130(T) Transverse Butt Welds Containing Intentional Weld Defects	48
4.1	Distribution of Fatigue Lives and Causes of Failure . .	49

LIST OF FIGURES

Number

- 2.1 Details of Fatigue Test Specimens
- 2.2 Illinois' Fatigue Testing Machine as Used for Axial Loading of Welded Joints
- 2.3 Set-Up for Radiographic Study of Crack Propagation
- 2.4 Ultrasonic Testing Equipment
- 2.5 Scanning Procedure for Ultrasonic Examination
- 3.1 Results of Fatigue Tests of HY-130(T) Plain Plate Specimens
- 3.2 Welding Procedure P130(T)-USS-A
- 3.3 Welding Procedure P130(T)-L140-A
- 3.4 Welding Procedure P130(T)-M140-A
- 3.5 Side Bend Test Specimens of Weldments in 1 in. Thick HY-130(T) Plates
- 3.6 Macro-Structure of Weldments in 1 in. Thick HY-130(T) Plates
- 3.7 Typical Fracture Surfaces of HY-130(T) Transverse Butt Welds in the As-Welded Condition
- 3.8 Comparison of Fatigue Test Results of As-Welded Butt Joints from Current Study with Data from Previous Investigation
- 3.9 Results of Fatigue Tests of As-Welded HY-130(T) Transverse Butt Joints
- 3.10 Results of Fatigue Tests of As-Welded HY-130(T) Transverse Butt Joints Initiating Failure at Toe of Weld
- 3.11 Results of Fatigue Tests of HY-130(T) Transverse Butt-Welded Specimens with Reinforcement Removed
- 3.12 Typical Fracture Surfaces of HY-130(T) Transverse Butt Welds with Reinforcement Removed
- 3.13 Effect of Various Weld Defects on Fatigue of HY-130(T) Transverse Butt Welds (Stress Cycle: 0 to +80 ksi)
- 3.14 Effect of Various Weld Defects on Fatigue of HY-130(T) Transverse Butt Welds (Stress Cycle: 0 to +50 ksi)

LIST OF FIGURES (Continued)

Number

- 3.15 Scanning Electron Microscope Image of Pore Initiating Fatigue Crack in Specimen ND-30
- 3.16 Tracings of Radiographs Taken During Fatigue Test of Specimen ND-6
- 3.17 Tracings of Radiographs Taken During Fatigue Test of Specimen ND-8
- 3.18 Tracings of Radiographs Taken During Fatigue Test of Specimen ND-21
- 3.19 Tracings of Radiographs Taken During Fatigue Test of Specimen ND-20
- 3.20 Tracings of Radiographs Taken During Fatigue Test of Specimen ND-10
- 3.21 Tracings of Radiographs Taken During Fatigue Test of Specimen ND-18
- 3.22 Tracings of Radiographs Taken During Fatigue Test of Specimen ND-17
- 3.23 Tracings of Radiographs Taken During Fatigue Test of Specimen ND-19
- 3.24 Tracings of Radiographs Taken During Fatigue Test of Specimen ND-14
- 3.25 Tracings of Radiographs Taken During Fatigue Test of Specimen ND-15
- 3.26 Propagation of Internal Fatigue Cracks in 1 in. HY-130(T) Transverse Butt Welded Specimens
- 3.27 Propagation of Internal Fatigue Cracks in 3/4 in. HY-80 and HY-100 Transverse Butt Welded Specimens
- 3.28 Cycles of Crack Propagation Prior to Failure in 1 in. HY-130(T) Transverse Butt Welded Specimens
- 3.29 Cycles of Crack Propagation Prior to Failure in 3/4 in. HY-80 and HY-100 Transverse Butt Welded Specimens
- 3.30 Fracture Surface, and Ultrasonic Indications Recorded for Specimen ND-8
- 3.31 Fracture Surface, and Ultrasonic Indications Recorded for Specimen ND-21
- 3.32 Fracture Surface, and Ultrasonic Indications Recorded for Specimen ND-20
- 3.33 Fracture Surface, and Ultrasonic Indications Recorded for Specimen ND-10
- 3.34 Fracture Surface, and Ultrasonic Indications Recorded for Specimen ND-18

LIST OF FIGURES (Continued)

Number

- 3.35 Fracture Surface, and Ultrasonic Indications Recorded for Specimen ND-17
- 3.36 Fracture Surface, and Ultrasonic Indications Recorded for Specimen ND-14
- 3.37 Fracture Surface, and Ultrasonic Indications Recorded for Specimen ND-15
- 3.38 Cycles to Failure Following Internal Fatigue Crack Initiation in HY-130(T) Transverse Butt Welds With Reinforcement Removed

I. INTRODUCTION

1.1 Object of Study

Considerable research has been undertaken to determine the fatigue characteristics of HY-130(T) steel subjected to various environments and loadings in anticipation of its use in naval construction. This report presents the latest results in a continuing investigation^(1,2) of the fatigue behavior of HY-130(T) plates and butt welded joints tested under constant amplitude, axial fatigue loading.

Previous tests of butt welds fabricated using "first-generation" gas metal-arc (GMA) welding wires have indicated that even small, widely scattered internal weld defects can serve as critical locations for fatigue crack initiation, often at lives well below those anticipated from a comparison with surface initiated failures of similar HY-80 and HY-100 steel weldments.⁽²⁾ One of the objectives of the current investigation was to extend these fatigue tests to include joints prepared using two experimental "second-generation" GMA wires and one coated electrode, to determine if an improvement in fatigue resistance can be realized when the new wires are used in specimens where care has been exercised to insure nominally high quality welds.

An additional phase of the current study has consisted of an investigation of the effects of weld defects introduced in the welding process, including porosity, slag, lack of fusion, and lack of penetration, on the axial fatigue lives of the test weldments. The initiation and subsequent propagation of fatigue cracks originating at such internal defects have been studied using both radiographic and ultrasonic techniques.

* Numbers in parentheses refer to corresponding entries in list of references.

1.2 Scope of Investigation

The fatigue tests of the plain plates and transverse butt welds were conducted using specimens of 1-in. thick HY-130(T) base material. All tests were performed using a stress cycle of zero-to-tension. The butt-welded joints were fabricated using experimental GMA wires, supplied by U. S. Steel Corporation and Linde Division of Union Carbide Corporation, and with an experimental coated electrode supplied by the McKay Company.

Twenty-seven welded specimens were tested in the "as-welded" condition to determine the effect of surface geometry on the fatigue behavior of the joints in the HY-130(T) material and for comparison with similar joints fabricated using HY-80 and HY-100 base materials. In addition, twenty specimens, most of which contained intentional internal defects, were tested with the weld reinforcement removed. In the case of those specimens used to examine crack initiation and propagation, the weld reinforcement was removed to permit better resolution of the radiographs taken during cycling, and, when ultrasonic techniques were employed, to provide a good contact surface between the plate and the test probe. Moreover, removal of the reinforcement precluded the possibility of fatigue cracks initiating at the notch associated with the surface geometry at the toe of the weld.

The 1-in. thick HY-130(T) base plates used in the present investigation were received descaled and one-coat painted. Fatigue tests were conducted on two specimens of this base plate for comparison with the results of earlier axial tests of plates that had the mill scale intact, and with the results of tests of other specimens in which the surfaces were polished to remove the mill scale and oxidized sub-layer.

The studies reported herein were conducted during the period from November, 1967 to November, 1968.

1.3 Acknowledgments

The tests reported in this study are the result of an investigation conducted in the Civil Engineering Department of the University of Illinois, Urbana, Illinois. The program was supported by funds provided by the Naval Ship Systems Command, U. S. Navy, under Contract N00024-68-C-5125, Project Serial No. SF020-01-01, Task 729.

This investigation constitutes a part of the structural research program of the Department of Civil Engineering, of which Dr. N. M. Newmark is the Head. The program is under the supervision of W. H. Munse, Professor of Civil Engineering; the fatigue and associated tests were conducted by P. N. Panjwani, L. S. Hirsch and G. J. Patterson, Research Assistants in Civil Engineering, under the direction of Dr. J. B. Radziminiski, Assistant Professor of Civil Engineering. Metallurgical studies associated with the program have been conducted by Dr. S. Mukai, Visiting Research Associate in Civil Engineering, and by R. Mah and R. Johnson, Research Assistants in Metallurgical Engineering, under the direction of Dr. F. V. Lawrence, who holds a joint appointment as Assistant Professor in Civil Engineering and Metallurgical Engineering.

The authors wish to express their appreciation for the conscientious work of the Civil Engineering Department's laboratory technicians, especially R. Williams, who was responsible for welding of the fatigue test specimens, and to the secretarial staff of the Department, for the typing of the reports.

II. DESCRIPTION OF TEST PROGRAM

2.1 Material

The plain plate and butt-welded specimens were fabricated from HY-130(T) base material, a quenched and tempered steel obtained from the U. S. Steel Corporation in accordance with contract provisions. The chemical composition and mechanical properties of the base metal, including plates used in an earlier investigation,⁽²⁾ are presented in Tables 2.1 and 2.2, respectively. Fatigue specimen numbers designated by the prefix NC were fabricated with plates from heat number 5P0540; those identified by the prefix ND were from heat number 5P2456. The plates from heat 5P0540 had the mill scale surface intact, those from heat 5P2456 were received descaled and painted (one coat).

The chemical compositions of the two GMA welding wires and of the one covered electrode used in the investigation are given in Table 2.3. The GMA wires, supplied by U. S. Steel Corporation and by Linde Division of Union Carbide Corporation, and the coated electrode, supplied by the McKay Company, have been received from the same lots as those used in the fabrication of a cylindrical vessel under construction at the Newport News Shipbuilding and Dry Dock Company.⁽⁴⁻⁷⁾

2.2 Fabrication of Specimens

The details of the welded test specimens are presented in Fig. 2.1. The fabrication technique for all specimens was similar except for differences in the welding procedures. Specimen blanks, 9 in. by 48 in., were first flame cut from the 72 in. by 96 in. HY-130(T) steel plates (1 in. thick). For the transverse butt-welded specimens, the blanks were sawed in half (9 in. x 24 in.) and the cut edges were machined to provide a double "V" groove for the weld deposit. The included angle

of the groove was 60° for all procedures examined. All welding was performed in the flat position with the specimens loosely clamped in a jig which could be rotated about a horizontal axis (the longitudinal axis of the weld). The final procedures adopted for the welding of the HY-130(T) specimens are presented in Section 3.2.1.

After the welding operation was completed, holes were drilled in the ends of the specimens, Fig. 2.1, as required for insertion of the member in the fatigue testing machine. The specimen was then milled to shape so that a 5-in. long straight section remained at mid-length to form a test section which included the butt weld. No material in the region of the test section was removed by flame cutting. The net width at the test section was governed by the test load range and the capacity of the fatigue testing machine, the width being made as large as possible within the capacity of the machine.

In the final stage of fabrication, the edges of the specimen in the region of the test section were ground smooth and any sharp burrs filed off. For those butt joints tested with the reinforcement removed, the specimen faces were first planed, and then rough polished in the direction of subsequent loading (longitudinal) with a belt sander.

2.3 Fatigue Testing Equipment and Procedure

The fatigue tests were conducted using the University of Illinois' 250,000 lb. and 200,000 lb. lever-type fatigue machines. The operating speeds of the machines are approximately 100 and 180 cycles per minute, respectively.

The essential features of the fatigue machines are shown schematically in Fig. 2.2. The lever system provides a force multiplication ratio of approximately 15 to 1. The load range is adjusted through the

throw of the eccentric, while the maximum load is controlled by the adjustable turnbuckle mounted just below the dynamometer.

The testing procedure was similar for all specimens. After the load had been set and the machine started, a micro-switch was set so that the machine would automatically shut off when a crack had propagated partially through the specimen. The load was maintained within limits of about ± 0.5 ksi by periodic checks, with adjustments made when necessary. Fatigue failure as reported herein was taken as the number of cycles at which the micro-switch shut off the testing machine. Cycling was then continued until complete fracture occurred so that the fracture surfaces could be examined and photographed. In each case, less than a 1 percent increase in fatigue life existed from the time of the micro-switch cut-off to the point of complete separation.*

2.4 Non-Destructive Testing Equipment and Procedures

Prior to fatigue testing all welded specimens were subjected to radiographic examination using a sensitivity level of two percent. The specimens were rated in accordance with the requirements for weld quality established by U. S. Steel Corporation⁽⁸⁾ and NAVSHIPS Specification No. 0900-006-9010.⁽⁹⁾ The results of the defect examinations and weld ratings are reported in the tables containing the fatigue results for each specimen. With one exception, all specimens that failed the specifications were tested without being repaired to evaluate the effect of these flaws on the fatigue behavior of the welds.

* For several of the welded joints tested at high stress levels, complete fracture occurred abruptly and with a loud report before the micro-switch was tripped.

For the specimens examined radiographically during the course of fatigue cycling (initiation and propagation studies), the X-ray equipment was mounted on a portable platform and positioned so that the exposures could be made with the test specimen mounted in the fatigue machine. The radiographic apparatus, less a protective lead enclosure, is pictured in position in Fig. 2.3. With this arrangement, radiographs were taken periodically during the fatigue tests. The initial cyclic interval between radiographs was approximately 10 percent of the expected total life of the test specimen. After crack initiation, radiographs were taken at shorter cyclic intervals to obtain a measure of internal crack growth. This procedure was continued until the fatigue crack was visible on both surfaces of the specimen, thus indicating crack progression through the entire thickness of the plate.

Ultrasonic examination procedures were used with several specimens to obtain another indication of initial weld defect density and in an attempt to detect internal fatigue crack initiation for comparison with the radiographic information.

The ultrasonic testing apparatus, together with the auxiliary equipment, is shown in Fig. 2.4. The transducer is a miniature 45° shear element which operates at 5 MHz. The transducer is mounted in a ball bushing and spring loaded against the test specimen to ensure reproducibility of response from one scan to another. This device is mounted on a movable platen which is traversed across the test surface while the specimen is in the fatigue machine.

The position of the transducer on the surface of the specimen is sensed by two linear resistors, connected to the platen, and plotted on an X-Y recorder. In this manner, the position of an individual response

is projected and plotted on a plane parallel to the surface of the test specimen. The apparent depth of this signal into the specimen is scaled from the oscilloscope screen.

The ultrasonic tests were performed with the welded specimen in the fatigue machine and set at the maximum tensile load used for the particular fatigue test under study. The specimen faces were polished, as described earlier, to improve contact between the probe and the test surface, and to minimize wear on the face of the probe. Light machine oil was used as an acoustic couplant. As illustrated in Fig. 2.5, the weld area of a specimen was scanned by traversing horizontally across the specimen face below the weld and in 1/8 in. vertical increments until the weld area and adjacent heat affected zones had been searched. The detector test range and trace position were adjusted so that the echo between the first reflection from the rear surface and the second reflection from the front surface was observed (see Fig. 2.5).

The methods used to record the ultrasonic responses and the interpretation of these responses are discussed in Section 3.3.

2.5 Metallurgical Studies

Several welding procedures employing each of the two second-generation GMA wires and one coated electrode were used to develop satisfactory procedures for the double "V" butt welds. These experimental weldments were examined for proper placement of weld beads, severity of weld bead lobe (nugget papilla)⁽¹⁰⁾ formation, and degree of tempering of surface beads. The welding procedures were further evaluated by standard metallographic techniques to determine type and concentration of internal defects; the most promising procedures were then qualified in accordance with the appropriate specifications and used in the preparation of the fatigue specimens.

The exposed fracture surfaces of the welded fatigue test specimens were examined to determine the type of weld defect and the nature of the microstructure of the weld deposit at the location of internal fatigue crack initiation. The results of these examinations are presented in Section 3.2.4.

III. STUDIES OF HY-130(T) PLATES AND BUTT WELDS

3.1 Fatigue Tests of Plain Plates

For purposes of comparison with earlier fatigue test data,^(1,2) two plain plate specimens fabricated using the descaled and painted plate material were tested at a stress level of 0 to +80 ksi. The results of these tests are compared in Table 3.1 and Fig. 3.1 with the test data from as-rolled plates and from control specimens which were prepared with the mill-scale removed and the test section polished parallel to the longitudinal axis of the specimens.*

At the 0 to +80 ksi stress level examined, the fatigue lives of the descaled and painted plates were approximately four times the lives of the corresponding specimens containing mill-scale, or only slightly below the average life for the two specimens with the polished surfaces. The significant reduction in fatigue life of the as-rolled plates may be attributed in part to the presence of a coarse oxidized layer located just beneath the exterior mill-scale in those specimens.⁽²⁾ This hard, oxidized layer provided severe geometrical stress raisers which initiated fatigue cracks in several of the fatigue test specimens.

From these few tests, it appears that descaling and painting the surfaces of the HY-130(T) plate material will substantially improve its subsequent behavior under high stress axial loadings (in the absence of other external stress raisers such as weld reinforcement, etc.). Additional fatigue tests are required to determine if this relative behavior persists in the region of long life, low stress fatigue.

* The milling and polishing procedure was the same as that used for the welded specimens in which the reinforcement was removed, Section 2.2.

3.2 Tests of Transverse Butt Welds

3.2.1. Welding Procedures, Qualification Tests

The first phase of the current study consisted of the development of suitable welding procedures for the fabrication of butt welds using each of the three electrodes (chemical compositions presented in Table 2.3) supplied for this investigation. The wire designation and manufacturer of each of the electrodes are:

<u>Manufacturer</u>	<u>Designation</u>	<u>Type</u>
U. S. Steel Corporation	5 Ni-Cr-Mo	1/16" bare-electrode wire
Linde Division, Union Carbide Corporation	Linde 140	1/16" bare-electrode wire
McKay Company	McKay 14018	5/32", 3/16" covered electrode

Several experimental weldments were fabricated using the three electrodes, each including minor modifications to the procedures recommended by the suppliers. The procedures which proved most satisfactory for the preparation of the full penetration butt welds (flat position) were then used in the fatigue studies; these procedures are shown in Figs. 3.2, 3.3, and 3.4.

Each of the three procedures, using the 1-in. thick base material, was successfully qualified in accordance with procedures recommended by the U. S. Steel Corporation,⁽⁸⁾ and those required by the U. S. Navy for fabrication of HY-80 submarine hulls.⁽⁹⁾ The qualification tests included the reduced-section tension test, side bend test (except that a bend test radius of 2t was used instead of the 3t required), macro-etch specimens, and radiographic inspection. The results of the reduced-section tension tests and side bend tests are summarized in Table 3.2; photographs of typical side bend test specimens are shown in Fig. 3.5. A photograph

of a macro-etch specimen prepared from each of the three welding procedures is shown in Fig. 3.6.

From the weldability studies, it was found that, to consistently achieve weldments as free of internal defects as possible, the following measures are required in the preparation of fatigue test specimens welded using each of the three electrodes:

- a) Surfaces to be joined by welding should be prepared just prior to welding to prevent the accumulation of organic matter and hygroscopic materials.
- b) Mill-scale surfaces adjacent to the beveled edges of the plates to be welded are to be removed as indicated in Figs. 3.2, 3.3, and 3.4 to prevent the formation of porosity in surface weld beads.
- c) The beveled edges of the plates to be welded are to be filed and cleaned with acetone immediately preceding welding.
- d) The root pass of the weldment is to be back ground using a carbide grinding wheel following the deposition of the first two weld beads.
- e) As a result of the convex shape of the deposited weld bead, a sharp notch is created between the edge of the bead and the sidewall of the beveled plates; such notches should be removed by light grinding (carbide wheel) following the deposition of weld passes 2 through 4 to minimize the possibility of lack of fusion occurring in these regions.

The above procedures were followed in the preparation of all of the HY-130(T) butt welds investigated, with the exception of those which were to contain intentional defects.

3.2.2. Fatigue Tests of As-Welded Joints

A total of twenty-seven specimens were tested in the as-welded condition at a stress cycle of zero-to-tension. The number of specimens prepared using each of the three electrodes was as follows:

<u>Electrode Designation</u>	<u>Welding Procedure</u>	<u>No. of Fatigue Test Specimens</u>
USS 5Ni-Cr-Mo	P130(T)-USS-A	8
Linde 140	P130(T)-L140-A	9
McKay 14018	P130(T)-M140-A	10

After welding, each of the specimens was radiographed and rated in accordance with the specifications noted in Section 2.4.* The radiographic ratings and defect descriptions are reported in Table 3.3. Also reported in this table are the stress cycle, fatigue life, and location of failure for each of the as-welded specimens. Ten specimens originally exhibited observable defects, four of which failed the specification requirements for weld quality. However, with the exception of Specimen NC-41, the welds that failed radiographic inspection were tested in fatigue without being repaired to obtain a broader indication of the effect of weld flaws on the fatigue behavior of the members. Specimen NC-41, which initially contained a 1-1/4 in. long surface crack, was rewelded after the region containing the crack was ground to sound weld metal; a second radiograph taken after repair showed no other defects to be present.

Thirteen of the fatigue specimens tested (approximately one-half the total) exhibited fatigue failures that initiated at locations

* There was no ultrasonic inspection performed for the as-welded joints.

within the welds, while the remainder exhibited surface crack initiation either at the toe of the weld or in the test section adjacent to the weld. Typical fracture surfaces for specimens having failed at the toe of the weld, and for those having failed at internal defects are shown in Fig. 3.7. The single specimen exhibiting failure on the surface of the base metal, NC-35, was fabricated using plate material which had the mill-scale surface intact.

From examination of Table 3.3, it is evident that those specimens which initiated failure at internal defects exhibited shorter fatigue lives (and greater scatter in lives) than those in which failure initiated at the toe of the weld. Within the range of flaws included in this study, it was difficult to obtain a correlation between the size and type of defect identified by radiographic examination and the location of crack initiation. Indeed, eight of the thirteen specimens failing at internal defects were identified as "sound" weldments by radiography, whereas only three of the weldments in which internal flaws were detected actually initiated internal cracking. It is also noteworthy that, for the specimens tested at 0 to +50 ksi and 0 to +60 ksi, the longest fatigue lives were attained by those specimens that had failed the weld inspection requirements,^(8,9) but had, nonetheless, fatigue cracks that initiated at the toe of the weld.

A comparison of the results obtained for the three welding procedures indicates that the specimens fabricated using the U. S. Steel and Linde 140 GMA wires exhibited the lowest incidence of internal crack initiation, whereas those prepared with the McKay electrode exhibited the highest incidence of internal crack initiation (in most instances, at lack of fusion not initially detected by radiography). However, these observations are based on a very limited number of test specimens, and should not be construed as

conclusive or even necessarily indicative of the results which might have been obtained if a larger number of specimens were available, if slightly different welding procedures were used, or if other than a flat welding position were employed.

The fatigue lives of the as-welded specimens tested in the present study are compared in Fig. 3.8 to the data from an earlier investigation⁽²⁾ in which several "first-generation" GMA welding wires were used. Even with the wide scatter in fatigue lives exhibited by those specimens which initiated failure at internal defects, it is apparent that the specimens using the second-generation electrodes and the new procedures performed more satisfactorily than those fabricated with the first-generation wires. This improvement may be explained in part by the fact that although lack of fusion was the predominant cause of internal failure for the specimens with the lower lives, it was generally less extensive in those weldments prepared using the later wires.

The fatigue data for the current as-welded specimens are compared, in Figs. 3.9 and 3.10, with the zero-to-tension S-N curves obtained for similar as-welded joints of HY-80 and HY-100 steel which were also subjected to axial, constant amplitude cycling.^(2, 11-13) (The S-N curve for the HY-80 material includes specimens that were fabricated using both 3/4 in. and 1-1/2-in. thick plate stock, while the curve for the HY-100 material represents specimens fabricated from 3/4 in. stock.) Figure 3.10 shows the fatigue response of the HY-130(T) welds failing at the toe of the weld to be at least equal to the performance of the HY-80 and HY-100 weldments. At a stress cycle of 0 to +80 ksi, for example, the fatigue life of the butt welds in all three materials was approximately 25,000 cycles, whereas, at 0 to +60 and 0 to +50 ksi, the average fatigue lives of the HY-130(T) welds were considerably longer

than those using the HY-80 and HY-100 base materials. It must be emphasized, however, that the longer lives associated with the weld toe failures in the HY-130(T) material will be realized under axial loading only if weld flaws which precipitate internal crack nucleation are eliminated.* Toward this goal, metallurgical examinations of the fatigue fracture surfaces have been conducted to better define the conditions at the point of internal crack initiation. These studies, in turn, have suggested means of modifying the current welding procedures to hopefully further improve the weld quality; the results are reported in Section 3.2.4.

3.2.3. Fatigue Tests of Joints with Reinforcement Removed

In order to determine the fatigue behavior of defective butt welds, several specimens utilizing each of the three second-generation electrodes were fabricated containing intentionally induced flaws. The weld reinforcement was removed from these specimens: (1) to insure internal fatigue crack initiation; and (2) to permit better resolution and interpretation of radiographic and ultrasonic inspection data for those specimens included in the studies of crack initiation and propagation.

Of the total of twenty specimens tested with the reinforcement removed, the number fabricated using each of the three electrodes was as follows:

* The problem of internally initiated fatigue failure is less critical under purely flexural loading, since the plate surface is more highly stressed than the internal regions where weld defects are prevalent; thus, in flexure, the importance of defects in establishing fatigue resistance should be minimal and fatigue lives commensurate with the toe failures reported in Table 3.3 should be readily attainable.

<u>Electrode Designation</u>	<u>Welding Procedure</u>	<u>No. of Fatigue Test Specimens</u>
USS 5Ni-Cr-Mo	P130(T)-USS-A	9
Linde 140	P130(T)-L140-A	5
McKay 14018	P130(T)-M140-A	6

The welding procedures employed in the fabrication of the specimens were the same as those illustrated in Figs. 3.2, 3.3, and 3.4, except that specific measures were followed (wetting of welding wire, weaving back over slag, etc.) to induce the formation of a certain type of defect in an individual weldment. A list of the specimens and the type and size of the detected defects are presented in Table 3.4, together with similar information for six specimens fabricated using a first generation welding wire. The defect types were identified by radiographic examination using the same two percent sensitivity level followed in X-raying the as-welded members. (The report "Guide for Interpretation of Non-Destructive Tests of Welds in Ship Hull Structures", Ref. 14, was used as an aid in the identification of defects appearing on the radiographs.) It should be noted that the attempts to induce specific amounts and types of defect were met with only limited success; i.e., as shown in Table 3.4, some specimens were found to be radiographically "sound" even when welding procedures were used which were intended to introduce porosity, lack of penetration, etc. Further, as with the as-welded members, radiography did not necessarily reveal the type of flaw present at the eventual location of fatigue crack initiation under cyclic loading.

All of the specimens with the reinforcement removed were tested at a stress cycle of zero-to-tension to permit comparison of the results with the behavior of the as-welded members reported earlier. The

results of the fatigue tests, together with a description of the type(s) of defect observed on the fracture surfaces at the location of fatigue crack nucleation, are presented in Table 3.4; the fatigue test data are also presented graphically in Fig. 3.11. A number of specimens are reported in Table 3.4 simply as having failed "in weld metal" because no physical internal flaw was discernible, with the unaided eye, on the fracture surfaces. These specimens were subsequently examined metallographically to study the weld microstructure and type of microscopic defect at the site of crack initiation; the results of this investigation are reported in Section 3.2.4. Photographs of the fracture surfaces of specimens having failed at various internal defects are pictured in Fig. 3.12.

Examination of Table 3.4 reveals the occasional disparity between the initial radiographic record of the weld quality and the actual defect later determined as the location of fatigue crack initiation. It is apparent, therefore, that unless a large single defect or gross amounts of a particular defect type are present in a given weldment, it is not possible to predict with any degree of certainty the point of fatigue crack initiation under direct axial loading simply from the results of a radiographic inspection conducted before testing.

No firm relationship between the crack-initiating defect type (as determined by fracture surface examination) and fatigue life could be established. The wide variation in fatigue behavior is clearly illustrated in Figs. 3.13 and 3.14 for specimens tested at stress levels of 0 to +80 ksi and 0 to +50 ksi, respectively. The data for as-welded specimens in which failure initiated at internal defects are also presented in these figures. From the data for tests conducted at 0 to +80 ksi, it appears that the irregularly shaped defects and the

linear defects, such as slag and lack of fusion, generally resulted in lower lives than those obtained for specimens containing isolated pores or clustered porosity. This could be expected, since the notch acuity and corresponding stress concentrations associated with the sharp, linear defects are considerably greater than for the approximately spherical configuration of the individual pores in porosity clusters. This expected performance was not enforced, however, by the data for specimens tested at 0 to +50 ksi (Fig. 3.14). For these tests, the scatter in data for all defect types is so large that it precludes drawing conclusions regarding the influence of any single flaw type. It should be noted, however, that the majority of specimens tested at 0 to +50 ksi had failed the radiographic inspection, and that greater consistency might be obtained if smaller defect densities were present.

Although the welded HY-130(T) specimens examined in this study exhibited a wide range in fatigue lives at the several test stress levels, it will be shown, in Section 3.3, that the number of cycles from crack initiation to failure was relatively consistent for specimens failing at a variety of internal flaws. This information is, of course, quite meaningful in that it may suggest reasonable limits which could be established between periodic inspections of structural components in service (subjected to axial fatigue loading), especially after the first indication of fatigue cracking had been noted.

3.2.4. Metallurgical Examination of Fracture Surfaces

3.2.4.1 Introductory Remarks

The fracture surfaces of all specimens listed in Tables 3.3 and 3.4 have been examined using low power optical microscopy. The

Metz Reference Room
Civil Engineering Department
B106 C. E. Building
University of Illinois

location and nature of the most serious defects apparent on the fracture surfaces were noted. These observations confirmed the listed sources of failure given in Tables 3.3 and 3.4.

In addition, sections were cut through many of the fractured specimens which failed through internal defects. The sectioned surfaces were polished and etched to reveal the location of the fatigue crack initiation and the path chosen by the propagating crack relative to the principal metallurgical zones in the weld; i.e., weld metal, heat affected zone (HAZ), or base metal.

In the following sections, a brief description of these metallographic observations will be given for specimens exhibiting toe failures and internal failures.

3.2.4.2 Specimens Failing at Toe of Weld

Of the specimens tested in the as-welded condition, with the reinforcement intact, approximately 50 percent failed at the toe of the weld. The remainder failed internally from a variety of causes and will be discussed in the next section.

Toe initiated failures invariably started at or near the line of fusion and propagated first through the HAZ and finally into the base metal. Crack initiation in and propagation through weld metal was seldom observed. Substantial improvement of fatigue lives beyond those obtained in this study does not seem too promising because of the inherent stress raiser existing at the toe of the weld. A temper bead technique was used in all of the specimens tested to try to obtain an optimum condition at the toe of the weld. Nevertheless it is felt that a more effective procedure may exist which could improve the fatigue resistance of reinforced weldments somewhat further and that studies of this question should be continued.

3.2.4.3 Specimens Exhibiting Internal Failure

Approximately 50 percent of the as-welded and all of the specimens with the reinforcement removed failed as a result of internal defects or discontinuities, many of which were intentionally incorporated in the weld. About one-half of the failures initiated at large linear defects such as slag and/or lack of fusion. Other causes were porosity and cold cracks.

In general, the failures originated near the center of the weldment, in the vicinity of the root passes. Many of these proved to be lack of fusion (cold shuts) and were located very close to the line of fusion. It was not always possible to determine exactly whether the crack had initiated in the weld metal, at the line of fusion, or in the grain coarsened portions of the HAZ, but it was observed that the fracture surfaces often passed through an appreciable fraction of the HAZ.

In a few cases, notably in Specimens NC-20, NC-31, NC-37 and NC-47, the fatigue cracks preferentially propagated within the HAZ. These observations suggest that the HAZ provides a harsh region through which the crack can readily propagate. Hardness traverses have confirmed this condition. Areas in the HAZ exhibited Vickers hardnesses of 450 VHN while both the base and weld metals averaged about 350 VHN. These higher values in the HAZ would indicate the presence of a material that is less ductile and more notch sensitive than in the surrounding weld and base metals.

The tendency of the internally initiated failures to occur in the vicinity of the root passes, even in those specimens not containing intentional defects, needs to be studied further. This effect may be due to minor variations in the welding techniques during the first and most troublesome welding passes. A second possible factor may be the existence

of unfavorable residual stresses. A third cause may be the presence of a high alternating plastic strain which is concentrated in these areas due to the geometry of the welds.

Details on the fracture surfaces of several fatigue specimens have been studied using a scanning electron microscope. Figure 3.15 shows a view of a pore which initiated the critical fatigue crack in Specimen ND-30. From the surface steps radiating from the pore in the center, it is apparent that it is this object at which failure initiated. A further observation is that the interior of the pore appears to be crazed with a number of intersecting cracks suggesting that the interior surfaces of such pores may be reticulated by microcracks prior to fatigue loading.

3.3 Fatigue Crack Initiation and Propagation

Both radiographic and ultrasonic techniques were used to detect the nucleation of fatigue cracks at internal defects; radiography was further employed to examine the patterns of internal crack propagation beyond the stage of initiation. A description of the ultrasonic equipment, of the X-ray equipment, and of the procedures followed for the periodic examination of the defective butt welds is presented in Section 2.4.

3.3.1. Results of Radiographic Crack Detection Studies

Thirteen HY-130(T) butt-welded specimens, with the reinforcement removed, were subjected to radiographic inspection at periodic intervals during the course of cycling; the results of the surveys of crack initiation and cycles of propagation are summarized in Table 3.5. Twelve of specimens were tested at a stress level of 0 to +50 ksi to permit comparison of the results with similar tests of butt welds fabricated of HY-80 and HY-100 steels.

Tracings of selected radiographs obtained during the progress of fatigue cycling are illustrated in Figs. 3.16 through 3.25 for ten of the thirteen specimens examined in this phase of the investigation. (For Specimens NC-20 and NC-23, the anticipated fatigue lives were much longer than those actually obtained. Thus, the first X-ray taken after the start of cycling indicated that considerable crack growth had taken place and an insufficient number of radiographs obtained to adequately describe the complete crack progression process for these two weldments. Similarly, no radiographs of Specimen ND-12 were taken between 175,000 cycles, at which time no internal fatigue cracking was evident, and 219,200 cycles, when complete failure occurred.)

Examination of the tracings of the radiographs clearly demonstrates the complex and often unpredictable nature of the progression of a fatigue crack or cracks in the test weldments. In Specimen ND-21 (Fig. 3.18), for example, the fatigue crack which eventually extended to complete failure was not the first fatigue crack observed nor was it the longest crack until the latter stages of propagation. Further, in Specimen ND-17, fatigue cracks initiated near the tip of weld hot cracks oriented parallel to the direction of stress rather than at a seemingly more critical elongated slag deposit, Fig. 3.22. Despite these instances of unexpected behavior, the fatigue cracks in most of the specimens were found to propagate on planes perpendicular to the direction of external loading until such time as they had penetrated to one surface of the specimen; thereafter, during the latter stages of cycling, the cracks extended to complete failure along oblique planes in a typical "shear" mode of rupture.

For each of the specimens welded using the second-generation wires and X-rayed during cycling, the horizontal projection of the length

of the critical internal fatigue crack,^{*} expressed as a ratio of the total specimen width, is plotted in Fig. 3.26, as a function of the percentage of fatigue life to failure. Similar data for HY-80 and HY-100 specimens tested at 0 to +50 ksi are presented in Fig.

3.27. (2,16) It must be recognized that the propagation patterns indicated in the figures are approximate at best since only a limited number of radiographs were obtained for each specimen; a continuous trace of internal crack extension was not determined. Nevertheless, certain general observations may be deduced by comparison of the tests of three different materials. The occurrence of internal fatigue crack initiation was found to vary from approximately 20 to 80 percent of the total fatigue life of a specimen; as discussed later, this explains in part the wide scatter in lives obtained for those welds tested at a particular stress level. Following initiation, the specimens tested at 0 to +50 ksi often exhibited somewhat erratic crack growth patterns, with short periods of extension followed by periods of apparent stagnation. For Specimens ND-10, ND-14, and ND-15, a sharp jump in crack length was recorded at those cycles where two or more individual cracks had merged to form one continuous crack. The general trend, however, was one of a gradually increasing growth rate as cycling progressed and the fatigue cracks extended over an

* For Specimens ND-10, ND-14, and ND-15, the length of the first observed fatigue crack was used, until such time as two or more separate cracks had merged into a single continuous crack. For Specimen ND-21, the crack which eventually extended to complete failure was used.

ever-increasing area of the specimen cross-section.* Then, toward the completion of the test, the final few load repetitions were associated with a shear-type failure which concluded with complete specimen separation.

Although the scatter in the total fatigue lives of the HY-130(T) specimens which were welded using the second-generation wires and which failed at internal flaws was large (27,500 to 651,900 cycles at 0 to +50 ksi), the number of cycles for a crack to propagate to failure from the time of its initiation appears to be much more consistent. As illustrated in Fig. 3.28, the cracks in specimens for which there is radiographic data appeared to initiate at from 15,000 to 45,000 cycles prior to failure. However, the range in "total" lives for these specimens generally was much greater. The same general pattern was exhibited by the HY-80 and HY-100 weldments, as shown in Fig. 3.29, where the numbers of cycles for propagation prior to failure ranged from approximately 12,000 to 30,000 cycles, and the total fatigue lives for the same specimens varied from 17,300 to 130,500 cycles.⁽¹⁶⁾

* The latter stages of crack propagation were marked by a continuous change in local stress in the vicinity of the crack front. This was occasioned by the fact that, as the cracked area of the specimen reached appreciable size (approximately one-fourth of the initial specimen cross-sectional area), the peak tensile load on the fatigue machine would gradually drop with continued cycling. At the same time, however, the remaining net cross-sectional area capable of transmitting this applied tensile load was becoming substantially reduced. Further, depending upon the position of the cracked region, the remaining load-carrying area generally became eccentrically loaded, resulting in a superposition of tensile stresses due to the combined axial and flexural components. The net result of these factors was that the maximum stresses were continually increasing at the crack tip (at lives beyond about 80 percent of the member life) which, in turn, explains the rapid acceleration in the rate of crack propagation during the final cycles before fracture.

The data of Figs. 3.28 and 3.29 exhibit crack propagation curves similar to those often reported in fatigue and appear to show three stages; an initial stage that is rather erratic, a relatively long approximately linear stage, and a final rapidly changing stage. The latter stage developed after the crack had propagated through approximately 30 percent of the section and occurred during the last 5,000 cycles or less. Thus, it appears that most of the propagation life is expended during the linear propagation stage.

This general consistency in the observed crack propagation behavior is to be expected since most of the defects initiating internal fatigue cracks were located at approximately mid-thickness in the test weldments (usually in the area of the root and second weld passes), in a region where residual stresses from welding would be expected to be similar from one specimen to another. Thus, once a fatigue crack has initiated (the cycles to initiation being governed primarily by the size of the weld defect and the notch acuity at the extremities of the defect), the geometry and state of stress at the tip of the progressing crack would be approximately the same for specimens tested at the same nominal stress level and duration of crack propagation should also be similar.

The above observations are restrictive, however, in that they are directly applicable to the behavior of specimens initiating cracks at a relatively small defect which is surrounded by a substantial body of sound metal. Where the internal flaw occupies a more significant portion of the weld, as in Specimen NC-20 (see Table 3.5), which had a linear discontinuity extending almost the full length of the weld, crack initiation may occur at or near the beginning of cycling, and the crack may soon thereafter progress at a rate equivalent to that observed in

the latter stages of growth in other specimens. This would explain the very short total fatigue life of Specimen NC-20, 6,600 cycles, and the correspondingly short lives of three previously tested as-welded HY-130(T) specimens,⁽²⁾ NB-3, NC-11, and NC-12, all of which also contained linear discontinuities extending nearly the total length of the welds and which displayed internal fatigue failures in less than 15,000 cycles at a stress level of 0 to +50 ksi.

3.3.2. Results of Ultrasonic Crack Detection Studies

As outlined previously, ultrasonic techniques have been utilized, in addition to radiography, to detect the presence of defects in several of the butt welds and to attempt to establish the initiation or early stage of propagation of fatigue cracks originating at these defects. A description of the ultrasonic equipment and the general procedures employed during this phase of the investigation are given in Section 2.4.

For the current program, the ultrasonic equipment was calibrated in accordance with procedures and sensitivity standards established by NAVSHIPS 0900-006-3010⁽¹⁵⁾ for the inspection of full penetration butt welds. (However, due to space limitations in the testing machines, a 45° beam angle was used instead of the 60° to 70° beam angle required for plates of 1 in. thickness.) The scanning technique consisted of traversing the probe across the face of the specimen in the transverse direction in 1/8 in. vertical increments until a response exceeding the disregard level (DRL) was detected. The probe position was then adjusted to maximize the signal amplitude from the internal defect or crack; this position was recorded on an X-Y plotter together with the depth beneath the surface of the test specimen from which the peak response originated and the pulse energy required to establish the response. Following this,

the probe was traversed both vertically and horizontally from the point of peak response, with the four positions at which the signal amplitude fell below the DRL being recorded on the plotter. It should be emphasized that no attempt was made to further identify the type of detected defect, nor were the points used to identify the limits of a recordable indication intended to represent, necessarily, the physical extremities of the actual defect or crack. The technique was employed simply as a means of determining whether the initiation (or early stage of propagation) of a fatigue crack, as verified by radiographic inspection, could be detected by an increase in the amplitude of the ultrasonic response in the vicinity of the initial flaw, and/or by a lengthening of the distance over which the response remained above the DRL.

Sketches of the ultrasonic responses obtained before testing, and after the presence of fatigue cracking had been determined by radiography, are presented in Figs. 3.30 through 3.37 for several of the HY-130(T) butt welds examined in this study. Also shown on the figures are sketches and photographs of the specimen fracture surfaces, and the radiographs taken prior to testing; on the sketches of the fracture surfaces are indicated the position of the weld defects, and extent of fatigue crack growth at approximately the time of intersection of the progressing crack with the specimen surface. The ultrasonic plots represent the projection of all detected responses above the DRL onto a cross-sectional plane through the weld perpendicular to the longitudinal axis of the fatigue specimen. The crosses represent the limits of the probe scan for which the echo amplitude remained above the DRL. The numbers corresponding to each response indicate a relative measure of the amplitudes of the peak signals; they are not a

direct measure of the pulse energy required to establish the responses. The letter designation indicates the vertical position of the maximum or peak response in the direction of the longitudinal axis of the test specimen. It should be noted that many additional responses were established for most of the weldments, including areas in which no corresponding radiographic indications of defects were obtained. However, the peak amplitudes of these responses were generally below the DRL and are not shown in the figures.

The second ultrasonic trace shown in the sketches for the various welds indicate a definite increase in the relative height of the peak signal in the general vicinity where fatigue cracking had been detected by radiography. However, at the time these traces were obtained, cracking was already clearly evident on the corresponding radiographs, so that the increase in signal amplitude does not correspond to the actual time of crack initiation. Due to the considerable amount of time involved in obtaining a complete ultrasonic trace using the manual traversing technique described earlier, no attempt was made to obtain such traces periodically during the course of fatigue crack propagation. Although previous studies in this area have occasionally proven successful, ⁽¹⁾ it was noted in Ref. 2 that, when dense concentrations of porosity and/or slag are present in a weldment, it is virtually impossible to distinguish a slight change, indicative of crack nucleation or early growth, from among the complex series of peaks and troughs representative of the response from the original defect itself.

In general, it may be stated that ultrasonics can be a satisfactory adjunct to, or, in some instances, replacement for radiography

for the detection of internal fatigue cracking in welds, at least where the cracking is of such proportions that the ultrasonic response from the crack is clearly distinguishable from the internal defect at which cracking originated. That ultrasonics can be used to establish the exact profile of a fatigue crack at some stage during the cycling process still questionable but is a matter that is currently being examined at the U. S. Naval Applied Science Laboratory⁽¹⁷⁻²⁰⁾ and at other agencies.

3.4 Concluding Remarks

From the foregoing discussions of the as-welded specimens and of those with the reinforcement removed, it is readily apparent that the location of internal fatigue crack initiation, the cycles to initiation, the rate of fatigue crack propagation, and the resultant total fatigue lives of defective transverse butt welds tested under axial loading, whether they be fabricated of HY-130(T) or of other HY steels, are governed by a variety of factors not all of which can be adequately described by non-destructive examination of the weld defects prior to testing. These factors include, besides the range of applied external load and its maximum tensile component, the nature of the residual stress field, the notch acuity at defect boundaries, the dimensions of the defects, and the locations of the defects within the weld in proximity to one another and to the surface of the test specimen. As a result of these varied, and often conflicting factors, a wide scatter in the total lives, at the zero-to-tension stress cycles examined, was exhibited by those welds in which fatigue cracking was internally initiated. However, despite these wide variations in total life, illustrated in Figs. 3.8 and 3.11 respectively, for the as-welded specimens and those with the

reinforcement removed, non-destructive examination of several specimens during cycling revealed a relatively consistent pattern in the number of cycles for propagation to failure (for those specimens containing observable defects within specification limits)*. Thus, the measure of the cyclic life capacity of the welds beyond the point of internal nucleation, as illustrated in Fig. 3.38, might be a more meaningful parameter by which to establish periodic inspection intervals of service structures, if there is reasonable certainty that no severe linear defects which have eluded non-destructive examination are present in the welds.

The preceding discussion refers to structural components (transverse butt welds) which are subjected primarily to direct axial loading wherein the entire cross-section of the weld, including areas containing weld defects, are uniformly stressed. When the external loading is essentially flexural, the surface of the member withstands the highest nominal stresses and fatigue failure will more commonly be associated with the external geometry at the toe of the weld. Under such conditions, HY-130(T) butt welds can be expected to attain fatigue lives, Fig. 3.10, at least as long as those exhibited by HY-80 and HY-100 butt welds, at stress levels of 0 to +80 ksi and below.

* As noted earlier, very short total lives were obtained at all stress levels for those specimens containing linear internal defects extending over a major portion of the total weld length.

IV. ANALYSIS OF FATIGUE DATA

Because of the small number of tests performed at any one stress level it is difficult to evaluate the effects on the fatigue strength of variables such as removal of reinforcement and differences in filler wire. In an attempt to overcome this difficulty, the fatigue performance of the welded specimens has been compared to the behavior of the unwelded HY-130 specimens and their lives expressed as a percentage of base metal fatigue life.

Using the fatigue data from HY-130 specimens with the mill scale intact and the few tests on specimens with machined surfaces, shown in Figure 3.1, the estimated lives of unwelded HY-130 specimens with machined surfaces tested in zero-to-tension stress cycle are:

<u>Stress, ksi</u>	<u>Cycles at Failure</u>
100	100,000
80	250,000
60	700,000
50	1,200,000

4.1 Effect of Removal of Reinforcement

Using the "percentage of base metal life" concept, the range of fatigue life, the arithmetic mean life, and the distribution of "failure causing defects" for six classes of welded specimens have been calculated and are listed in Table 4.1.

Seventy-three percent of the as-welded specimens failed at less than 10 percent of base metal life. The arithmetic mean life was approximately 9 percent of the base metal life. The most common causes of failure were the toe-initiated cracks (53 percent of all specimens) and large planar defects such as slag or lack of fusion (35 percent of all specimens).

Seventy-four percent of the specimens tested with the reinforcement removed failed at less than 10 percent of base metal life. The arithmetic mean life was higher than in the as-welded case and was roughly 15 percent, reflecting a greater distribution of lives. The most common cause of failure was the larger, planar defects of slag and lack of fusion (52 percent of all specimens); these defects were responsible for the failure in most of the short lived specimens at each stress level examined.

Since a number of the specimens contained intentionally deposited defects which would have been cause for their rejection by radiographic inspection standards,^(8,9) the lives of "as-welded" and "reinforcement removed" specimens passing the Navy's radiographic inspection requirements have been compared separately. Since few as-welded specimens contained unacceptable flaws, the exclusion of specimens failing radiographic inspection makes little difference upon the statistics of this case. This is not so, however, for the specimens with the reinforcement removed. Approximately one-half of the latter failed radiographic inspection because of the intentionally incorporated flaws. The exclusion of these tests from the data results in a two-fold increase in arithmetic mean life (from 15 percent to 25 percent) and a marked decrease in the number of specimens failing in less than 10 percent of base metal life (down from 74 percent to 50 percent).

4.2 Effect of Filler Wire

To determine whether any significant difference in fatigue behavior could be attributed to the type of filler wire and welding procedure, the fatigue data were also analyzed as a function of filler wire. There was little difference in fatigue life for specimens welded using the Linde filler wire and McKay coated electrodes; they exhibited the lower mean fatigue lives. However, the U. S. Steel-GMA procedure consistently produced fatigue

specimens, tested with reinforcement removed, capable of sustaining lives in excess of 10 percent of the base metal life. Specimens welded using the U. S. Steel-GMA technique which passed radiographic inspection and were tested with reinforcement removed yielded an arithmetic mean life of 30 percent, roughly two times the average for all specimens, and appreciably better than the average for all specimens passing inspection and tested with reinforcement removed. It must be remembered, however, that these observations are based on a limited amount of data and must be interpreted accordingly.

4.3 Concluding Remarks

Specimens which sustained the longer fatigue lives at each test stress level were those in which no detectable flaw was observed and in which the time (cycles) to crack nucleation was very long. The specimens that failed at lives of less than 10 percent base metal life initiated active fatigue cracks early in their fatigue life.

The elimination or reduction in severity of the sites for fatigue cracking, thereby increasing the time to crack initiation, offers real promise for greatly increasing the fatigue life of the butt-welded joints in HY-130 steel. Of the several wires and welding procedures used, the U. S. Steel-GMA procedure produced the greatest average fatigue resistance. However, further developments and improvements are desired to provide a weld metal that more nearly reproduces the fatigue resistance of the base metal when placed in butt-welded joints.

V. SUMMARY AND CONCLUSIONS

The studies reported herein are part of a continuing investigation to evaluate candidate high strength steels developed for use by the U. S. Navy. The purpose of the current investigation has been to investigate the axial fatigue behavior of plates and transverse butt-welded joints in HY-130(T) steel. The plain plate specimens, received descaled and painted, were tested at a stress cycle of zero-to-tension; the results have been compared to similar tests of plates containing mill scale, and plates with polished surfaces. The weldments were prepared using each of two experimental "second-generation" GMA welding wires and a coated electrode. Fatigue tests at a stress cycle of zero-to-tension were conducted using both sound weldments and weldments containing such defects as porosity, slag, lack of fusion, and lack of penetration. Radiographic and ultrasonic testing techniques were used to study the initiation and propagation of fatigue cracks originating at internal weld flaws.

Since the results reported herein represent a rather limited amount of test data, the evaluation of the data must be viewed as preliminary in nature. With this in mind, a number of basic observations have been made which are considered significant; these are briefly summarized in the following paragraphs.

Plain Plate Specimens

The fatigue lives exhibited by descaled and painted plain plate specimens at a stress cycle of 0 to +80 ksi were approximately four times the average life of corresponding specimens containing mill-scale, and slightly below the average life of specimens having polished plate surfaces. The average life at 0 to +80 ksi for specimens with each of the surface conditions is shown below:

<u>Surface Condition</u>	<u>Average Fatigue Life</u>	<u>Number of Tests</u>
As-Rolled (Mill-Scale Intact)	57,000	5
Descaled and Painted	218,000	2
Polished	257,000	2

Transverse Butt Welds, As-Welded

Approximately one-half of the as-welded specimens tested at various zero-to-tension stress levels initiated failure at internal weld defects; the remainder initiated cracking at the toe of the weld reinforcement. Internally initiated failures occurred nearly as often in specimens rated as "sound" weldments by radiography (2 percent sensitivity) as at the toe of the weld in the weldments.

The specimens which initiated failure at internal weld flaws exhibited shorter lives and greater scatter in lives than did those in which failure initiated at the toe of the weld. It was not possible to relate the point of internal crack initiation with a radiographic indication of defects present in the weld; based on examination of the fracture surfaces, however, it appears that planar discontinuities such as lack of fusion represent the most severe conditions with regard to lowering the fatigue life expectancy of the weldments. For those as-welded specimens which failed at the toe of the weld, the average life, at a stress cycle of 0 to +80 ksi, was approximately 25,000 cycles, or about the same as the lives of similar weldments fabricated of HY-100 or HY-80 steel.

Transverse Butt Welds, Reinforcement Removed

Twenty butt-welded specimens which contained several types of intentionally deposited weld defects and which had the reinforcement removed were tested at a stress cycle of zero-to-tension. As with the as-welded specimens, there was an occasional disparity between the initial radiographic record of weld quality and the location of fatigue crack

initiation. Further, consistent patterns could not be established for all test stress levels between the type of crack-initiating defect (as determined by fracture surface examination) and the fatigue life. However, for tests conducted at 0 to +80 ksi, it was found that specimens containing planar and irregularly shaped defects, such as lack of fusion and slag, generally exhibited lower lives than those obtained from specimens containing isolated pores or clusters of porosity.

From radiographs taken periodically during the fatigue testing, it was found that time to initiation of cracking at internal defects varied from twenty to eighty percent of the total cyclic life. Although the scatter in the total fatigue lives for the specimens with the reinforcement removed was great, e.g., from 4,300 to 170,000 cycles at 0 to +80 ksi, and from 27,500 to 651,900 cycles at 0 to +50 ksi,^{*} the number of cycles of crack propagation to failure beyond the point of initiation was found to be relatively consistent at a specific test stress level. At 0 to +50 ksi, for example, the cycles from initiation to failure for nine specimens varied from 15,000 to 45,000 cycles. These comments are applicable, however, to specimens containing no long, linear defects which can cause failure at total lives considerably lower than those noted above. (2)

Summary

It has been found, for the HY-130(T) weldments tested in either the as-welded condition or with the reinforcement removed, that the location of fatigue crack initiation, the cycles to initiation, and the total cycles to failure are determined by a variety of factors. The lives of specimens that developed toe failures in the as-welded members

* Exclusive of those specimens using "first generation" wires. (2)

exhibited only slight scatter; however, the specimens in which the failures initiated internally at weld defects were found to display a wide range in lives at each of the stress levels examined. In the studies of the internal failures it has not been possible to relate fatigue behavior to type or percentage of defect area (within the limited range studied), except that planar flaws (lack of fusion, etc.) appeared to be most detrimental. Despite the range of defect types and the scatter in total fatigue lives exhibited by these HY-130(T) weldments (for the specimens containing defects considered acceptable by current specifications), the cycles of crack propagation beyond the point of initiation were relatively consistent. This suggests that the cyclic life capacity beyond the time of internal initiation rather than the cycles to initiation or the total fatigue life may be the more important parameter by which to establish inspection requirements for service structures, especially in those members subjected to axial fatigue loading.

LIST OF REFERENCES

1. Munse, W. H., Bruckner, W. H., Radziminski, J. B., Hinton, R. W., and Leibold, J. W., "Fatigue of Plates and Weldments in HY-100 and HY-130/150 Steels," Civil Engineering Studies, Structural Research Series No. 300, University of Illinois, Urbana, Illinois, December, 1965.
2. Radziminski, J. B., Hinton, R. W., Meinheit, D. F., Osman, H. A., Bruckner, W. H., and Munse, W. H., "Fatigue of Plates and Weldments in High Strength Steels," Civil Engineering Studies, Structural Research Series No. 318, University of Illinois, Urbana, Illinois, February, 1967.
3. Connor, L. P., and Orehoski, R. M., "Qualification Testing of 5Ni-Cr-Mo Welding Wire," Project No. 39.018-015(2), Applied Research Laboratory, U. S. Steel Corporation, Monroeville, Pennsylvania, May 1, 1967.
4. Boblenz, T. L., and Connor, L. P., "First Progress Report: Fabrication of an HY-130(T) Steel Structure," Project No. 39.018-015(1), Applied Research Laboratory, U. S. Steel Corporation, Monroeville, Pennsylvania, January 1, 1967.
5. Connor, L. P., "Second Progress Report: Fabrication of an HY-130(T) Steel Structure," Project No. 39.018-015(3), Applied Research Laboratory, U. S. Steel Corporation, Monroeville, Pennsylvania, August 1, 1967.
6. Connor, L. P., "Third Progress Report: Fabrication of an HY-130(T) Steel Structure," Project No. 39.018-015(5), Applied Research Laboratory, U. S. Steel Corporation, Monroeville, Pennsylvania, January 1, 1968.
7. Connor, L. P., "Fourth Progress Report: Fabrication of an HY-130(T) Steel Structure," Project No. 39.018-015(8), Applied Research Laboratory, U. S. Steel Corporation, Monroeville, Pennsylvania, July 1, 1968.
8. Porter, L. F., Rathbone, A. M., Rolfe, S. T., Dorsch, K. E., Wilcox, W. L., Waite, R. G., Jenni, C. B., Telford, R. T., and DeLong, W. T., "The Development of an HY-130(T) Steel Weldment," Project No. 39.018-001(64), Applied Research Laboratory, U. S. Steel Corporation, Monroeville, Pennsylvania, July 1, 1966.
9. NAVSHIPS Specification No. 0900-006-9010, "Fabrication, Welding and Inspection of HY-80 Submarine Hulls," Naval Ship Engineering Center, Navy Department, Washington, D. C., June 1966.
10. Enis, A., and Telford, R. T., "Gas Metal-Arc Welding of HY-130(T) Steel," Welding Research Supplement, Welding Journal, Vol. 47, No. 6, June 1968, pp. 271s-278s.
11. Hartmann, A. J., Bruckner, W. H., Mooney, J., and Munse, W. H., "Effect of Weld Flaws on the Fatigue Behavior of Butt-Welded Joints in HY-80 Steel," Civil Engineering Studies, Structural Research Series No. 275, University of Illinois, Urbana, Illinois, December 1963.

12. Hartmann, A. J. and Munse, W. H., "Fatigue Behavior of Welded Joints and Weldments in HY-80 Steel Subjected to Axial Loadings," Civil Engineering Studies, Structural Research Series No. 250, University of Illinois, Urbana, Illinois, July 1962.
13. Sahgal, R. K. and Munse, W. H., "Fatigue Behavior of Axially Loaded Weldments in HY-80 Steel," Civil Engineering Studies, Structural Research Series No. 204, University of Illinois, Urbana, Illinois, September 1960.
14. "Guide for Interpretation of Non-Destructive Tests of Welds in Ship Hull Structures," Ship Structure Committee Report SSC-177, Prepared by National Academy of Sciences - National Research Council, Washington, D. C., September 1966.
15. NAVSHIPS Specification No. 0900-006-3010, "Ultrasonic Inspection Procedure and Acceptance Standards for Production and Repair Welds," Naval Ship Engineering Center, Navy Department, Washington, D. C., January, 1966.
16. Munse, W. H., Bruckner, W. H., Hartmann, A. J., Radziminski, J. B., Hinton, R. W., and Mooney, J. L., "Studies of the Fatigue Behavior of Butt-Welded Joints in HY-80 and HY-100 Steels," Civil Engineering Studies, Structural Research Series No. 285, University of Illinois, Urbana, Illinois, November 1964.
17. DiGiacomo, G., and Foster, M. L., "Ultrasonic Crack-Depth Measuring Methods and Their Application to High Strength Steel Tee-Welded Plates," Lab. Project 930-23, Progress Report 3, Material Sciences Division, U. S. Naval Applied Science Laboratory, Brooklyn, N. Y., August 18, 1967.
18. Rosen, M., and Gaites, R. A., "Fatigue of Large Scale Uniformly Loaded Simply Supported Butt Welded Rectangular Plates," Lab. Project 930-23, Progress Report 6, Material Sciences Division, U. S. Naval Applied Science Laboratory, Brooklyn, N. Y., February 5, 1968.
19. Gaites, R. A., and Rosen, M., "Fatigue of Large Scale Uniformly Loaded Simply Supported Tee-Fillet Welded Rectangular Rib-Stiffened Plates," Lab. Project 930-23, Progress Report 8, Material Sciences Division, U. S. Naval Applied Science Laboratory, Brooklyn, N. Y., July 22, 1968.
20. Gaites, R. A., and Rosen, M., "Fatigue of Large Scale Uniformly Loaded Simply Supported Butt Welded Rectangular Plates," Lab. Project 930-23, Progress Report 9, Material Sciences Division, U. S. Naval Applied Science Laboratory, Brooklyn, N. Y., November 20, 1968.

TABLE 2.1
 CHEMICAL COMPOSITION OF HY-130(T) BASE METAL
 (Data Supplied by Manufacturer)

Heat Number	5P0540	5P2456
Fatigue Specimen Designation	NC	ND
Chemical Composition, per cent		
C	0.12	0.10
Mn	0.79	0.84
P	0.004	0.007
S	0.003	0.004
Si	0.35	0.24
Ni	4.96	4.92
Cr	0.57	0.54
Mo	0.41	0.50
V	0.057	0.08
Al*	0.044	--
Al**	0.048	--
Ti	--	0.04
Cu	--	0.06
N	0.013	--
O	0.0019	--

* Acid soluble

** Total

TABLE 2.2

MECHANICAL PROPERTIES OF HY-130(T) BASE METAL

(Data Supplied by Manufacturer)

Heat Number	Fatigue Specimen Designation	Plate Thickness (inches)	Properties in Longitudinal Direction				Charpy V-Notch (ft-lbs @ 0°F)
			Yield Strength* (ksi)	Tensile Strength (ksi)	Elong. in 2 inches (per cent)	Reduction in Area (per cent)	
5P0540 [†]	NC	1	138.5	149.0	20.5	67.5	83
5P2456 ^{††}	ND	1	140.4	149.2	20.0	64.4	83

* 0.2 per cent offset

† Properties are average values for two plates; plates received with mill scale in place.

†† Plates received descaled and one coat painted.

TABLE 2.3
 CHEMICAL COMPOSITION OF ELECTRODES
 FOR WELDING HY-130(T) PLATES

Manufacturer	U. S. Steel Corporation *	Linde Division, Union Carbide Corporation **	McKay Company **	
Electrode Designation	5Ni-Cr-Mo	Linde 140	McKay 14018	
Electrode Type	1/16" bare-electrode wire	1/16" bare-electrode wire	5/32", 3/16" covered electrodes	
Heat Number	50646	106140	1P1375	
Chemical Composition (per cent)			5/32"	3/16"
C	0.11	0.11	0.077	0.081
S	0.006	0.007	0.003	0.004
P	0.004	0.008	0.003	0.003
Mn	0.75	1.72	1.91	1.85
Si	0.38	0.36	0.42	0.39
Ni	5.03	2.49	2.08	1.92
Cr	0.61	0.72	0.71	0.73
Mo	0.47	0.88	0.43	0.43
V	0.01	0.01	-----	-----
Cu	-----	0.08	-----	-----
Ti ⁺	0.015	-----	-----	-----
Al ⁺⁺	0.01	-----	-----	-----
N	0.004	-----	-----	-----

* Data from Ref. 3
 ** Data supplied by manufacturer
 + Total
 ++ Kjeldahl determination

TABLE 3.1

RESULTS OF FATIGUE TESTS OF HY-130(T) PLAIN PLATE SPECIMENS

Specimen Number*	Surface Condition	Stress Cycle (ksi)	Life** (cycles)	Location of Failure
NA-8	As-Rolled***	0 to +100.0	26,800	At mill scale surface in test section
NA-7	As-Rolled	0 to +100.0	21,000	At mill scale surface in test section
NA-1	As-Rolled	0 to + 80.0	64,200	At radius of test section
NA-2	As-Rolled	0 to + 80.0	60,900	At mill scale surface in test section
NC-13	As-Rolled	0 to + 80.0	59,800	At mill scale surface in test section
NA-5	As-Rolled	0 to + 80.0	51,100	At polished edge of specimen test section
NC-14	As-Rolled	0 to + 80.0	50,500	At mill scale surface in test section
NA-10	As-Rolled	0 to + 50.0	1,247,800+	Failure in pull-head
NA-6	As-Rolled	0 to + 50.0	712,000+	Failure in pull-head
NA-4	As-Rolled	0 to + 50.0	515,000+(a)	At mill scale surface in test section
NA-9	As-Rolled	0 to + 50.0	345,500	At mill scale surface in test section
NA-3	As-Rolled	0 to + 50.0	280,900	At radius of test section
NA-11	Polished	0 to +100.0	176,000	At radius of test section
NA-14	Polished	0 to +100.0	110,500	At radius of test section
NA-13	Polished	0 to + 80.0	304,300	At radius of test section
NA-15	Polished	0 to + 80.0	208,800	At two locations on polished edge of test section
ND-3	Descaled & Painted	0 to + 80.0	249,000	At radius of test section
ND-2	Descaled & Painted	0 to + 80.0	187,800	At a corner in test section

* Specimens designated by prefix NA or NC were tested in earlier studies (1,2)

** (a) Cycle counter on fatigue machine broke during test - failure occurred between 484,000 and 627,000 cycles

*** Mill scale intact on specimen surfaces

TABLE 3.2
RESULTS OF WELD QUALIFICATION TESTS
OF HY-130 (T) WELDMENTS

Reduced Section Tension Tests

Electrode Designation	Sample No.	Ultimate Tensile Strength, ksi	Reduction in Area, %	Location of Fracture
Linde 140	MX-24	153.5	40.9	Base Metal
	MX-26	152.8	52.9	Base Metal
U.S. Steel 5% Ni	MX-23	154.4	49.1	Base Metal
	MX-28	151.8	54.3	Base Metal

Side Bend Tests^{*}

Electrode Designation	Sample No.	Total Bend Angle, degrees	Maximum Load, lbs.	Remarks
Linde 140	MX-24	180	11,400	No cracks
	MX-26	180	11,700	No cracks
U.S. Steel 5% Ni	MX-23	180	10,050	No cracks
	MX-28	180	11,400	1/16 in. crack
McKay 14018	MX-31	180	11,350	No cracks

^{*} Bend test radius: 2t

TABLE 3.3
RESULTS OF DEFECT EXAMINATION AND FATIGUE TESTS OF HY-130(T)
TRANSVERSE BUTT WELDS IN THE AS-WELDED CONDITION

Specimen Number	Welding Procedure (See Figs. 3.2, 3.3 & 3.4)	Defective Area, percent (Based on Radiographic Examination)	Radiographic Rating*	Stress Cycle (ksi)	Life (cycles)	Location of Failure
ND-30	P130(T)-USS-A	0.038 (Single pore 0.03" d.)	P	0 to +100.0	4,100	In weld metal
ND-29	P130(T)-L140-A	Sound Weld	P	0 to +100.0	6,150	At lack of fusion, 0.09" long
ND-31	P130(T)-M140-A	Crack, 0.35" long, \perp weld axis, & weld undercut (0.02" deep, 0.25" long)	F	0 to +100.0	3,150	At crack perpendicular to weld axis, & at single pore, 0.02" d.
NC-32	P130(T)-USS-A	Sound Weld	P	0 to + 80.0	25,800	At toe of weld
NC-33	P130(T)-USS-A	Sound Weld	P	0 to + 80.0	19,600	At toe of weld
ND-23	P130(T)-USS-A	Sound Weld	P	0 to + 80.0	16,300	At toe of weld
NC-31	P130(T)-USS-A	Sound Weld	P	0 to + 80.0	14,700	At lack of fusion, 1.0" long
NC-37	P130(T)-L140-A	Lack of Fusion (0.15" long)	P	0 to + 80.0	>27,900** <35,500	At toe of weld, secondary crack at internal pore
NC-38	P130(T)-L140-A	Sound Weld	P	0 to + 80.0	29,100	At toe of weld
NC-39	P130(T)-L140-A	Sound Weld	P	0 to + 80.0	21,000	At toe of weld
NC-45	P130(T)-M140-A	Sound Weld	P	0 to + 80.0	25,800	At toe of weld
NC-46	P130(T)-M140-A	Sound Weld	P	0 to + 80.0	22,000	At two isolated pores, <0.01" d.
NC-44	P130(T)-M140-A	Sound Weld	P	0 to + 80.0	9,000	At lack of fusion, 0.09" long and at single pore, 0.02" d.
ND-1	P130(T)-M140-A	Weld undercut (0.02" deep, 0.08" long)	P	0 to + 80.0	6,200	At lack of fusion, 0.08" long
NC-35	P130(T)-USS-A	0.037 (Single pore, 0.04" d.)	P	0 to + 58.0	138,200	On surface of base metal
NC-36	P130(T)-USS-A	Weld undercut (0.03" deep, 0.4" long)	F [†]	0 to + 60.0	115,300	At toe of weld (not at undercut)
NC-42	P130(T)-L140-A	Sound Weld	P	0 to + 60.0	70,000	At toe of weld
NC-41	P130(T)-L140-A	Sound Weld***	P	0 to + 60.0	69,200	At toe of weld
NC-50	P130(T)-L140-A	0.041 (Single pore, 0.04" d.)	P	0 to + 60.0	56,200	At toe of weld
NC-40	P130(T)-L140-A	Sound Weld	P	0 to + 60.0	12,300	At intermittent lack of fusion, 0.6" total length
ND-4	P130(T)-M140-A	Sound Weld	P	0 to + 60.0	57,500	At lack of fusion, 0.05" long, and at single pore, <0.01" d.
NC-48	P130(T)-M140-A	Sound Weld	P	0 to + 60.0	27,000	At lack of fusion, 0.09" long
ND-5	P130(T)-M140-A	Sound Weld	P	0 to + 60.0	19,900	At lack of fusion, 0.14" long
NC-47	P130(T)-M140-A	Sound Weld	P	0 to + 60.0	18,400	In weld metal at linear discontinuity, 0.10" long
NC-34	P130(T)-USS-A	0.33 (Porosity cluster)	F	0 to + 50.0	526,100	At toe of weld
NC-43	P130(T)-L140-A	Lack of fusion (0.16" long)	P	0 to + 50.0	52,000	At lack of fusion, 0.06" long
NC-49	P130(T)-M140-A	Sound Weld	P	0 to + 50.0	119,500	At toe of weld

* Based on U. S. Steel Corporation recommendations⁽⁸⁾ and NAVSHIPS Specification No. 0900-006-9010⁽⁹⁾ (P: passed; F: failed).

** Microswitch did not shut off fatigue machine.

*** Weld originally contained surface crack, 1-1/4" long; area was repaired by grinding to sound metal and rewelding.

† Visual inspection rating.

TABLE 3.4

RESULTS OF DEFECT EXAMINATION AND FATIGUE TESTS OF HY-130(T)
TRANSVERSE BUTT WELDS WITH REINFORCEMENT REMOVED

Specimen Number	Welding Procedure* (See Figs. 3.2, 3.3 & 3.4)	Radiographic Examination			Stress Cycle (ksi)	Life (cycles)	Location of Failure
		Defect Description	Defective Area (percent)	Rating			
ND-9	P130(T)-USS-A	Sound Weld	None	P	0 to +80.0	170,000	In weld metal
ND-6	P130(T)-USS-A ⁽¹⁾	Sound Weld	None	P	0 to +80.0	95,300	At minute scattered porosity, <0.01" d.
ND-22	P130(T)-USS-A	Sound Weld	None	P	0 to +80.0	69,000	In weld metal
ND-24	P130(T)-USS-A	2 Pores, 0.07", 0.02" d.	0.238	P	0 to +80.0	17,800	At lack of fusion 0.25" long; and at irreg. shaped void, 0.35"x0.06"
ND-13	P130(T)-L140-A	4 Isolated Pores, 0.03" to 0.01" d.	0.66	P	0 to +80.0	110,000	At single pore, 0.03" d.
ND-11	P130(T)-L140-A	Sound Weld	None	P	0 to +80.0	4,300	At intermittent lack of fusion, 1.05" total length
ND-16	P130(T)-M140-A	Crack, 0.20" long \perp weld axis	--	F	0 to +80.0	6,200	At elongated slag deposit, 0.3" long
ND-25	P130(T)-USS-A	6 Isolated pores, 0.02"-0.05" d.	0.15	P	0 to +50.0	651,900	At 3 isolated pores, 0.05", 0.03", 0.02" d.
ND-7	P130(T)-USS-A ⁽²⁾	Single pore, 0.04" d.	0.034	P	0 to +50.0	258,300+	Failed in specimen pull-head
ND-8	P130(T)-USS-A ⁽²⁾	Lack of fusion, 0.38" long	--	F	0 to +50.0	59,500	At lack of fusion, 0.97" long
ND-21	P130(T)-USS-A ⁽²⁾	Slag deposits, 0.45"x0.12", 0.1"x0.06"; crack, 0.12" long; & 2 pores 0.04" d.	1.5	F	0 to +50.0	43,800	At large void, 0.35"x0.2"
ND-20	P130(T)-USS-A ⁽²⁾	Lack of penetration, 0.76" long; & irreg. shaped void, 0.24"x0.1"	0.61	F	0 to +50.0	36,000	At lack of penetration, 0.3" long; and at irreg. shaped void, 0.2"x0.1"
ND-12	P130(T)-L140-A ⁽¹⁾	Lack of penetration, 0.4" long; & 2 pores, 0.04", 0.02" d.	0.048	F	0 to +50.0	219,200	At lack of penetration, 0.52" long
ND-28	P130(T)-L140-A	6 Isolated pores, 0.02"-0.05" d.	0.18	P	0 to +50.0	72,300	At intermittent lack of fusion, 0.5" total length
ND-10	P130(T)-L140-A ⁽²⁾	Intermittent lack of fusion, 0.3" long; & 2 pores, 0.04" d.	0.072	P	0 to +50.0	27,500	At intermittent lack of fusion, 0.65" total length
ND-18	P130(T)-M140-A ⁽²⁾	Crack, 0.4" long \perp weld axis; & slag deposit 0.35"x0.15"	1.23	F	0 to +50.0	83,800	At slag deposit, 0.55" long
ND-17	P130(T)-M140-A ⁽¹⁾	2 cracks, 0.35", 0.3" \perp weld axis; & elongated slag, 0.95" long	--	F	0 to +50.0	71,300	At 2 cracks \perp weld axis; secondary crack at slag deposit
ND-19	P130(T)-M140-A ⁽²⁾	Crack, 0.3" long \perp weld axis; & slag deposit, 0.4"x0.15"	1.45	F	0 to +50.0	52,000	At slag deposit, 0.7" long
ND-14	P130(T)-M140-A ⁽²⁾	Porosity, pores 0.02"-0.04" d.	0.22	P	0 to +50.0	33,500	At porosity cluster, 0.38% area reduction
ND-15	P130(T)-M140-A ⁽²⁾	Porosity, pores 0.01"-0.10" d.	0.94	F	0 to +50.0	32,400	At porosity cluster, 0.92% area reduction
NC-22	P150-AX140-D	Porosity, pores 0.01"-0.08" d.	1.78	F	0 to +80.0	9,500	At isolated pores, 0.02", 0.04", 0.045", 0.05" d.
NC-21	P150-AX140-D	Lack of fusion, 0.5" long; & single pore, 0.07" d.	0.21	F	0 to +80.0	3,900	At lack of fusion, 0.9" long
NC-17	P150-AX140-D ⁽³⁾	Porosity, pores 0.02"-0.04" d.	0.15	P	0 to +50.0	1,406,400+	No failure
NC-23	P150-AX140-D ⁽³⁾	Lack of fusion, 0.6" long; & porosity, pores 0.01"-0.05" d.	0.29	F	0 to +50.0	21,000	In weld metal at linear discontinuity, 3.5" long
NC-20	P150-AX140-D ⁽³⁾	Porosity, pores 0.02"-0.05" d.	0.41	F	0 to +50.0	6,600	In weld metal at linear discontinuity, 2.4" long
NC-19	P150-AX140-D	Porosity, pores 0.01"-0.05" d.	0.75	F	0 to +43.0	2,272,500	At isolated pore, 0.08" d.

* Welding procedures altered slightly to intentionally introduce specific weld defects.

Procedure P150-AX140-D used "first generation" welding wire; properties given in Ref. 2.

(1) Specimen subjected to periodic radiographic examination during cycling, & to ultrasonic inspection before cycling; see Table 3.5.

(2) Specimen subjected to periodic radiographic examination during cycling, & to ultrasonic inspection before cycling and after radiographic indication of fatigue cracking; see Table 3.5.

(3) Specimen subjected to periodic radiographic examination during cycling; see Table 3.5.

TABLE 3.5

RESULTS OF FATIGUE CRACK INITIATION AND PROPAGATION STUDY OF
HY-130(T) TRANSVERSE BUTT WELDS CONTAINING INTENTIONAL WELD DEFECTS

Specimen Number	Welding Procedure*	Stress Cycle (ksi)	Estimated Cycles to Crack Initiation**	Total Life (Cycles)	Percent of Life at Crack Initiation	Defect Description at Site of Crack Initiation
ND-6	P130(T)-USS-A	0 to +80.0	86,000	95,300	90	Minute, scattered porosity
ND-8	P130(T)-USS-A	0 to +50.0	45,000	59,500	76	Lack of fusion, 0.97" long
ND-21	P130(T)-USS-A	0 to +50.0	27,500	43,800	63	Large void, 0.35" x 0.2"
ND-20	P130(T)-USS-A	0 to +50.0	5,000	36,000	14	Lack of penetration, 0.3" long; & irreg. shaped void, 0.2"x0.1"
ND-12	P130(T)-L140-A	0 to +50.0	>175,000	219,200	>80	Lack of penetration, 0.52" long
ND-10	P130(T)-L140-A	0 to +50.0	5,000	27,500	18	Intermittent lack of fusion, 0.65" total length
ND-18	P130(T)-M140-A	0 to +50.0	60,000	83,800	72	Slag deposit, 0.55" long
ND-17	P130(T)-M140-A	0 to +50.0	27,500	71,300	39	Two cracks \perp weld axis; secondary crack at slag
ND-19	P130(T)-M140-A	0 to +50.0	17,500	52,000	34	Slag deposit, 0.7" long
ND-14	P130(T)-M140-A	0 to +50.0	18,500	33,500	55	Porosity cluster
ND-15	P130(T)-M140-A	0 to +50.0	7,000	32,400	22	Porosity cluster
NC-23	P150-AX140-D	0 to +50.0	--	21,000	--	In weld metal at linear discontinuity, 3.5" long
NC-20	P150-AX140-D	0 to +50.0	< 2,300	6,600	<35	In weld metal at linear discontinuity, 2.4" long

* Welding procedures altered slightly to intentionally introduce specific weld defects.

** Estimated as one-half the number of cycles between last radiograph showing no fatigue crack and first radiograph showing crack growth.

TABLE 4.1

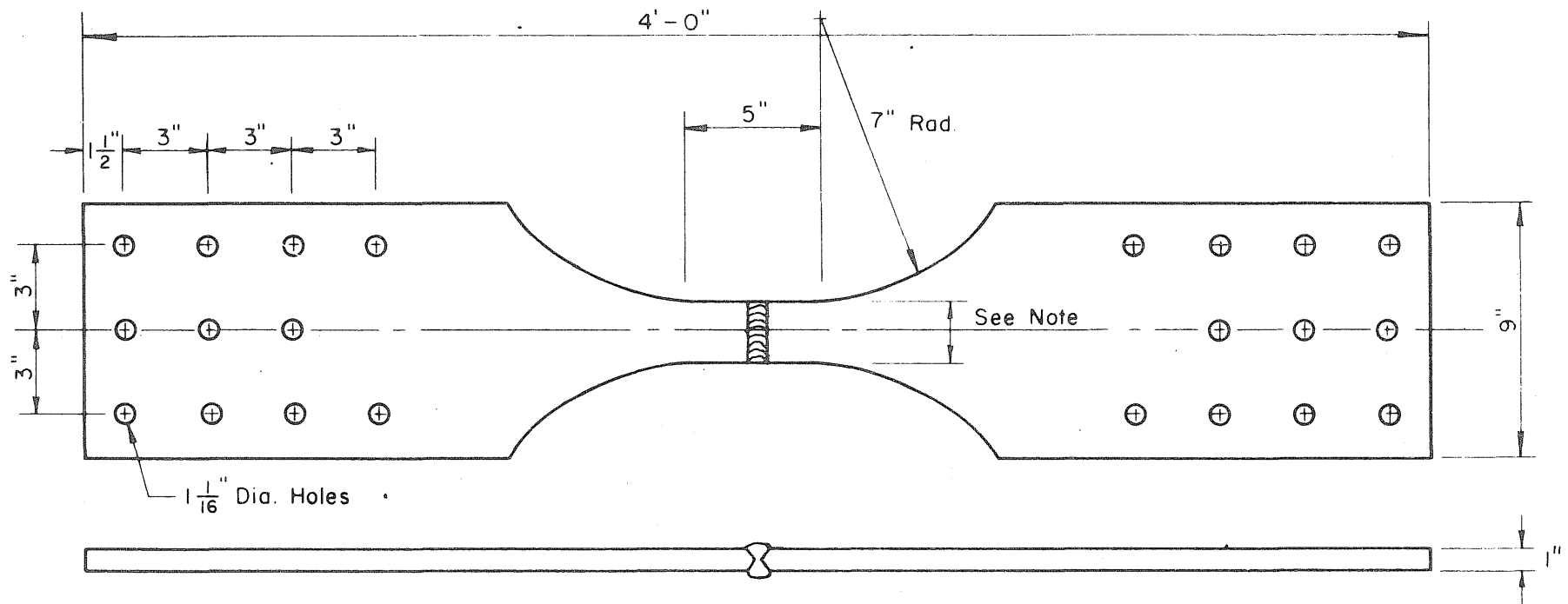
DISTRIBUTION OF FATIGUE LIVES AND CAUSES OF FAILURE

	Type*	No. of Specimens	Percent of Base Metal Life					Arithmetic Mean Life	Cause of Failure,** percent			
			0-10	10-20	20-30	30-40	40-50		Slag/LOF	Toe	Pore	Unknown
All Specimens	AW	26	73.0	23.0	0	0	4.0	8.9	34.6	53.4	4.0	8.0
	RR	23	74.2	0	8.7	4.35	13.05	14.57	52.2	-	26.1	21.7
Passed Radiographic Inspection***	AW	23	88.3	21.7	0	0	0	7.6	34.8	52.0	4.3	8.7
	RR	10	50.0	0	10.0	10.0	30.0	25.0	40.0	-	30.0	30.0
Failed Radiographic Inspection***	AW	3	33.3	33.3	0	0	33.3	21.4	33.3	66.6	0	0
	RR	13	92.4	0	7.6	0	0	6.4	61.5	-	23.0	15.5

* AW = as welded
RR = reinforcement removed

** Source of failures are defined as (a) Slag/LOF: slag inclusion or lack of fusion, (b) Toe: toe of the weld, (c) Pore: porosity in the weld metal, or (d) Unknown: the source or cause of failure is not clearly defined.

*** Based on U. S. Steel Corporation recommendations⁽⁸⁾ and NAVSHIPS Specification No. 0900-006-9010.⁽⁹⁾



Note:

3 1/4" for tests conducted at maximum stress up to 60 ksi

2" for tests conducted at maximum stress = 80 ksi

FIG. 2.1 DETAILS OF FATIGUE TEST SPECIMENS

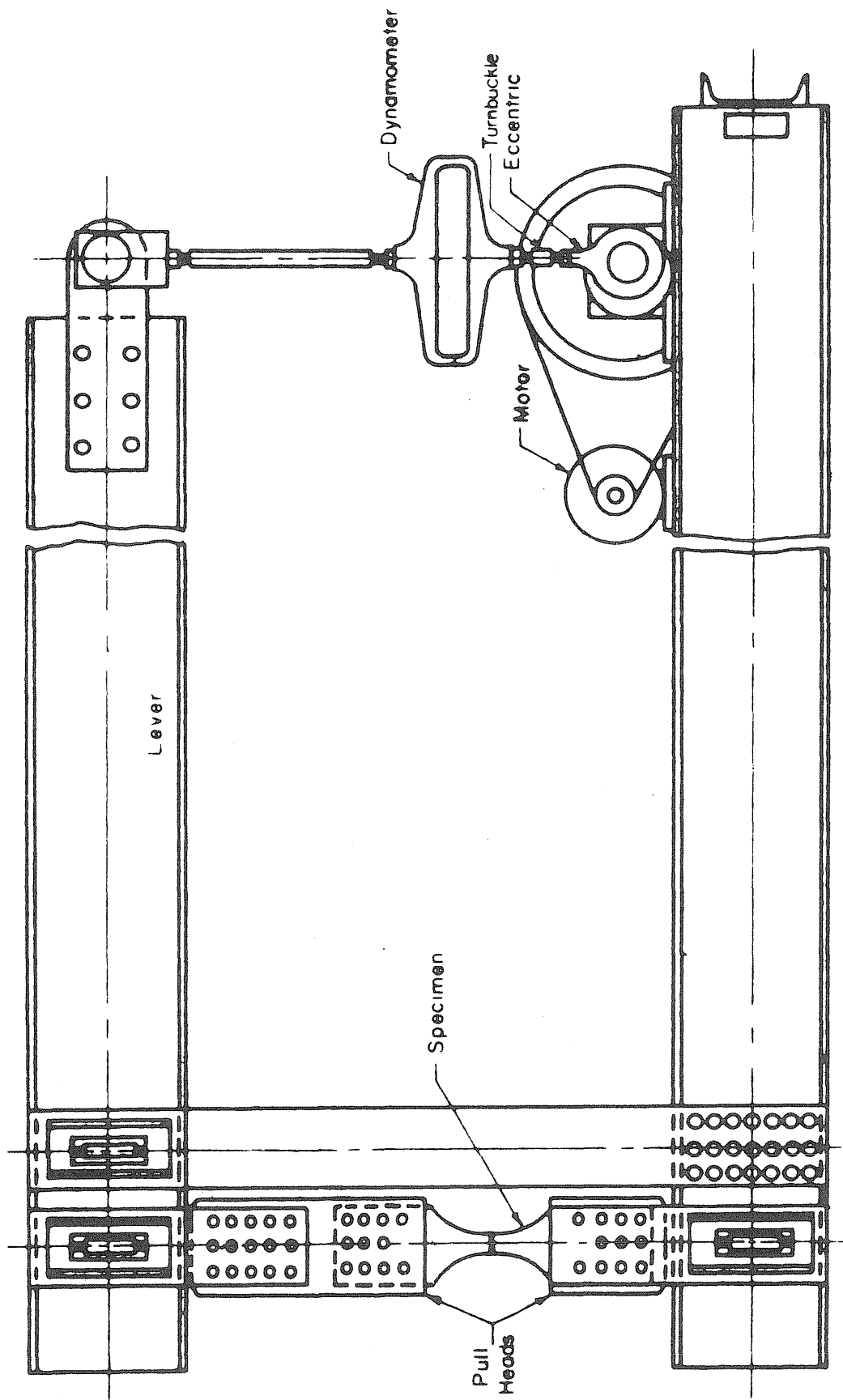
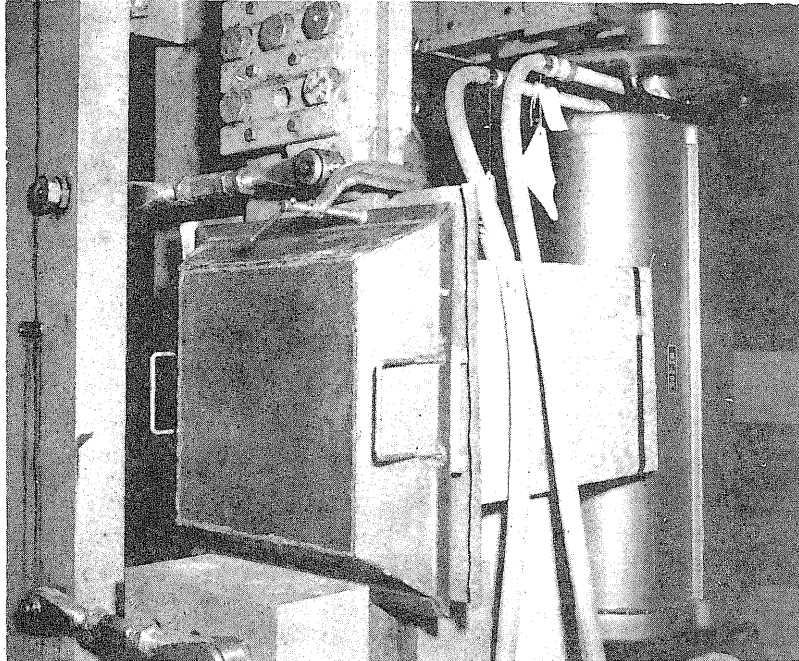
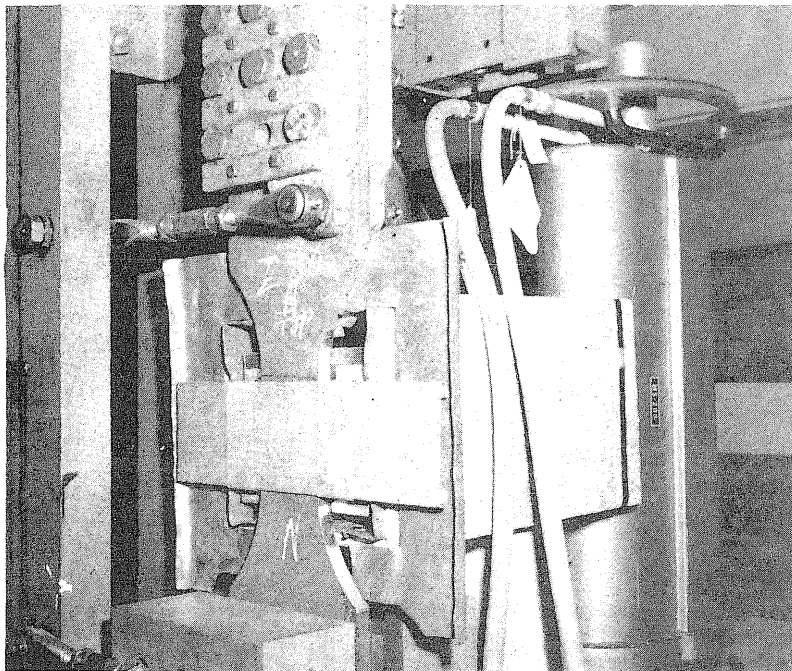


FIG. 2.2 ILLINOIS' FATIGUE TESTING MACHINE AS USED FOR AXIAL LOADING OF WELDED JOINTS

Metz Reference Room
 Civil Engineering Department
 B106 C. E. Building
 University of Illinois
 Urbana, Illinois 61801

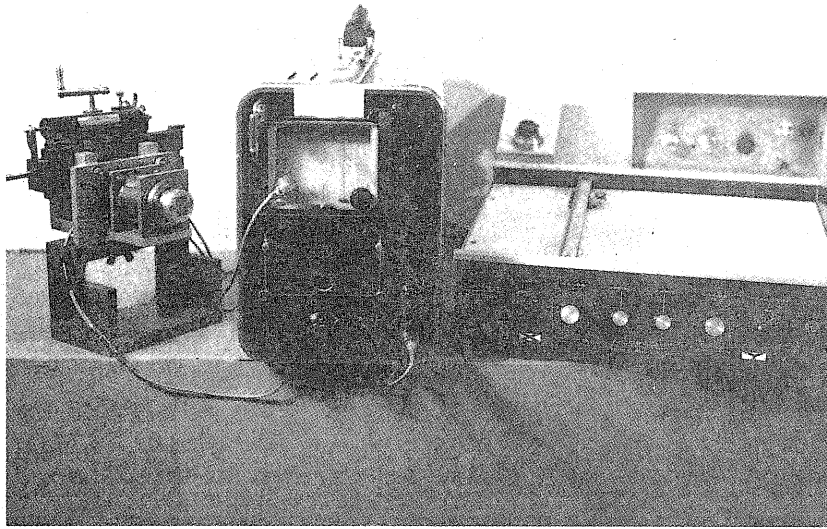


a) EQUIPMENT AND LEAD SHIELD IN POSITION

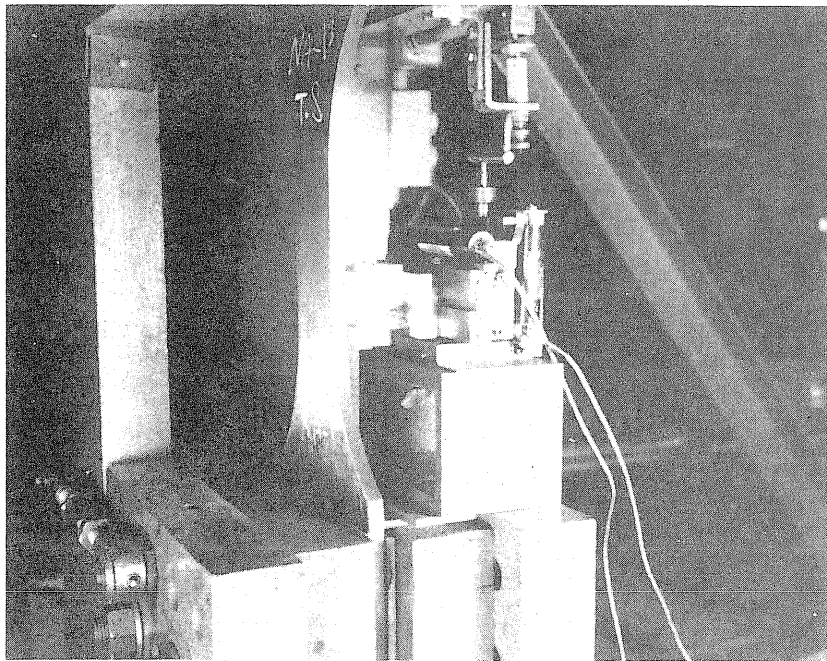


b) SPECIMEN AND X-RAY FILM HOLDER

FIG. 2.3 SETUP FOR RADIOGRAPHIC STUDY OF
CRACK PROPAGATION



a) Probe Support, Detector And X-Y Recorder



b) Unit In Position For Testing

FIG.2.4 ULTRASONIC TESTING EQUIPMENT

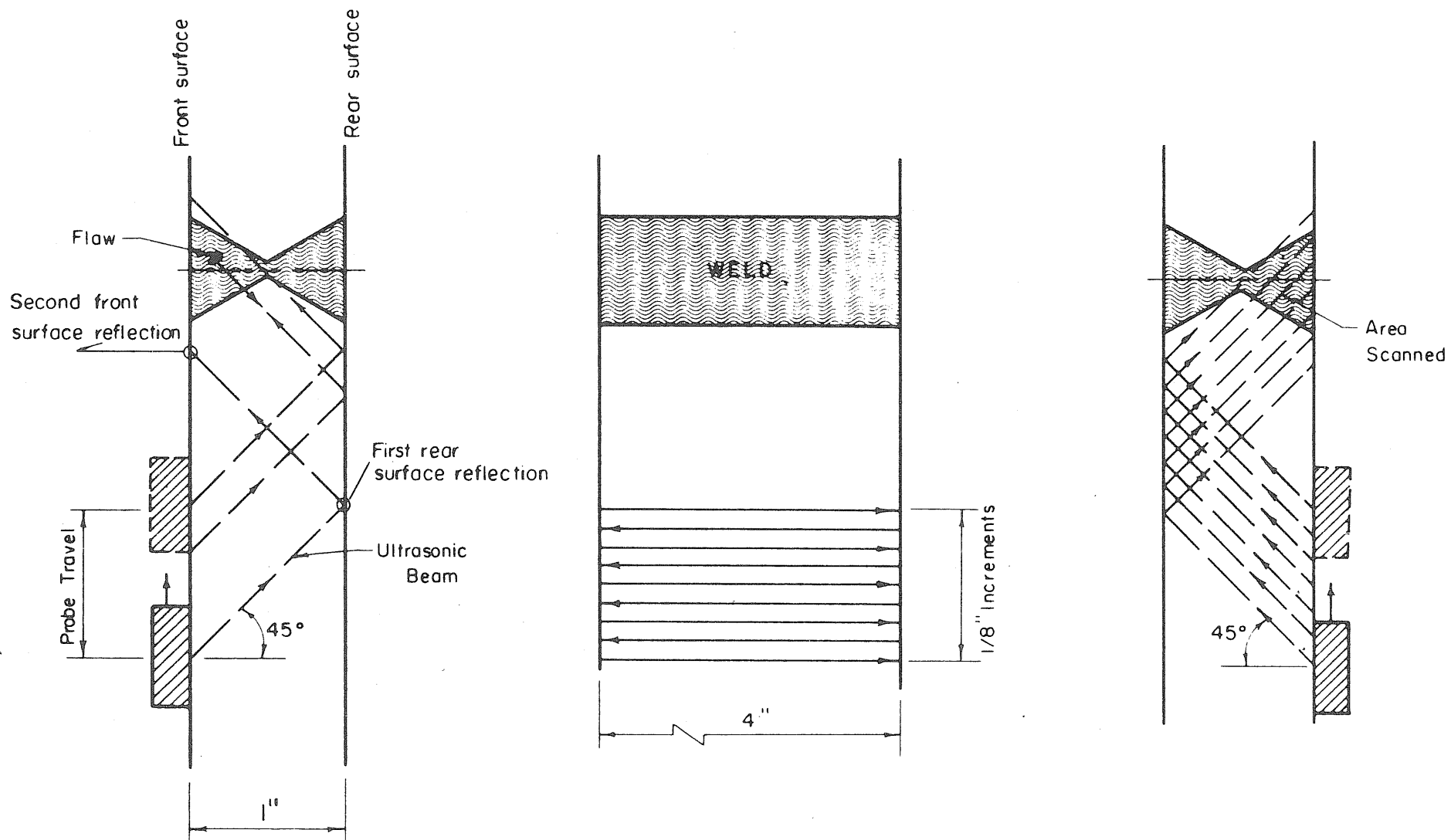


FIG. 2.5 SCANNING PROCEDURE FOR ULTRASONIC EXAMINATION.

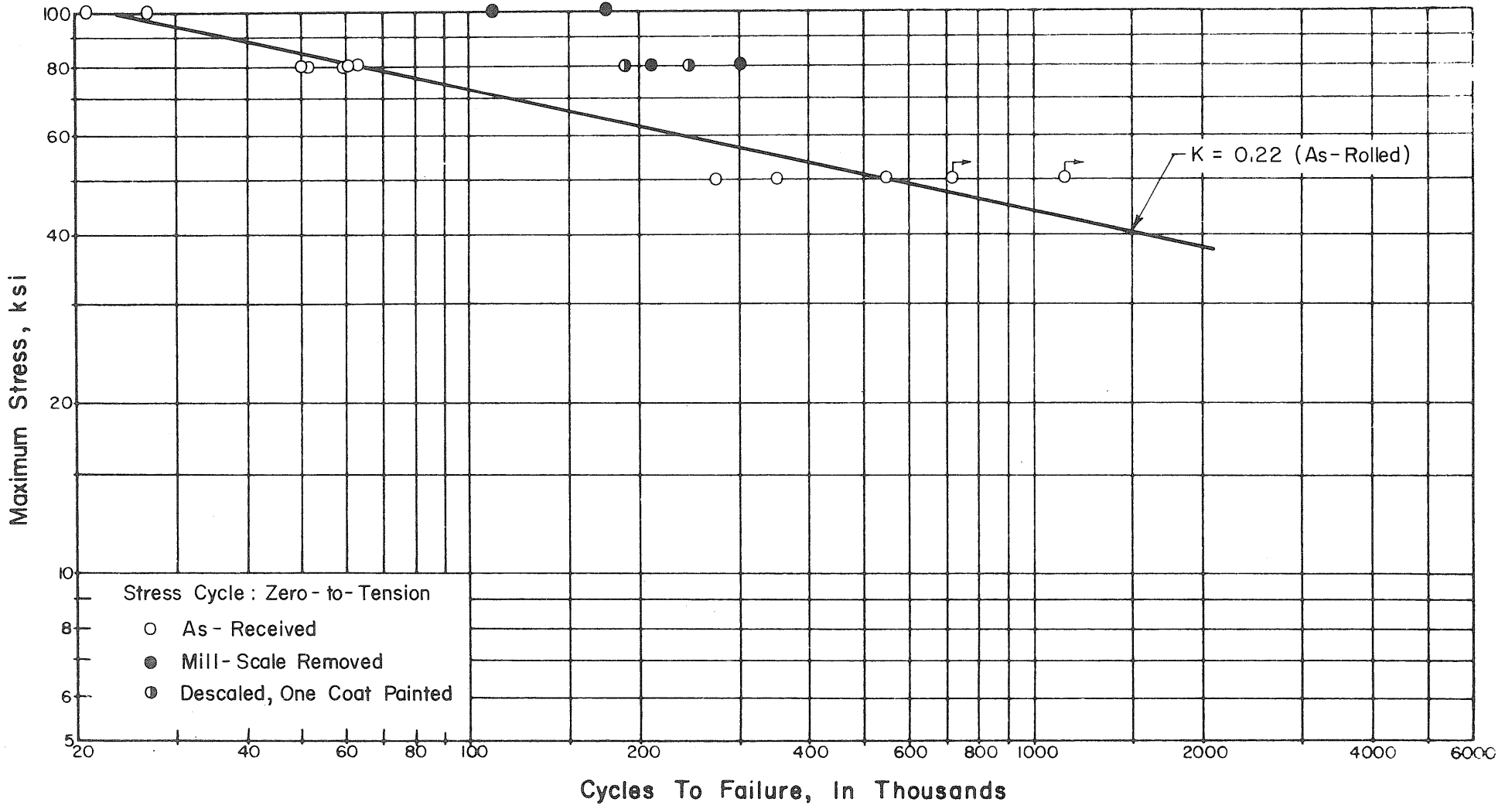
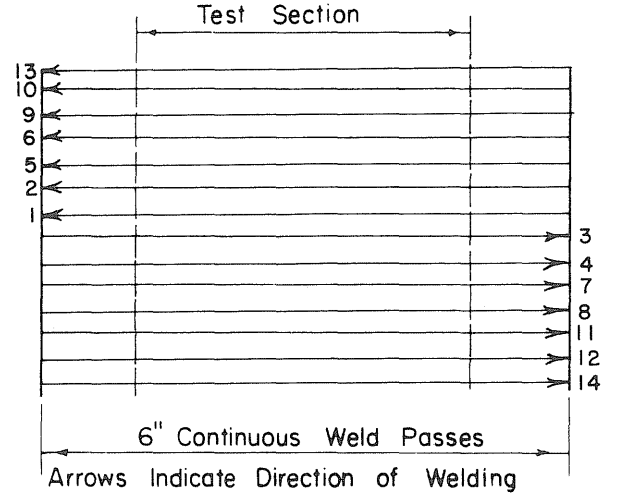
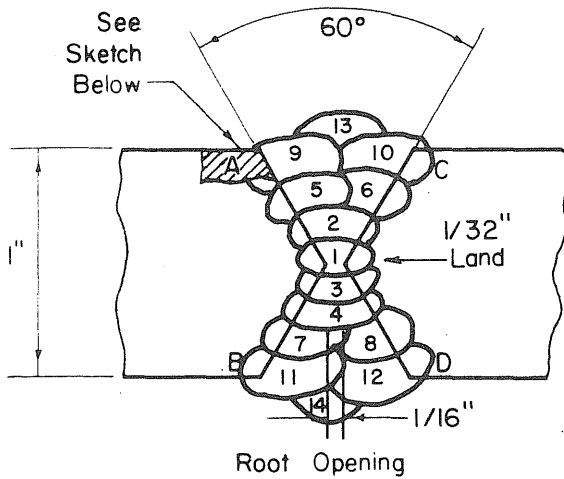


FIG. 3.1 RESULTS OF FATIGUE TESTS OF HY-130 (T) PLAIN PLATE SPECIMENS



Pass	Voltage Volts	Current, amps	Rate of Travel, in./min.
1	28	290	14
2-4	29	320	12.5
5-8	29	315	14
9-14	28	290	14

Welding Wire: USS 5Ni - Cr - Mo

Electrode Size: 1/16"

Polarity: DC Reversed

Preheat Temperature: 200°F

Interpass Temperature: 200°F

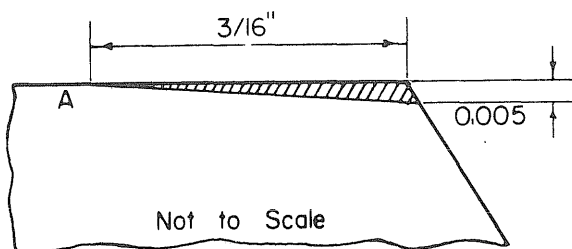
Heat Input: 45,000 joules/in. (Maximum)

All Welding in Flat Position

Underside of Pass 1 Ground With Carbide Wheel After Placing Pass 2

Shielding Gas: 98 % Argon

2 % Oxygen

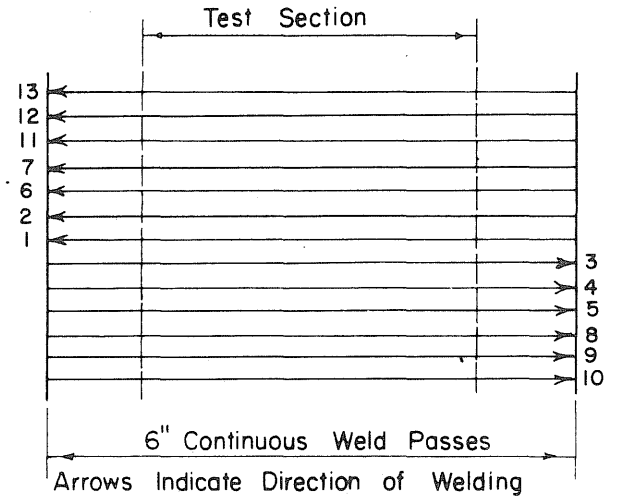
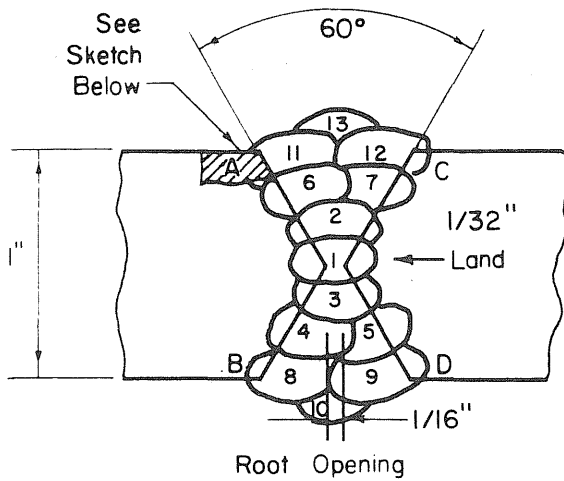


Preparation of Joint Before Welding:

Cross Hatched Area Removed by Milling on Corners A, B, C, D.

Beveled Joint Surfaces Filed and Cleaned With Acetone

FIG. 3.2 WELDING PROCEDURE PI30(T) - USS-A



Pass	Voltage Volts	Current, amps	Rate of Travel, in./min.
1	27.5	285	13
2	29	320	13
3	29	325	13
4, 5	29	330	13.5
6-13	29	320	13.5

Welding Wire : Linde 140

Electrode Size: 1/16"

Polarity: DC Reversed

Preheat Temperature: 225°F

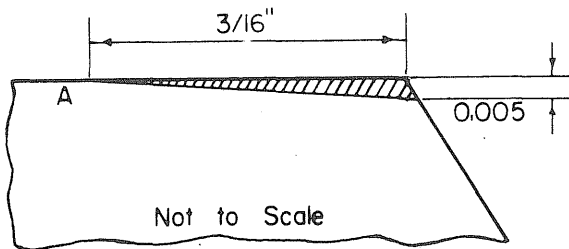
Interpass Temperature: 225°F

Heat Input: 45,000 joules/in. (Maximum)

All Welding in Flat Position

Underside of Pass 1 Ground With Carbide Wheel After Placing Pass 2

Shielding Gas: 98 % Argon
2 % Oxygen

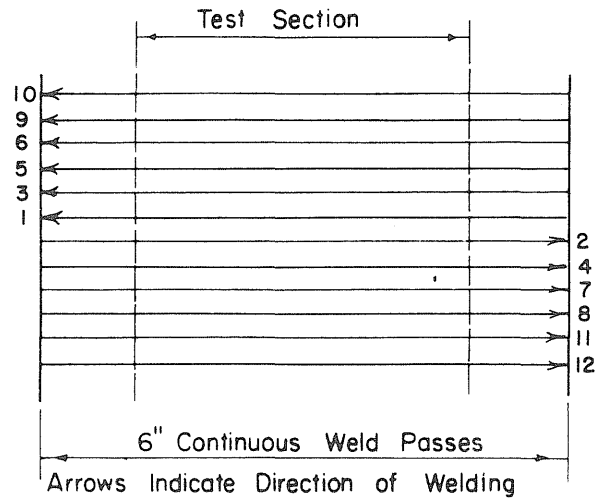
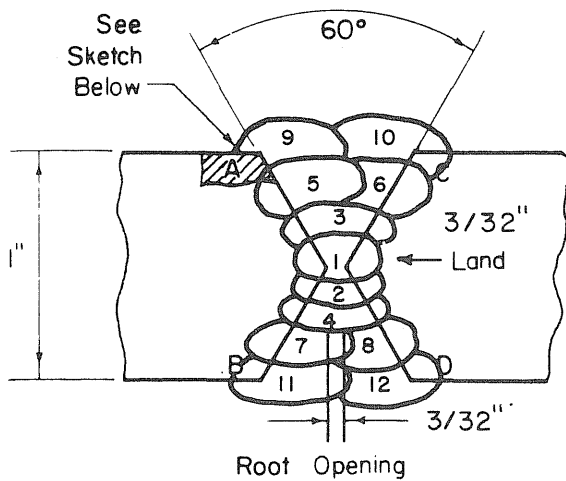


Preparation of Joint Before Welding:

Cross Hatched Area Removed by Milling on Corners A, B, C, D.

Beveled Joint Surfaces Filed and Cleaned With Acetone

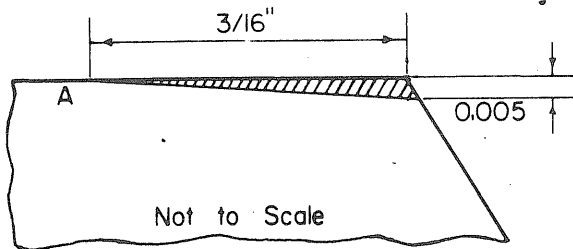
FIG. 3.3 WELDING PROCEDURE PI30(T)-L140-A



Pass	Electrode Size, in.	Current, amps	Rate of Travel, in./min.
1	5/32	150	6
2	5/32	170	6
3	3/16	200	7.5
4-12	3/16	210	8

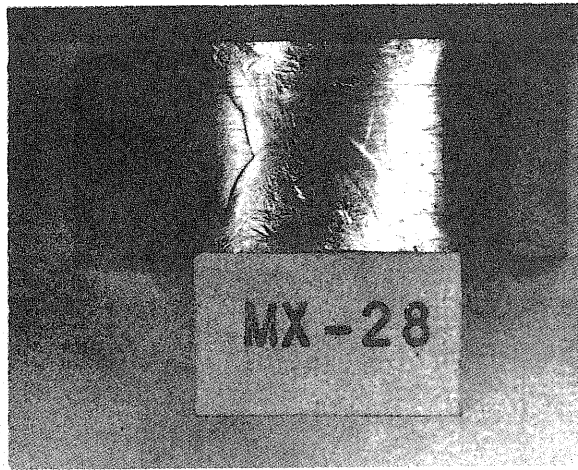
Welding Wire : Mc Kay 14018

Voltage: 22 Volts
Polarity: DC Reversed
Preheat Temperature: 200°F
Interpass Temperature: 200°F
Heat Input: 37,500 joules/in. (Maximum)
All Welding in Flat Position
Underside of Pass 1 Ground With Carbide Wheel Before Placing Pass 2

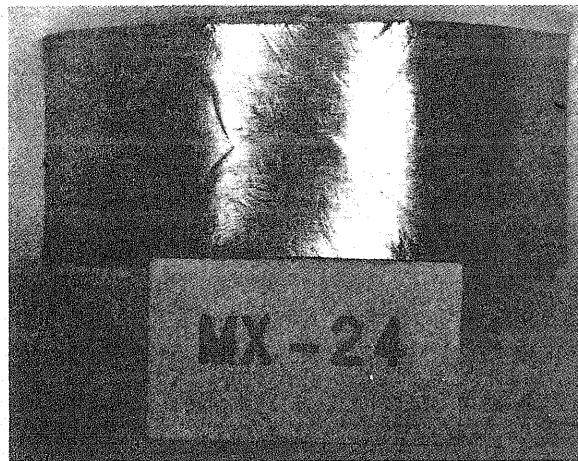


Preparation of Joint Before Welding:
Cross Hatched Area Removed by Milling on Corners A,B,C,D.
Beveled Joint Surfaces Filed and Cleaned With Acetone

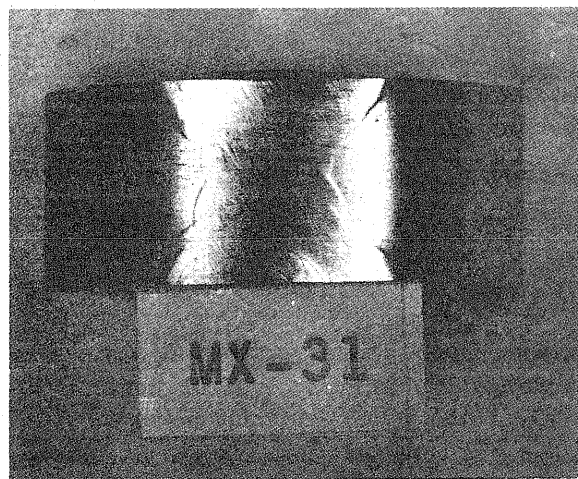
FIG. 3.4 WELDING PROCEDURE P130(T)-M140-A



(a) Welding Procedure P130(T)-USS-A

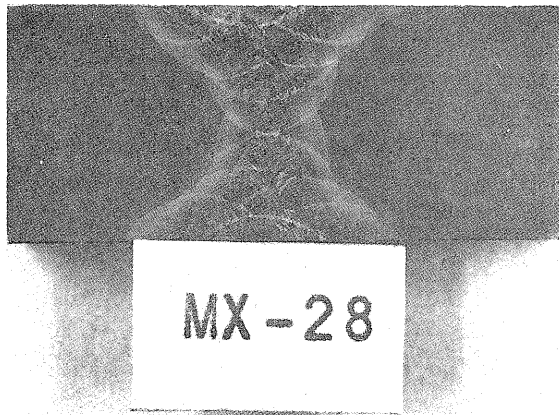


(b) Welding Procedure P130(T)-L140-A

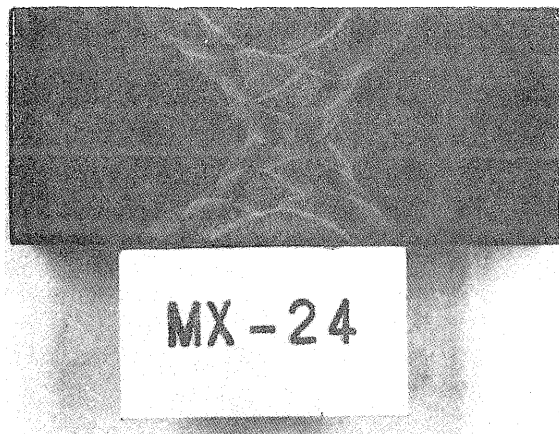


(c) Welding Procedure P130(T)-M140-A

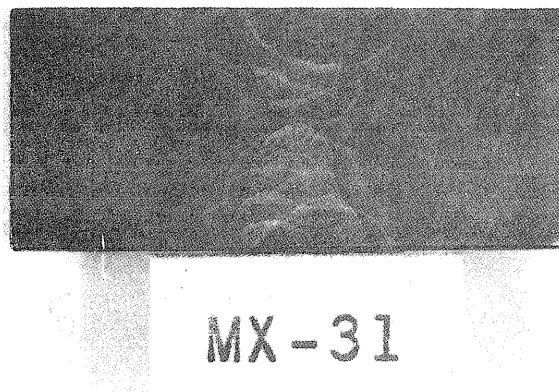
FIG. 3.5 SIDE BEND TEST SPECIMENS OF WELDMENTS IN
1 in. THICK HY-130 (T) PLATES



(a) Welding Procedure P 130 (T)-USS-A

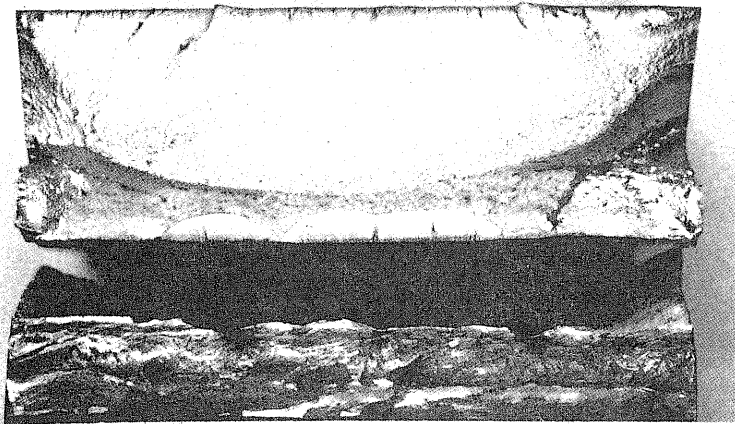


(b) Welding Procedure P 130 (T)-L 140-A



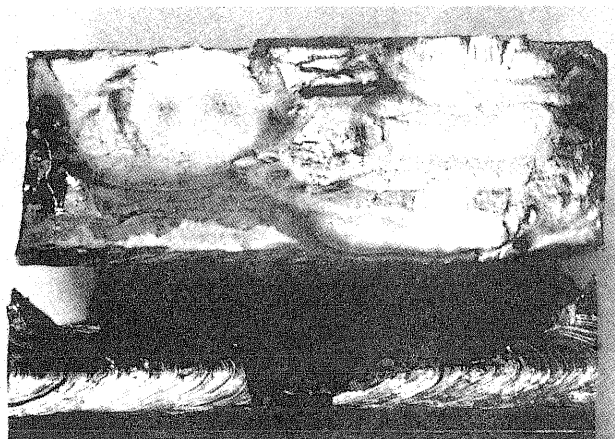
(c) Welding Procedure P 130 (T)-M 140-A

FIG. 3.6 MACRO-STRUCTURE OF WELDMENTS IN 1in. THICK HY-130 (T) PLATES.



NC-41 FRACTURE
Stress 0 to +80.0 ksi
Life 68,200

(a) Failure Initiated at Toe of Weld



ND-4 FRACTURE
Stress 0 to +80.0 ksi
Life 57,500

(b) Failure Initiated at Internal Defect

FIG. 3.7 TYPICAL FRACTURE SURFACES OF HY-130 (T) TRANSVERSE BUTT WELDS IN AS-WELDED CONDITION

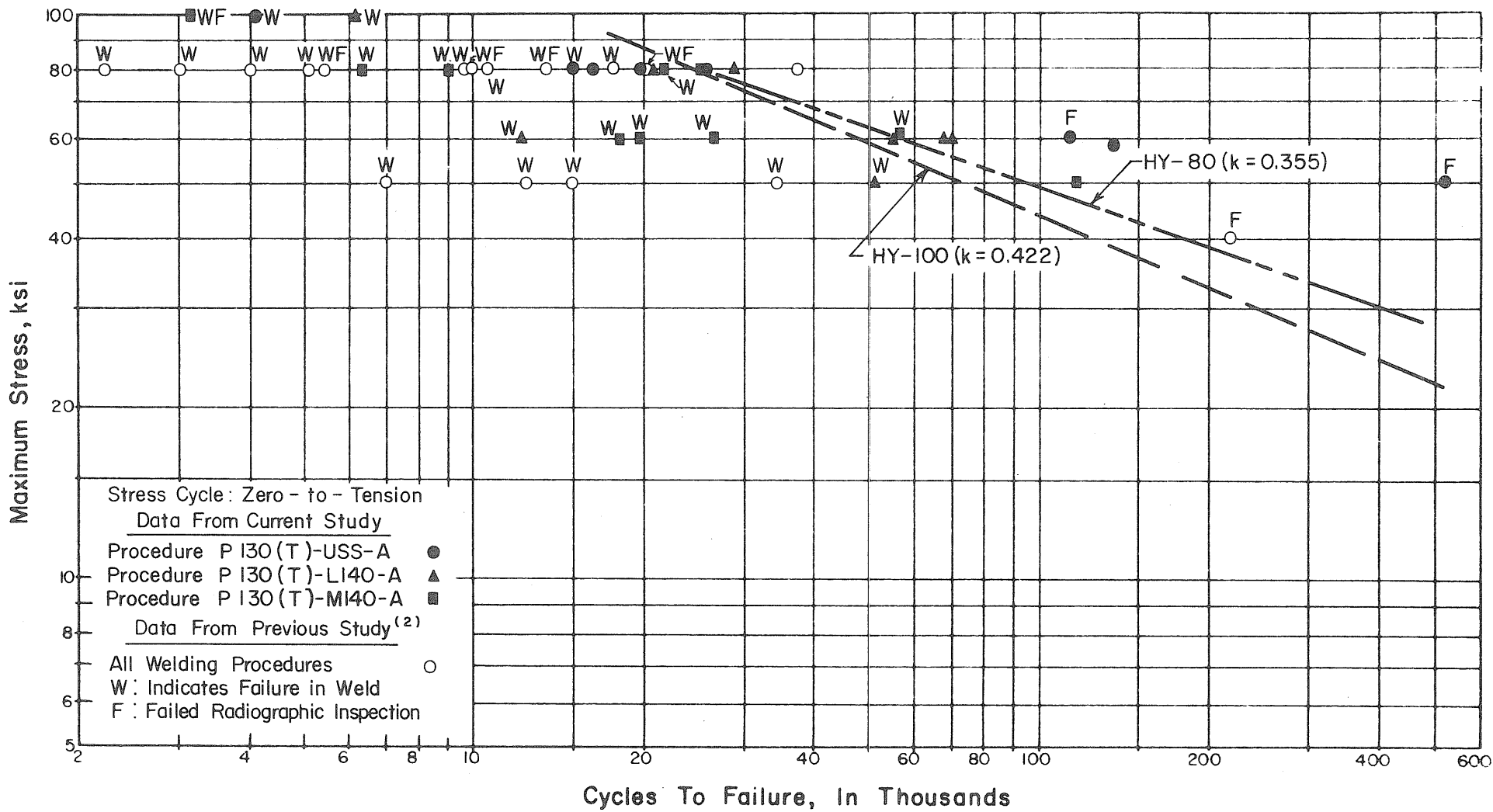


FIG. 3.8 COMPARISON OF FATIGUE TEST RESULTS OF AS-WELDED BUTT JOINTS FROM CURRENT STUDY WITH DATA FROM PREVIOUS INVESTIGATION

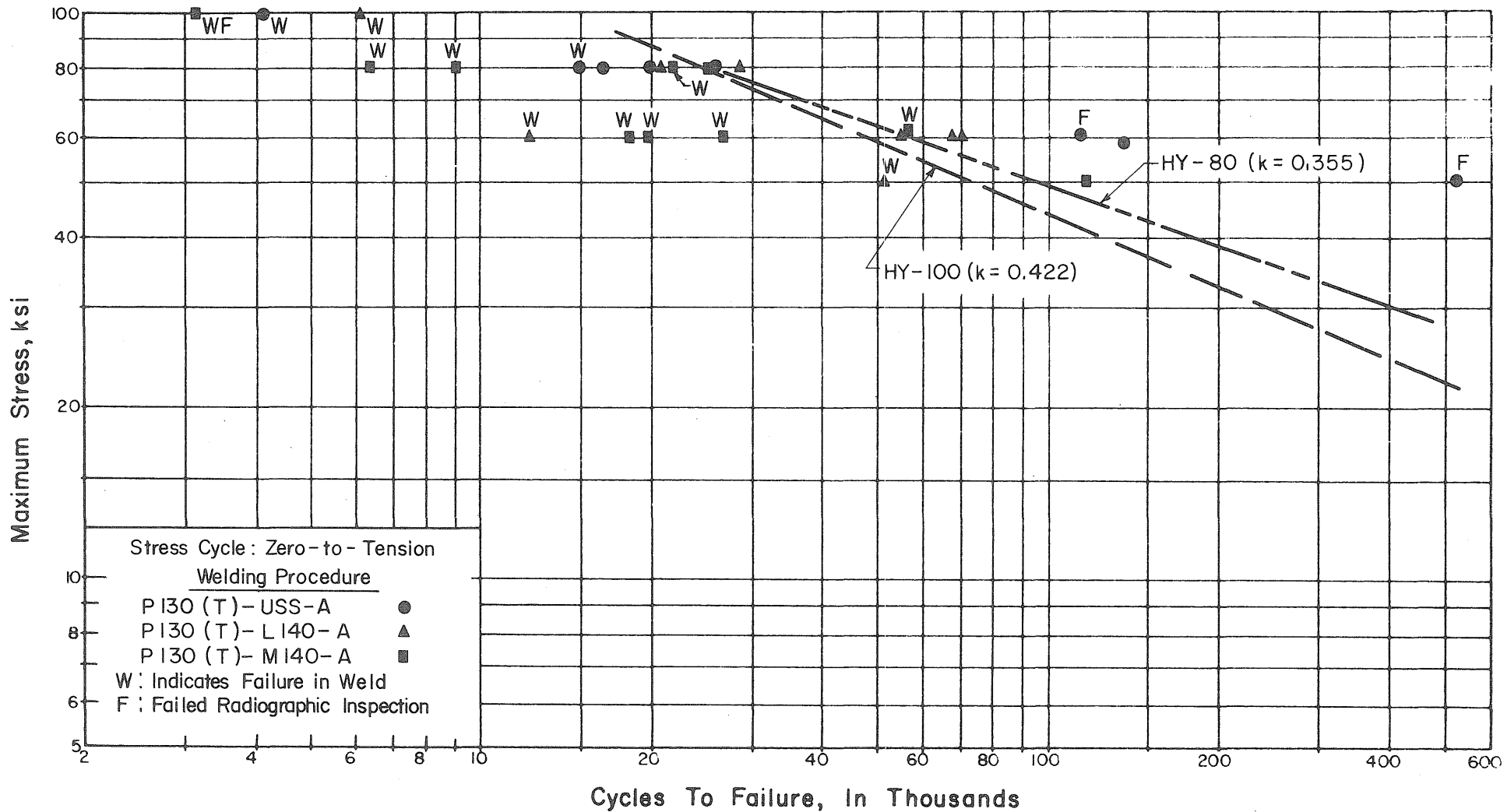


FIG. 3.9 RESULTS OF FATIGUE TESTS OF AS-WELDED HY-130 (T) TRANSVERSE BUTT JOINTS

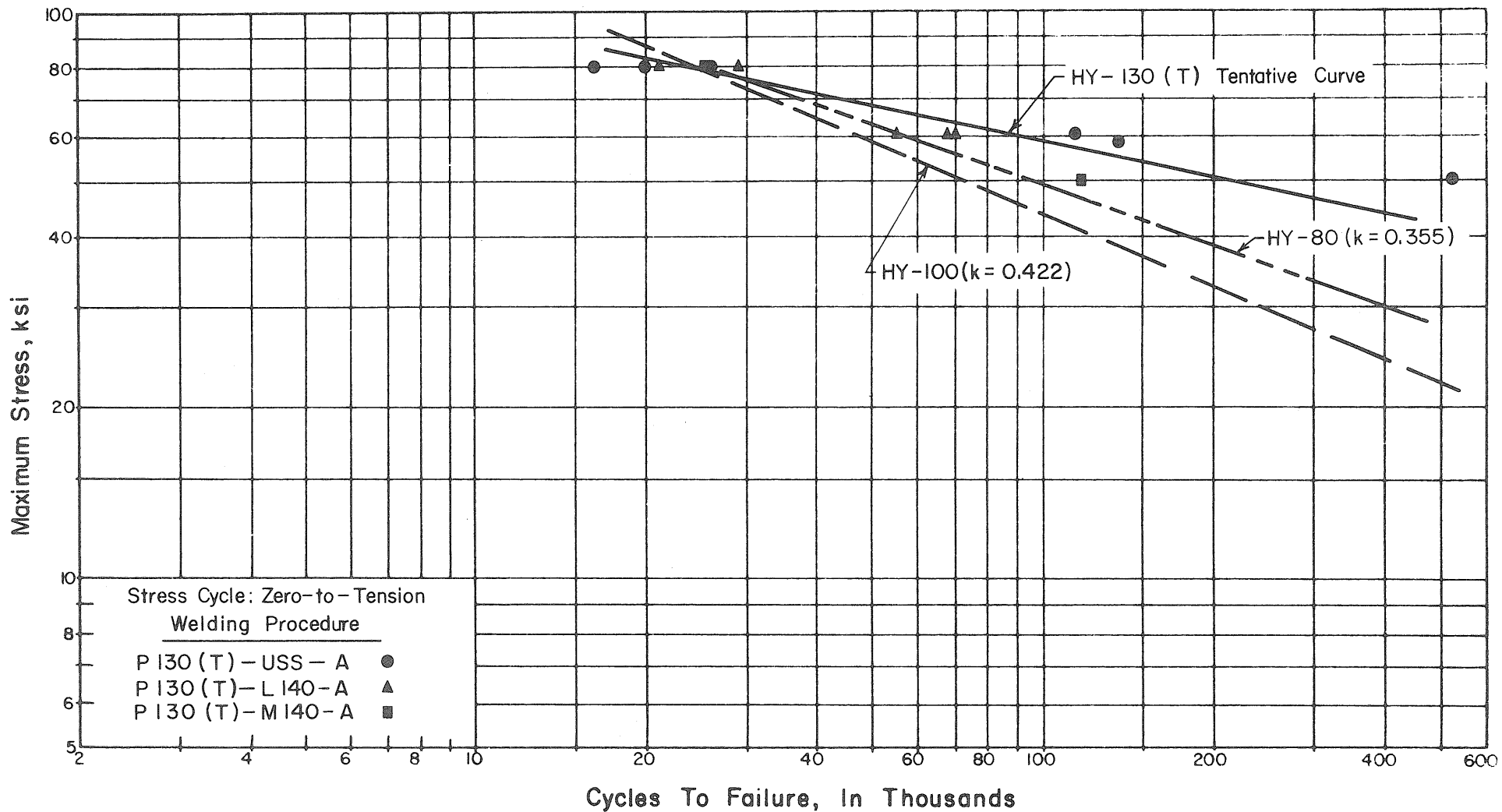


FIG. 3.10 RESULTS OF FATIGUE TESTS OF AS-WELDED HY-130 (T) TRANSVERSE BUTT JOINTS INITIATING FAILURE AT TOE OF WELD

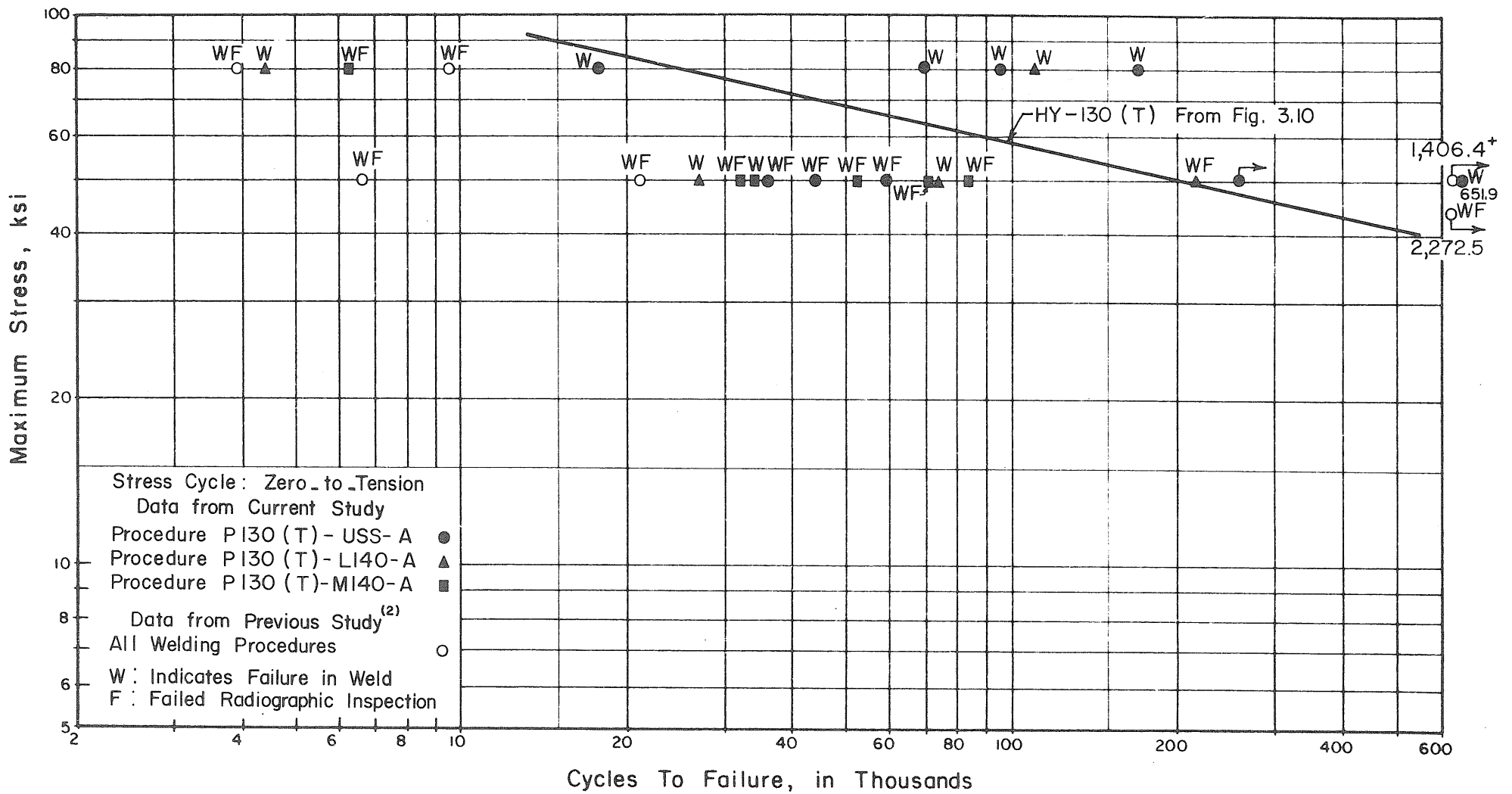
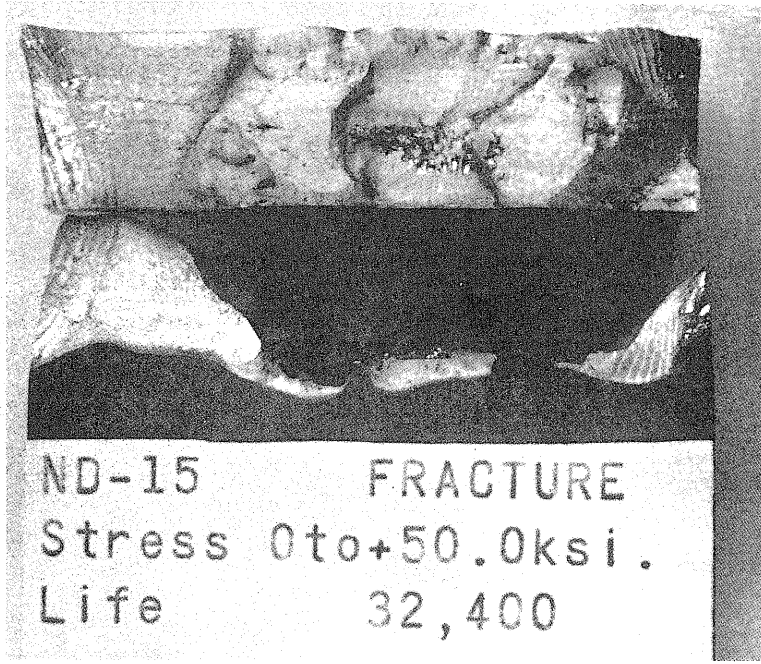
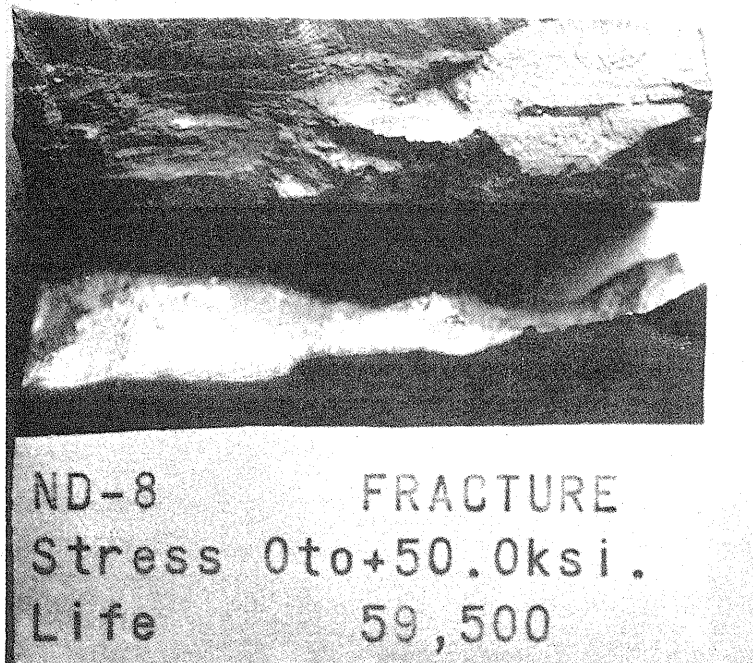


FIG. 3.11 RESULTS OF FATIGUE TESTS OF HY-130 (T) TRANSVERSE BUTT-WELDED SPECIMENS WITH REINFORCEMENT REMOVED

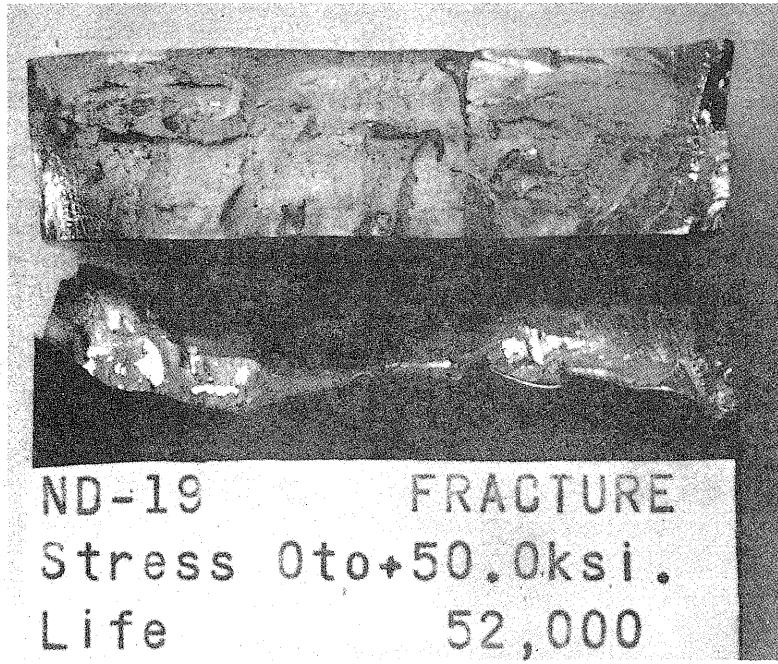


(a) Failure Initiated at Porosity

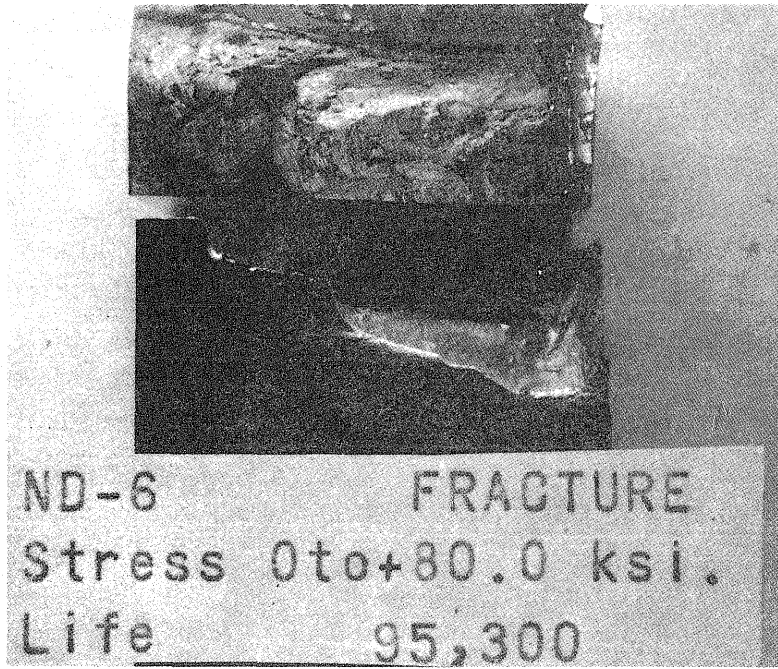


(b) Failure Initiated at Lack of Fusion

FIG. 3.12 TYPICAL FRACTURE SURFACES OF HY-130 (T) TRANSVERSE BUTT WELDS WITH REINFORCEMENT REMOVED



(c) Failure Initiated at Slag



(d) Failure Initiated "In Weld Metal"

FIG. 3.12 (CON'T.)

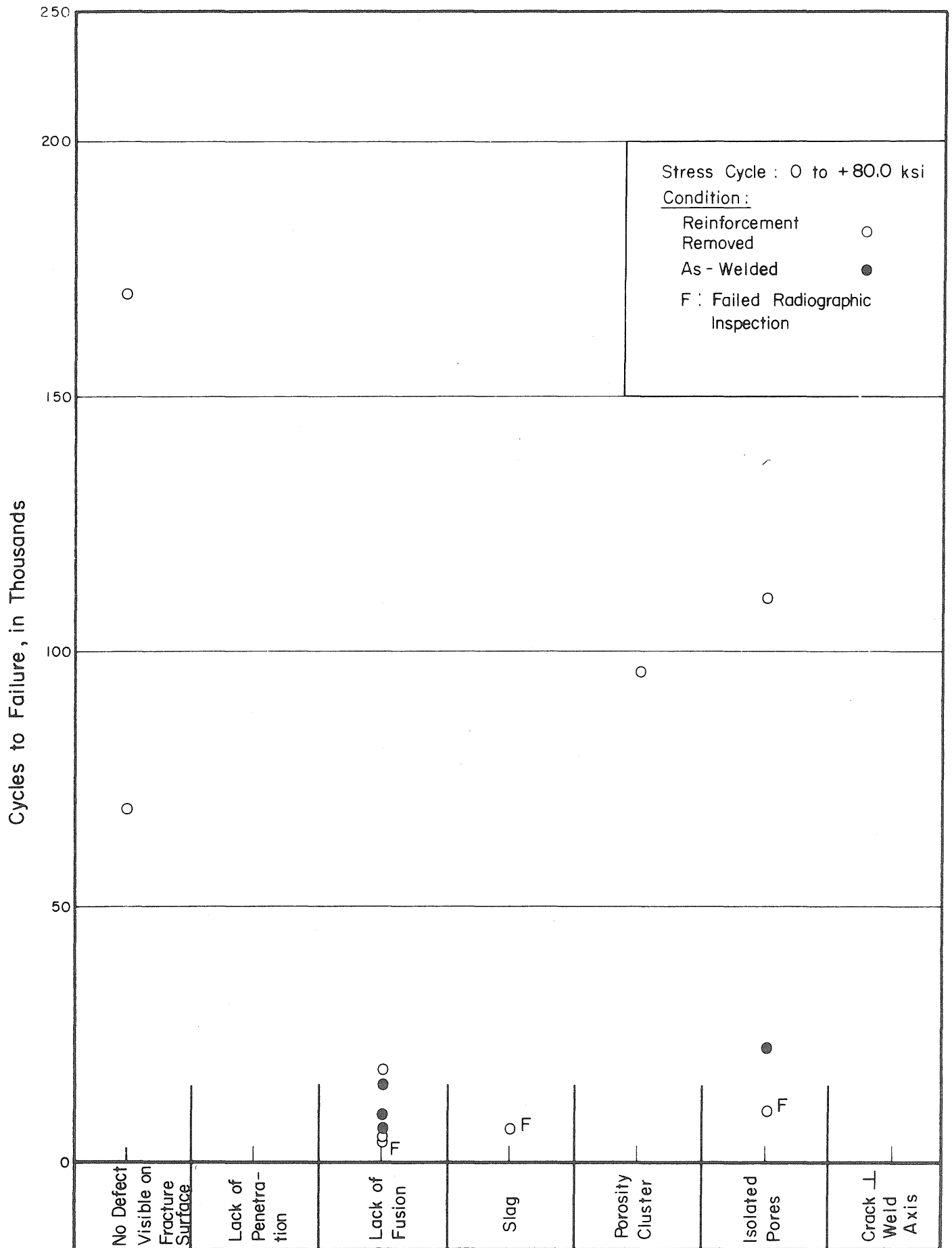


FIG. 3.13 EFFECT OF VARIOUS WELD DEFECTS ON FATIGUE OF HY-130 (T) TRANSVERSE BUTT WELDS (STRESS CYCLE : 0 TO +80 ksi)

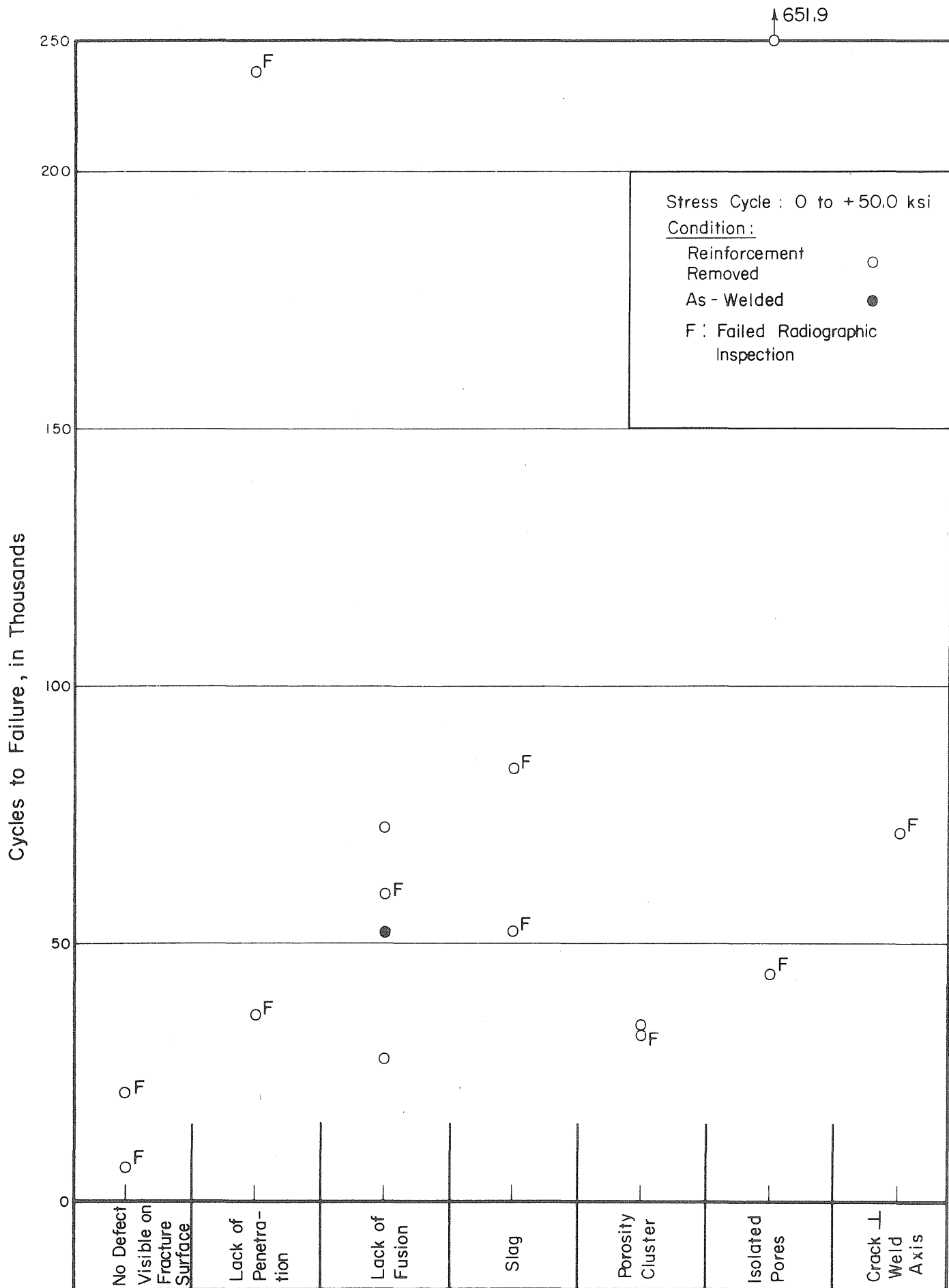


FIG. 3.14 EFFECT OF VARIOUS WELD DEFECTS ON FATIGUE OF HY-130 (T) TRANSVERSE BUTT WELDS (STRESS CYCLE : 0 TO + 50 ksi)

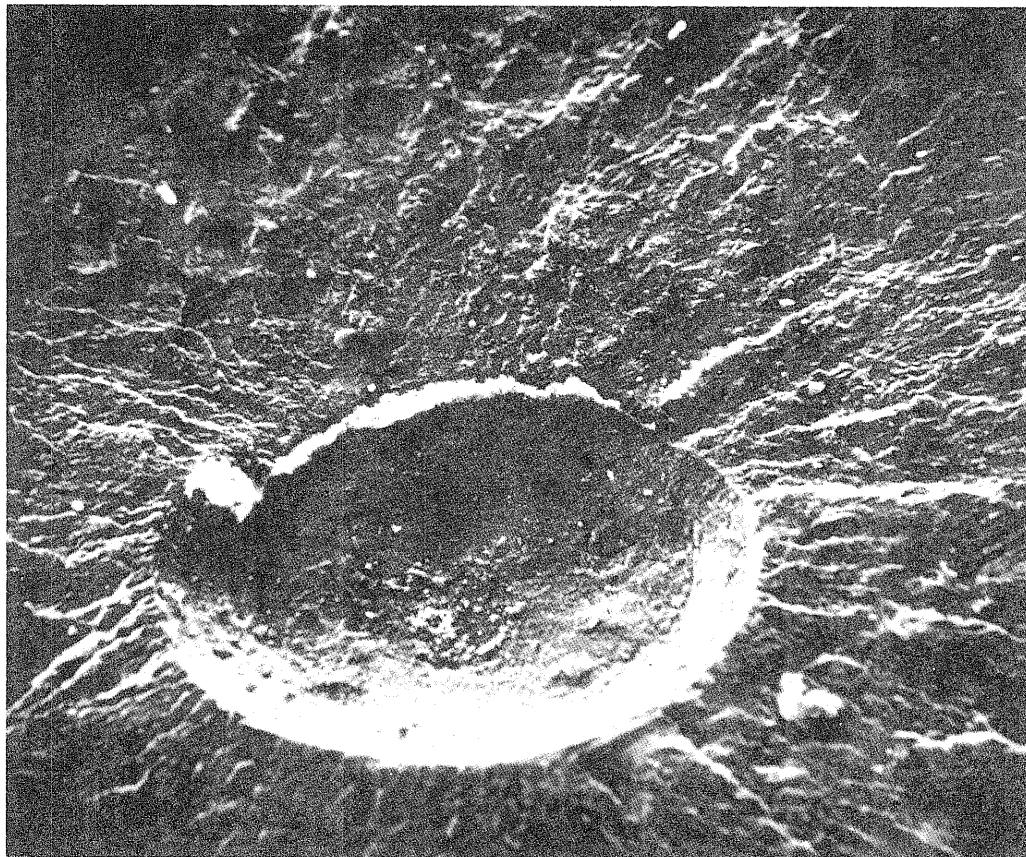
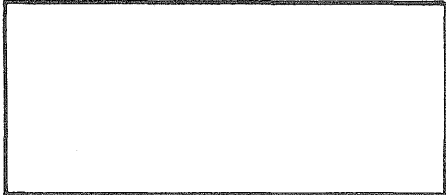
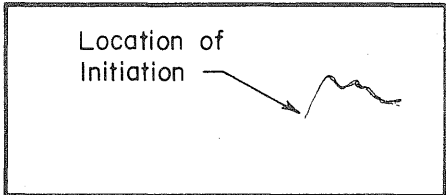


FIG. 3.15 SCANNING ELECTRON MICROSCOPE IMAGE OF PORE INITIATING FATIGUE CRACK IN SPECIMEN ND-30

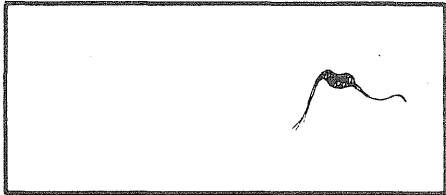
Number of Cycles



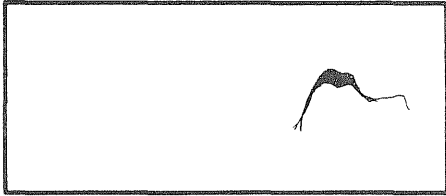
N = 0 to 80,000



N = 92,000



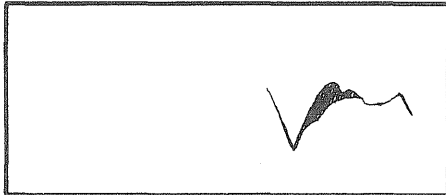
N = 92,500



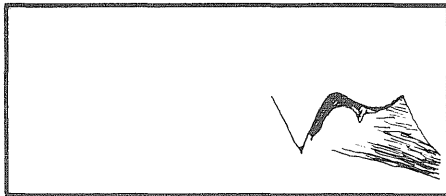
N = 93,000



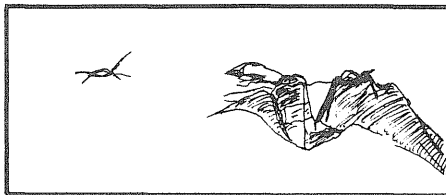
N = 93,300 (Fatigue Crack Visible on Specimen Surface)



N = 93,900



N = 94,400



N = 95,230 (Fatigue Crack Through Plate Thickness)

FIG.3.16 TRACINGS OF RADIOGRAPHS TAKEN DURING FATIGUE TEST OF SPECIMEN ND-6

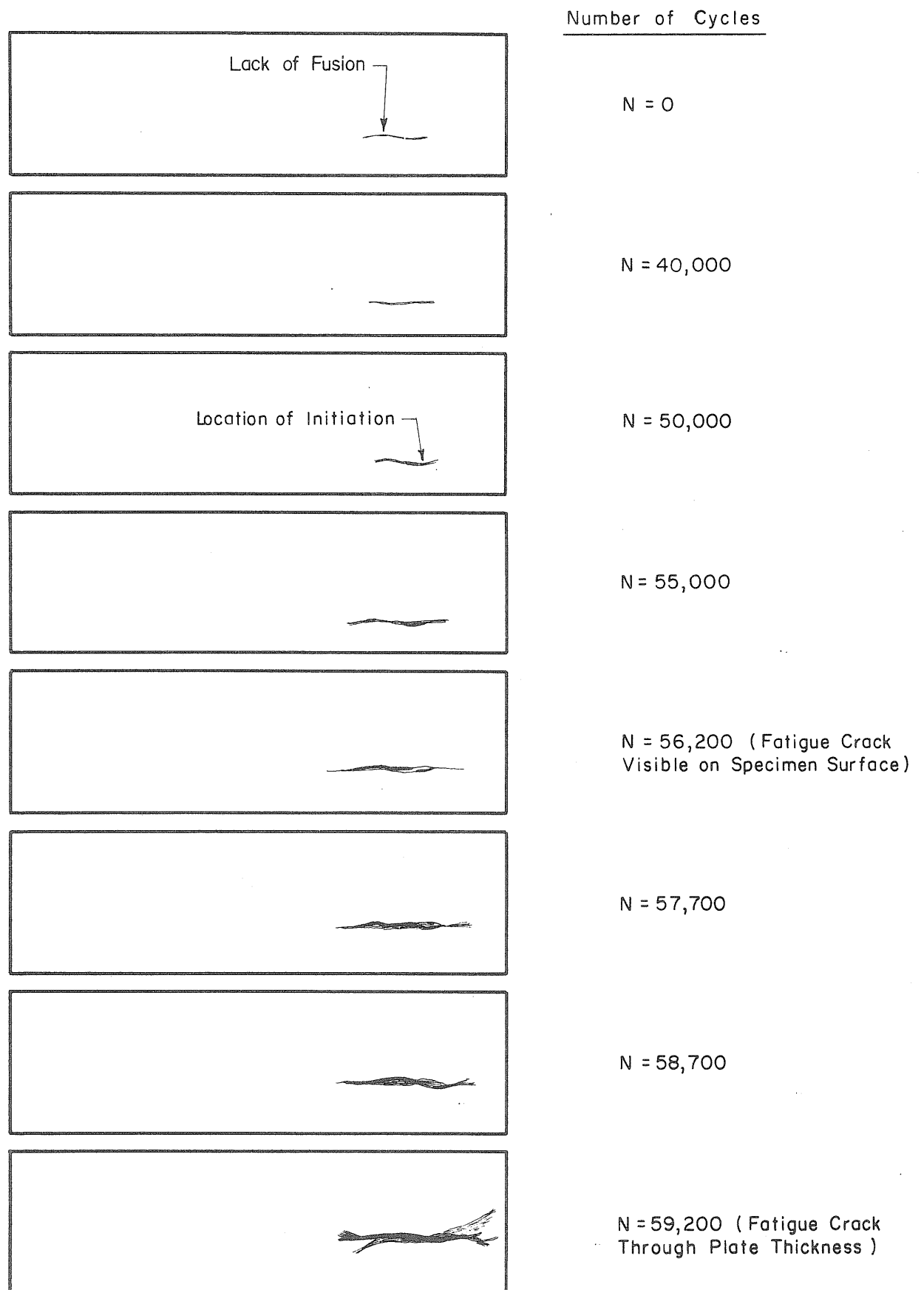
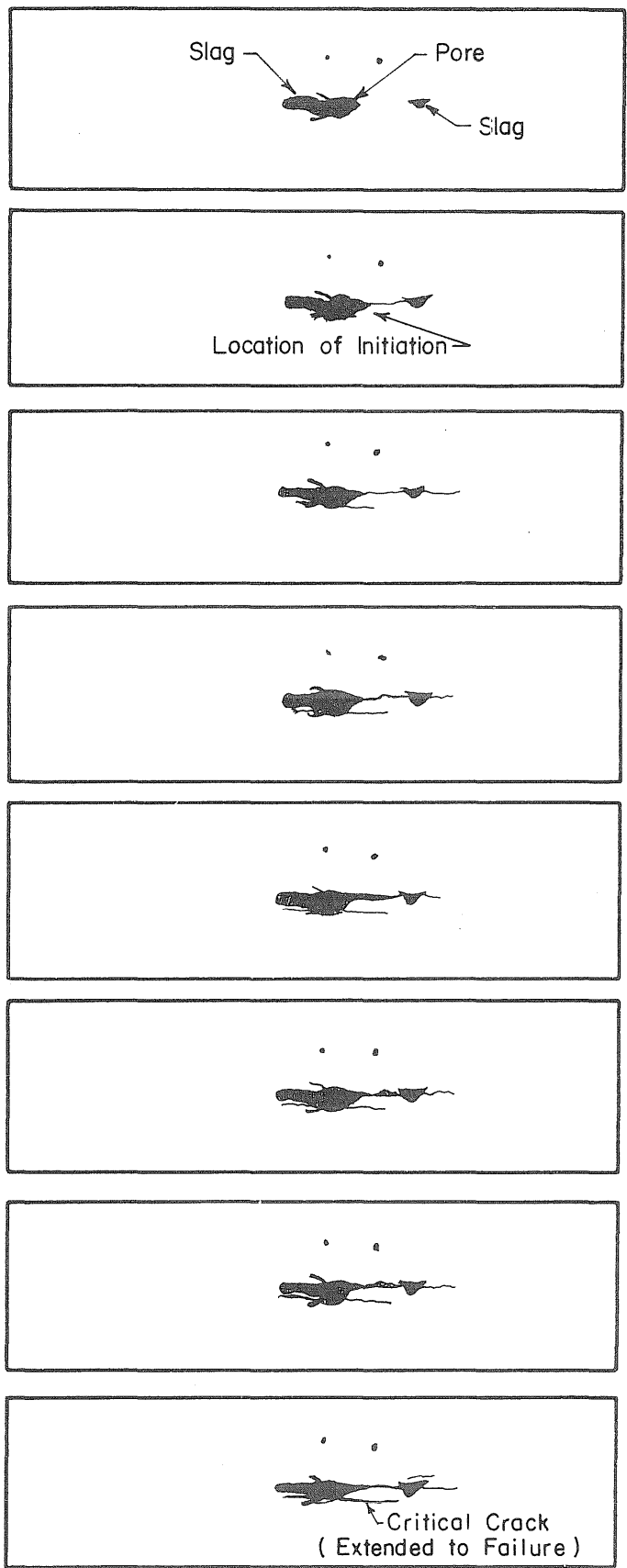


FIG. 3.17 TRACINGS OF RADIOGRAPHS TAKEN DURING FATIGUE TEST OF SPECIMEN ND-8



Number of Cycles

N = 0 to 25,000

N = 30,000

N = 31,000

N = 32,000 (Fatigue Crack
Visible on Specimen
Surface)

N = 33,000

N = 34,000

N = 36,000

N = 37,000 (Fatigue Crack
Through Plate Thickness)

FIG. 3.18 TRACINGS OF RADIOGRAPHS TAKEN DURING FATIGUE TEST OF SPECIMEN ND-21

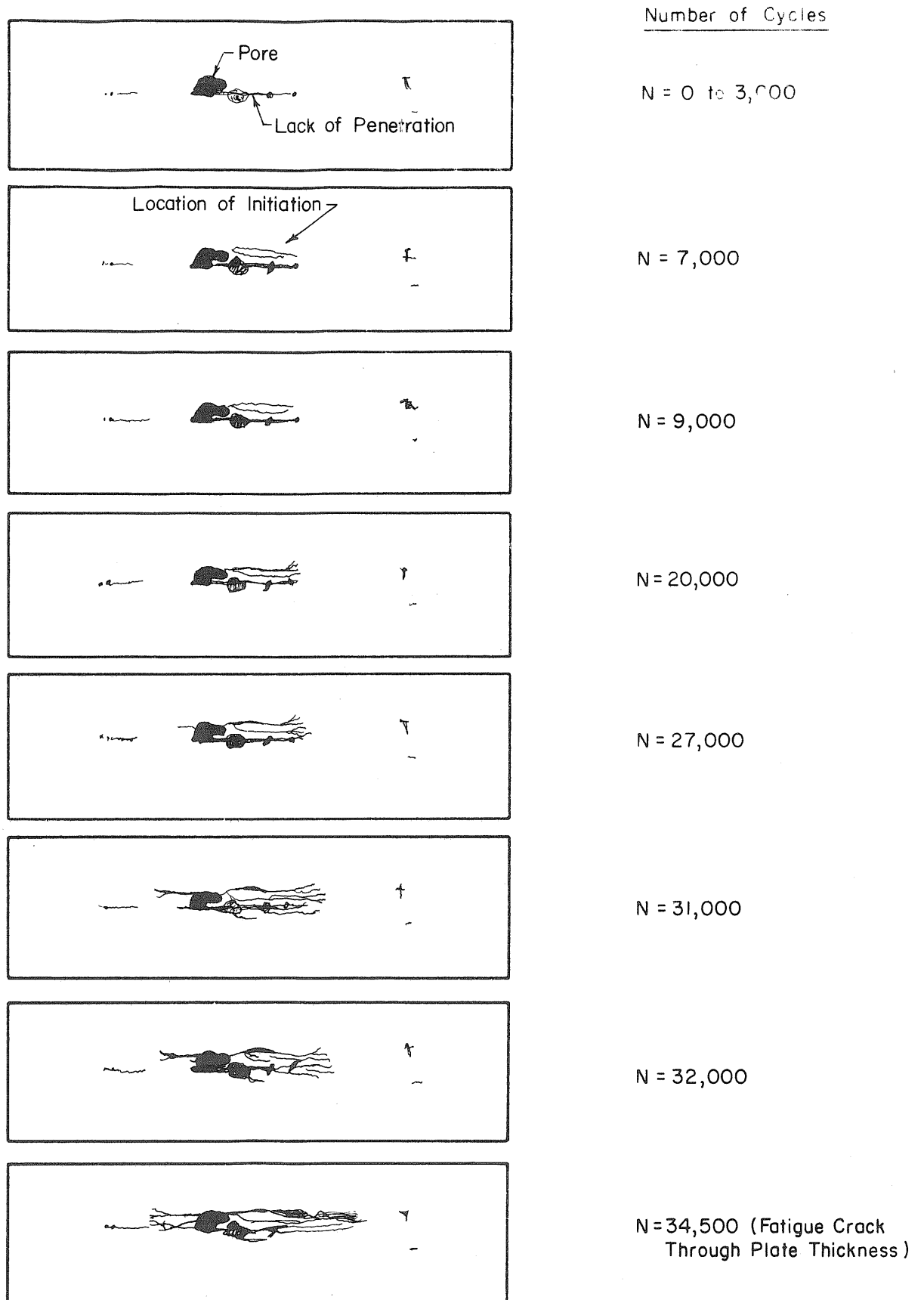
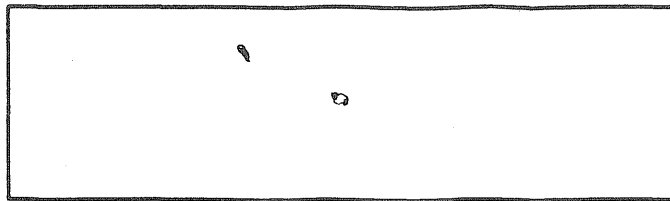
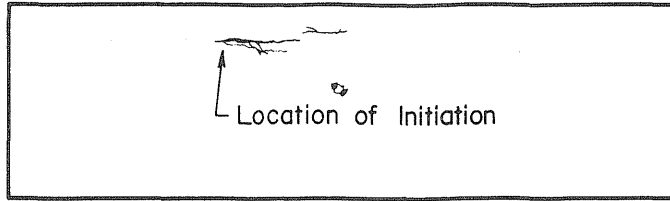


FIG. 3.19 TRACINGS OF RADIOGRAPHS TAKEN DURING FATIGUE TEST OF SPECIMEN ND-20

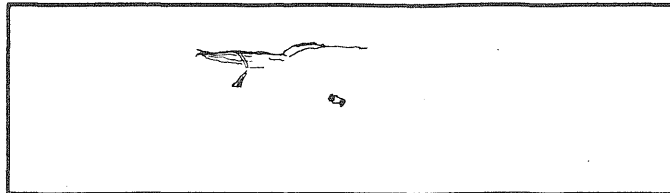
Number of Cycles



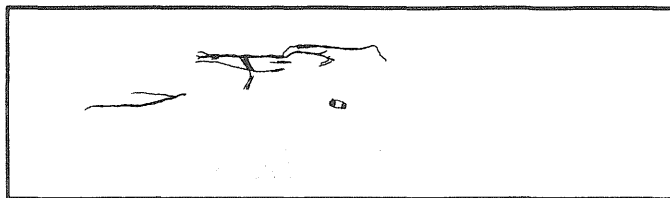
N = 0



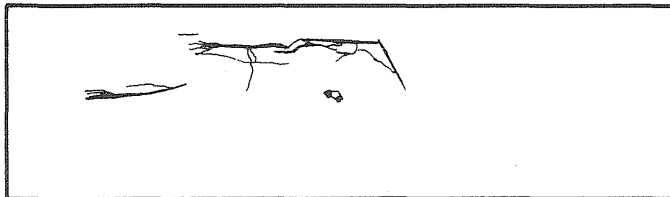
N = 10,000 (Fatigue Crack
Visible on Specimen Surface)



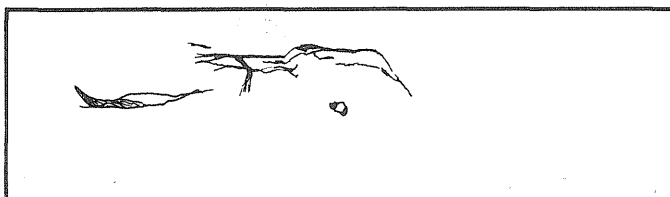
N = 15,000



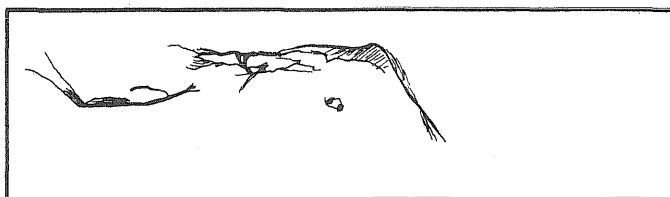
N = 19,000



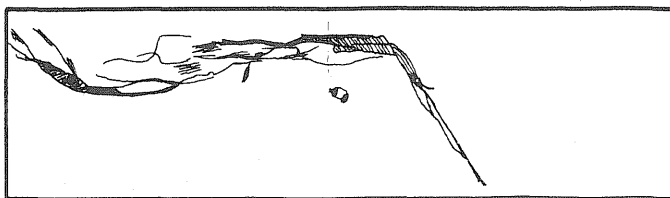
N = 21,000



N = 23,000



N = 25,000



N = 26,940 (Fatigue Crack
Through Plate Thickness)

FIG. 3.20 TRACINGS OF RADIOGRAPHS TAKEN DURING FATIGUE TEST OF SPECIMEN ND-10

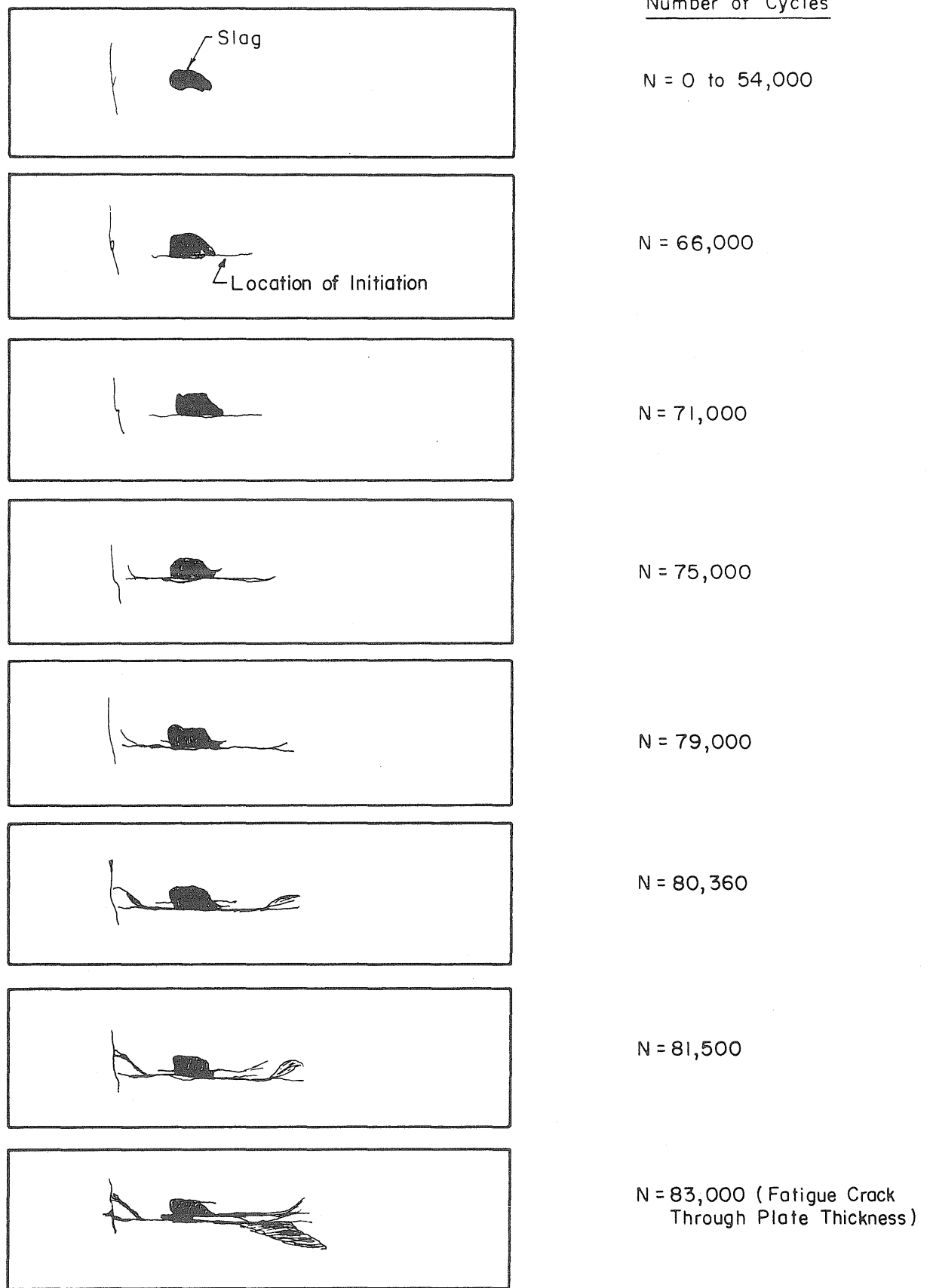


FIG. 3.21 TRACINGS OF RADIOGRAPHS TAKEN DURING FATIGUE TEST OF SPECIMEN ND-18

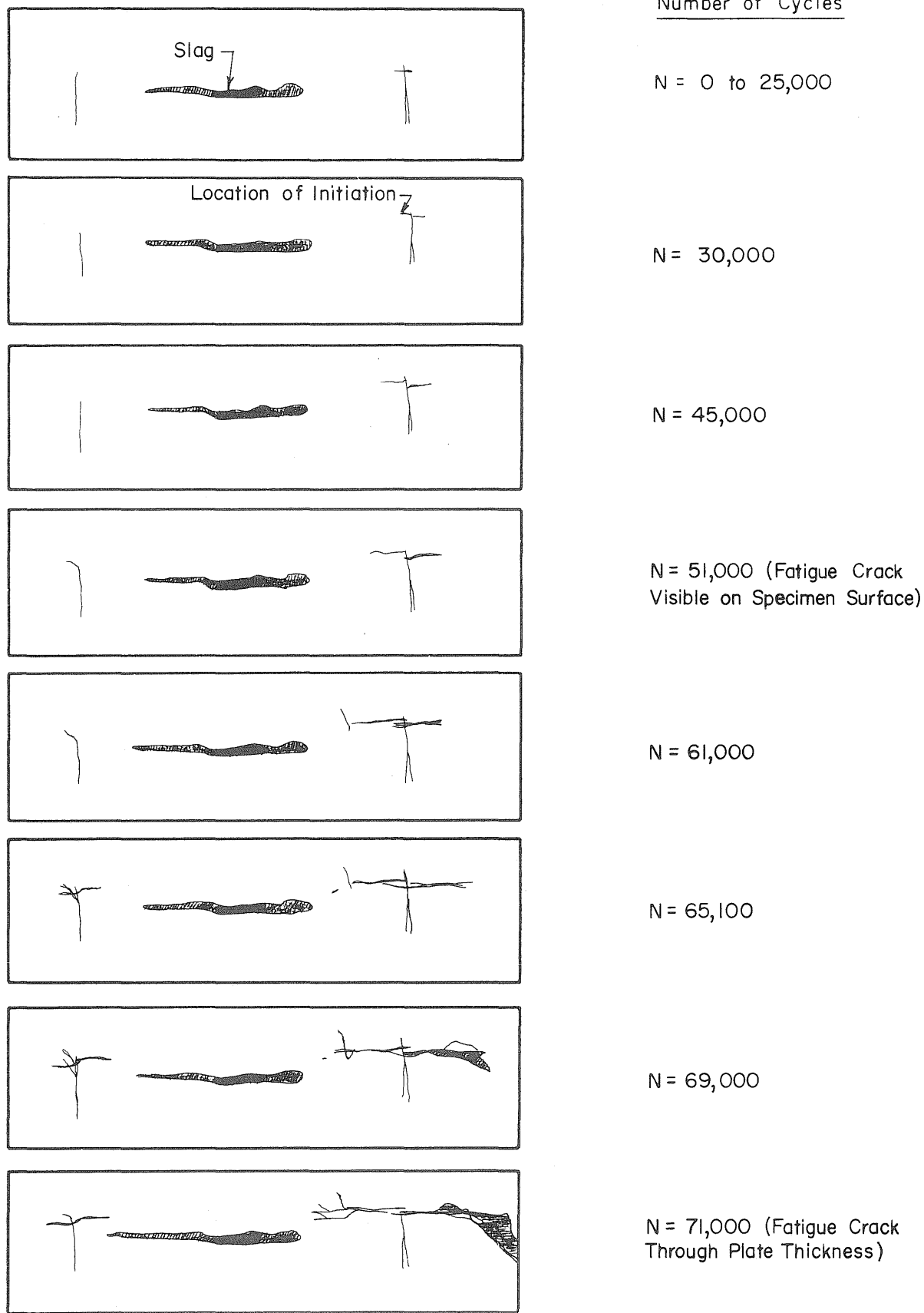


FIG. 3.22 TRACINGS OF RADIOGRAPHS TAKEN DURING FATIGUE TEST OF SPECIMEN ND-17

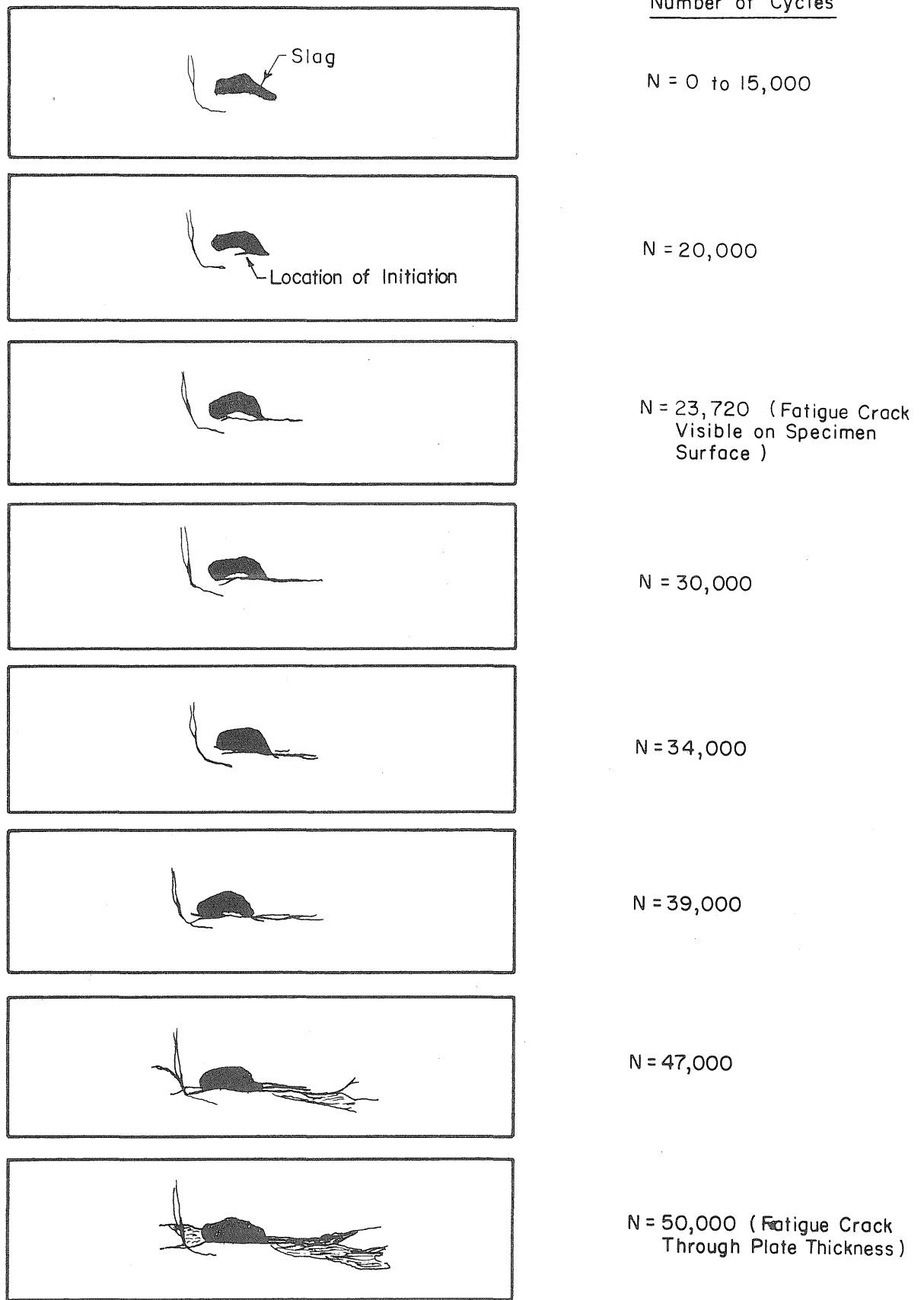


FIG. 3.23 TRACINGS OF RADIOGRAPHS TAKEN DURING FATIGUE TEST OF SPECIMEN ND-19

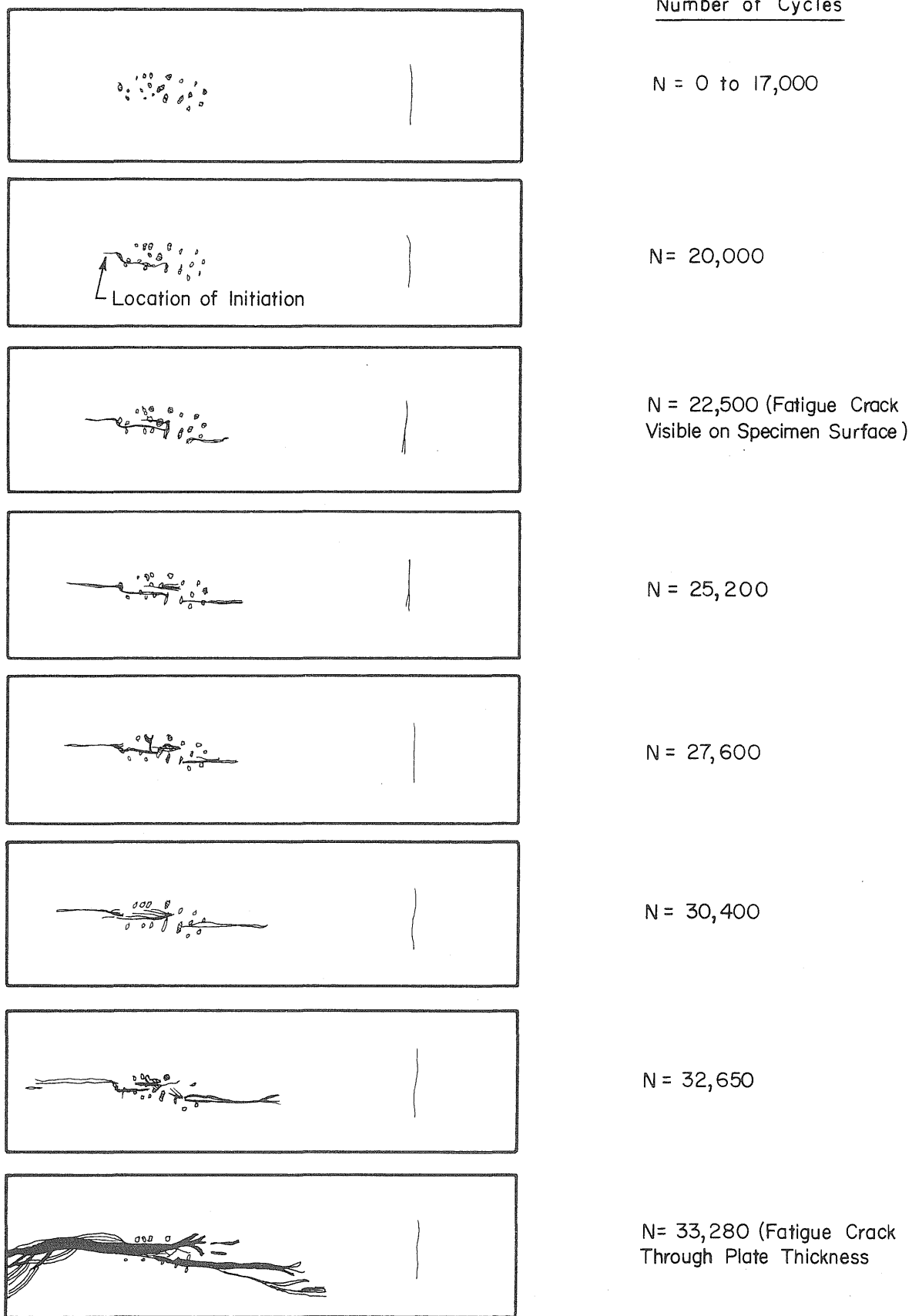
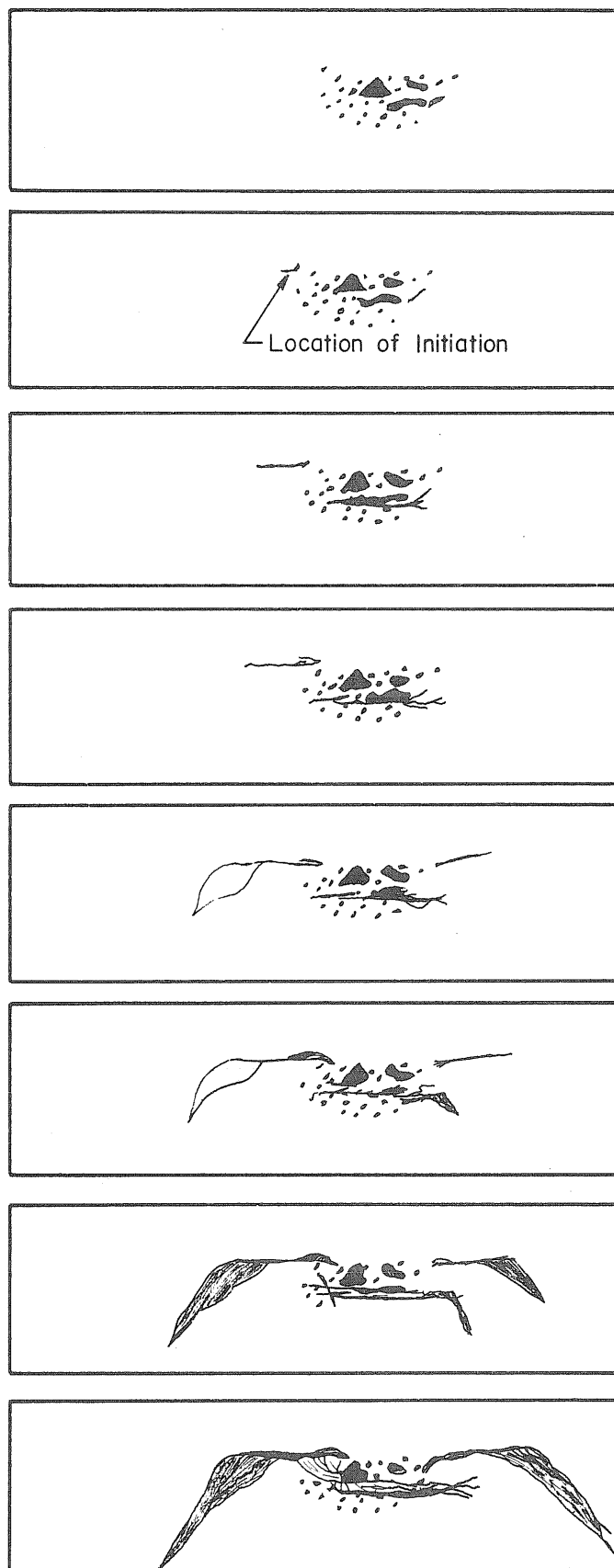


FIG. 3.24 TRACINGS OF RADIOGRAPHS TAKEN DURING FATIGUE TEST OF SPECIMEN ND-14



Number of Cycles

N = 0 to 6,000

N = 8,000

N = 14,844

N = 20,360

N = 26,139

N = 27,640

N = 30,420

N = 32,060 (Fatigue Crack
Through Plate Thickness)

FIG. 3.25 TRACINGS OF RADIOGRAPHS TAKEN DURING FATIGUE TEST OF SPECIMEN ND-15

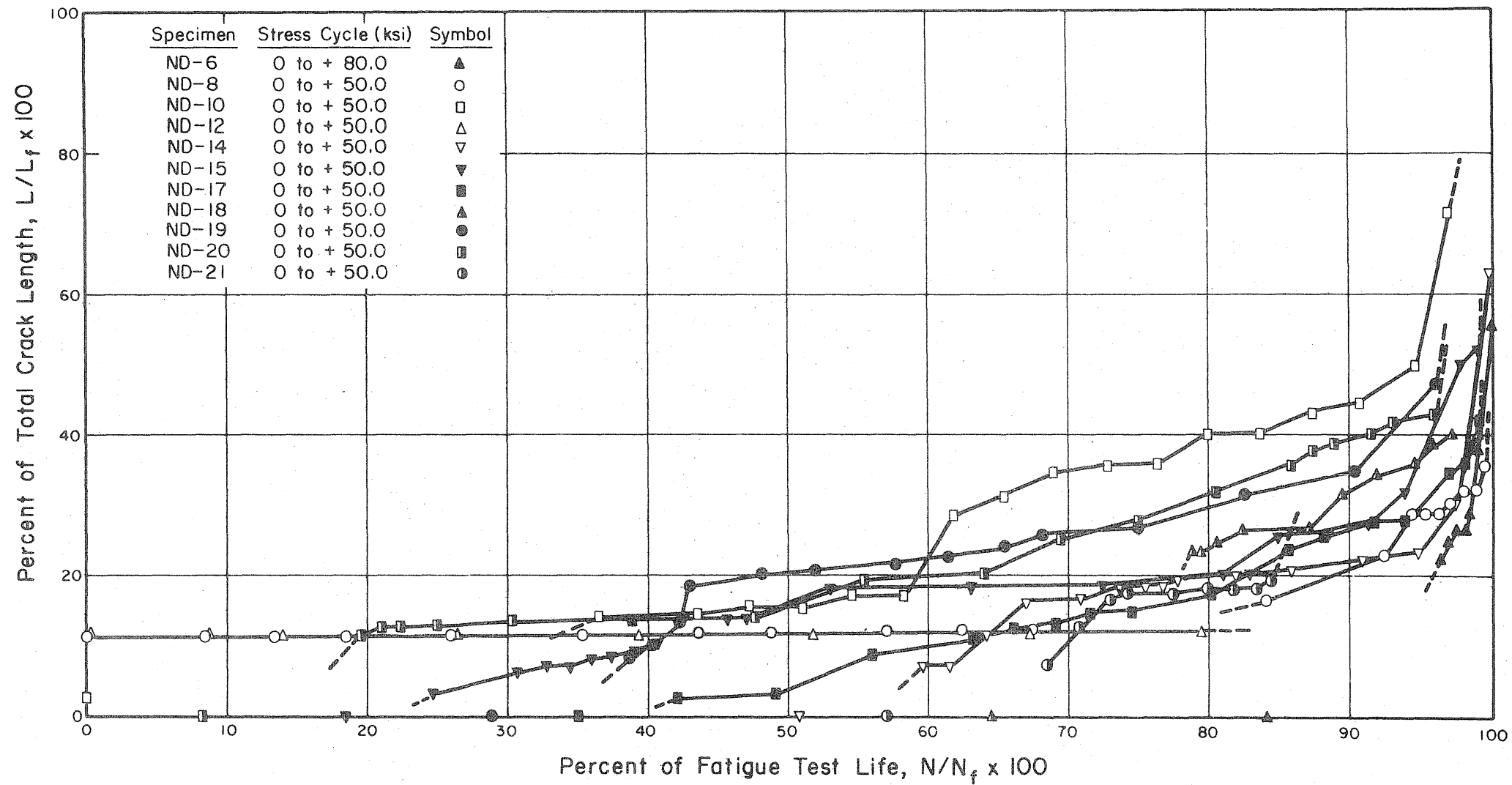


FIG. 3.26 PROPAGATION OF INTERNAL FATIGUE CRACKS IN 1 IN. HY-130 (T) TRANSVERSE BUTT WELDED SPECIMENS

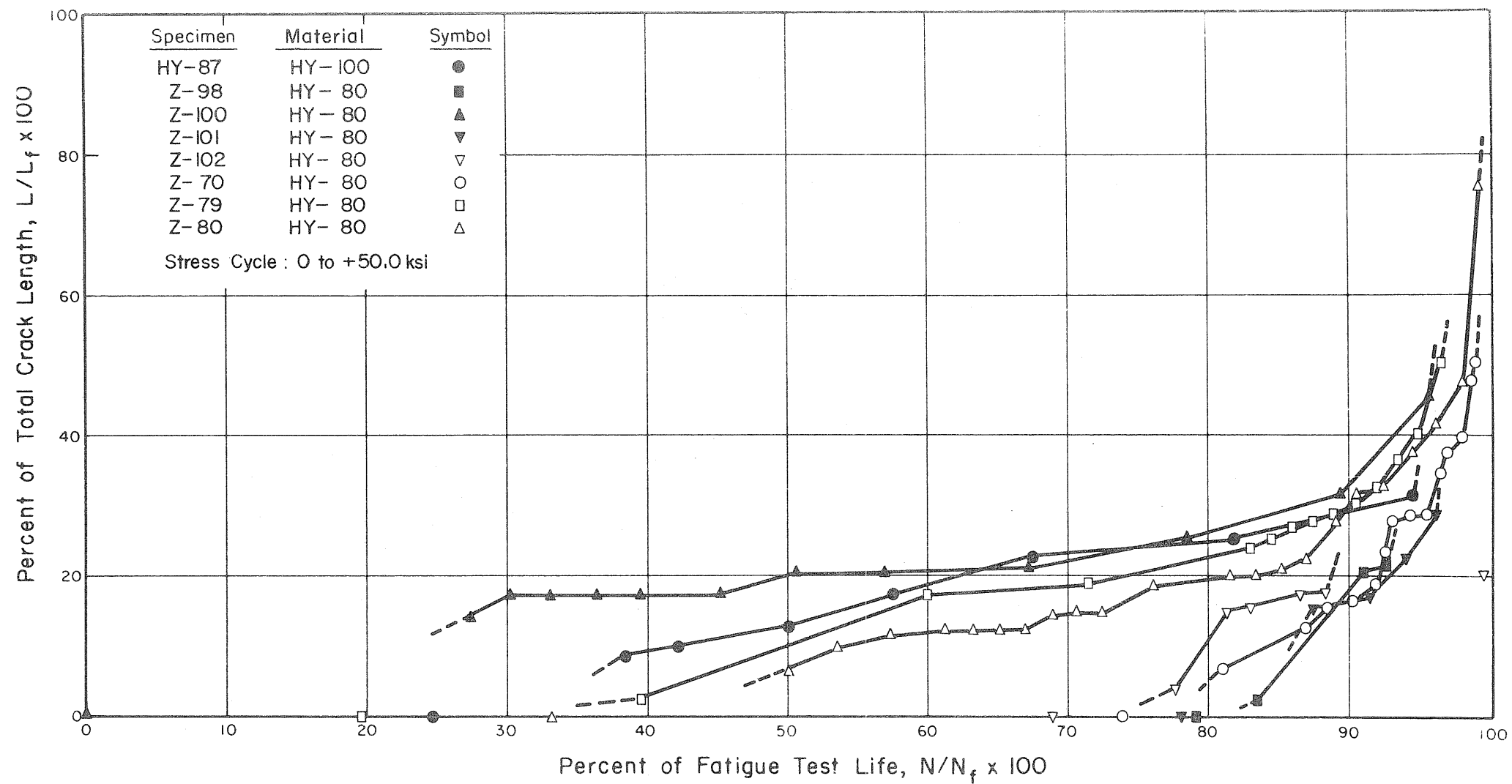


FIG. 3.27 PROPAGATION OF INTERNAL FATIGUE CRACKS IN 3/4 IN. HY-80 AND HY-100 TRANSVERSE BUTT WELDED SPECIMENS

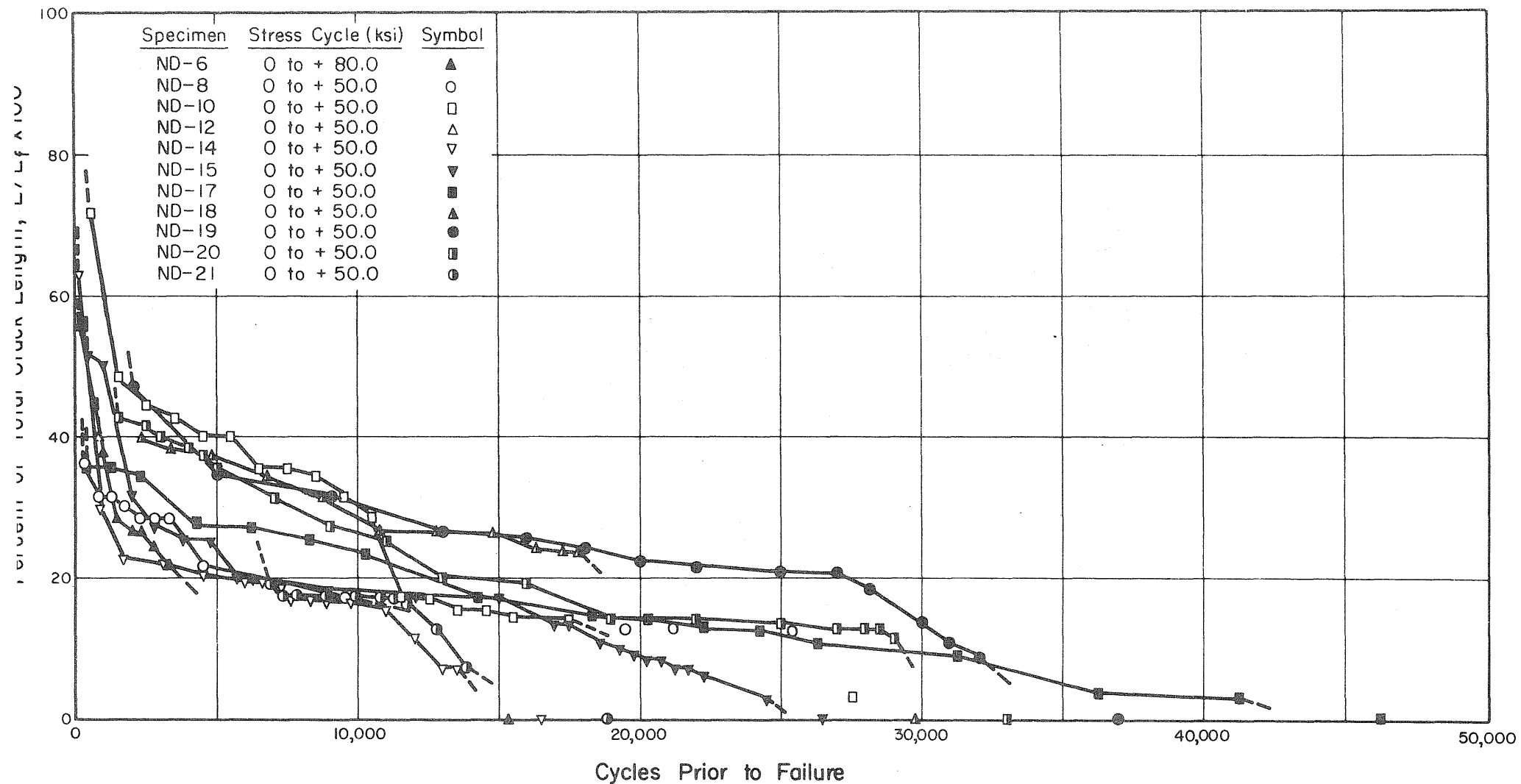


FIG. 3.28 CYCLES OF CRACK PROPAGATION PRIOR TO FAILURE IN 1 IN. HY-130(T) TRANSVERSE BUTT WELDED SPECIMENS

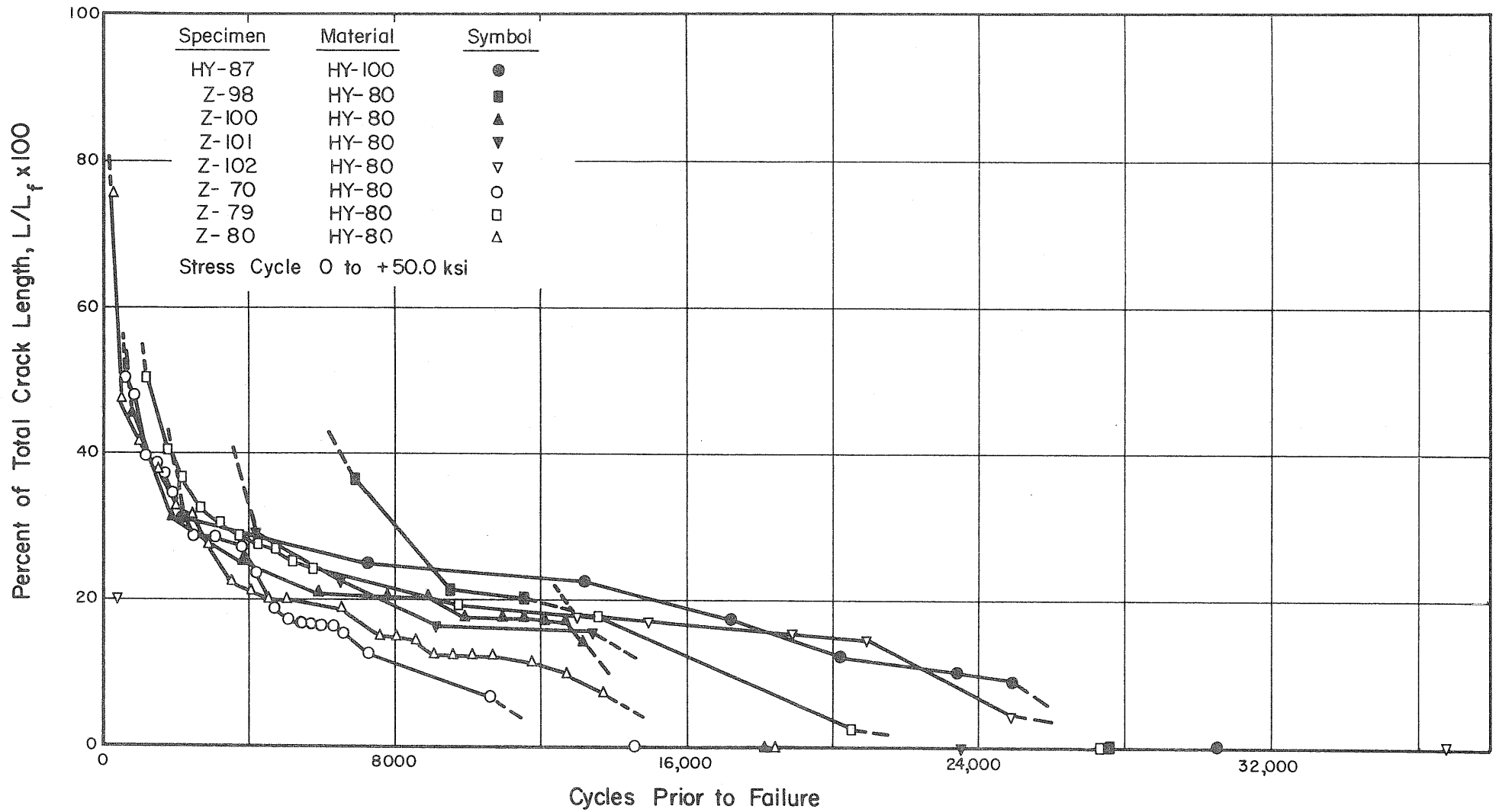


FIG. 3.29 CYCLES OF CRACK PROPAGATION PRIOR TO FAILURE IN 3/4 IN. HY-80 AND HY-100 TRANSVERSE BUTT WELDED SPECIMENS

SPECIMEN ND-8
Stress Cycle: 0 to + 50.0 ksi

Key:

Fracture Surface

- 1) Internal weld flaws visible on fracture surface
- 2) Extent of fatigue crack propagation at intersection with surface

Ultrasonic Readings

- 1) Location and extent of responses as indicated on detector scope
- 2) a. Number designation corresponds to magnitude of peak response as indicated on detector scope
- b. Letter designation corresponds to vertical location on specimen surface

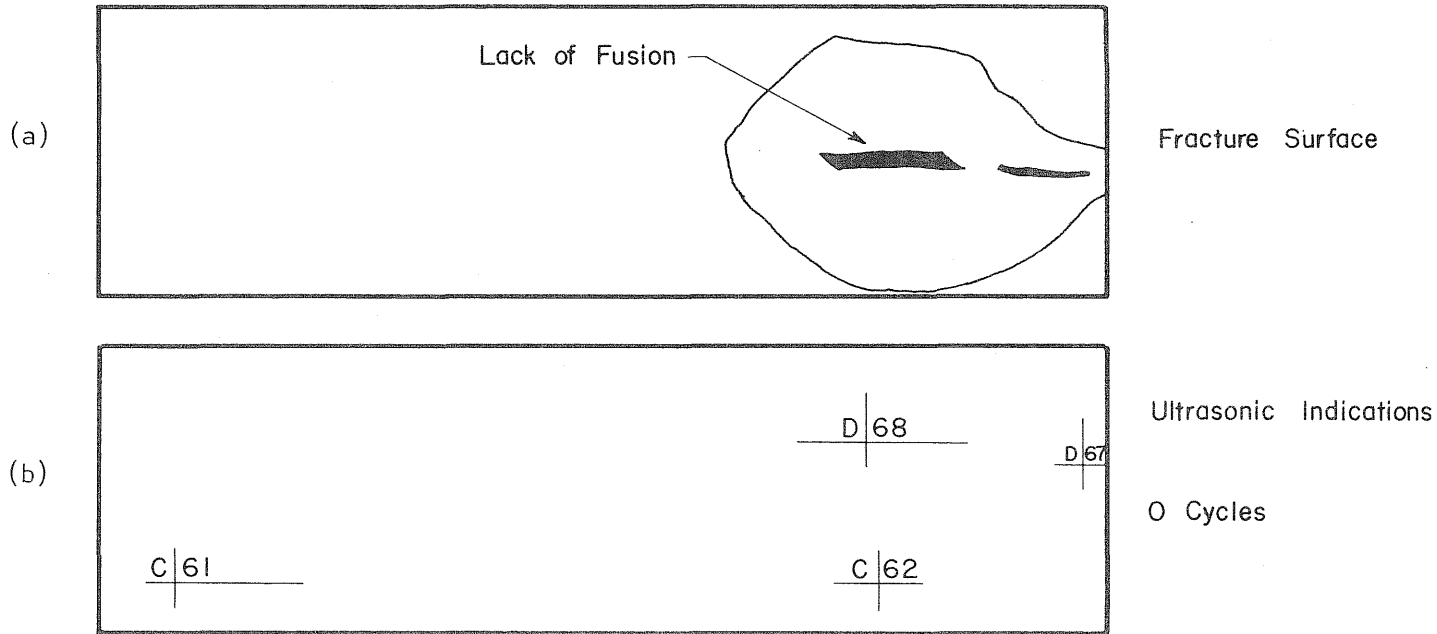
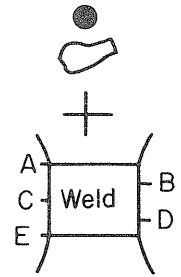


FIG. 3.30 FRACTURE SURFACE, AND ULTRASONIC INDICATIONS RECORDED FOR SPECIMEN ND-8

SPECIMEN ND-8 (Cont.)

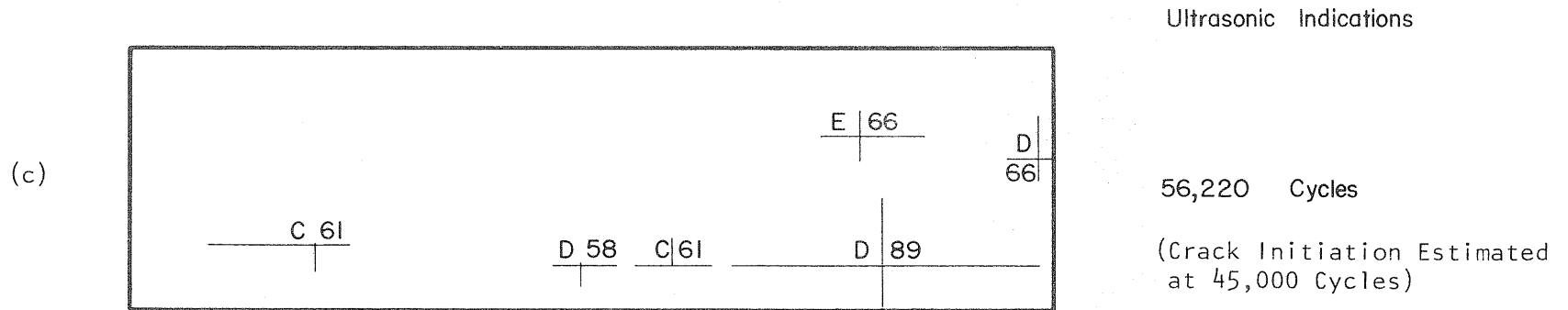
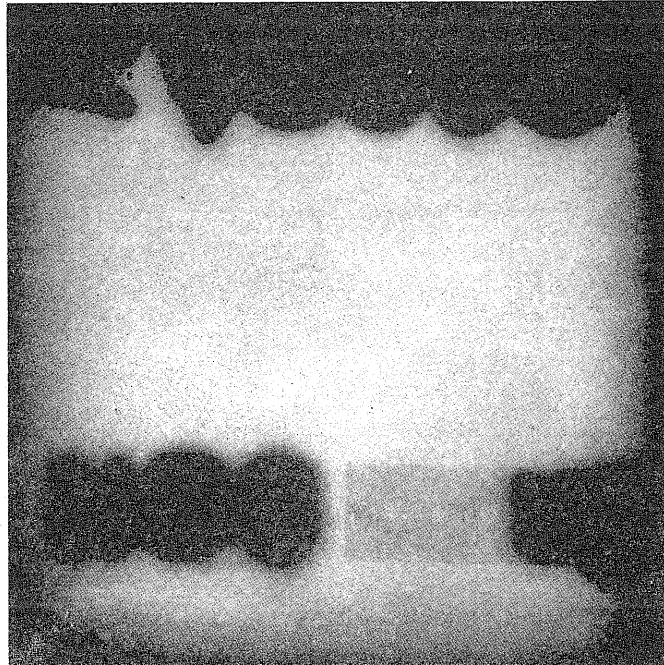
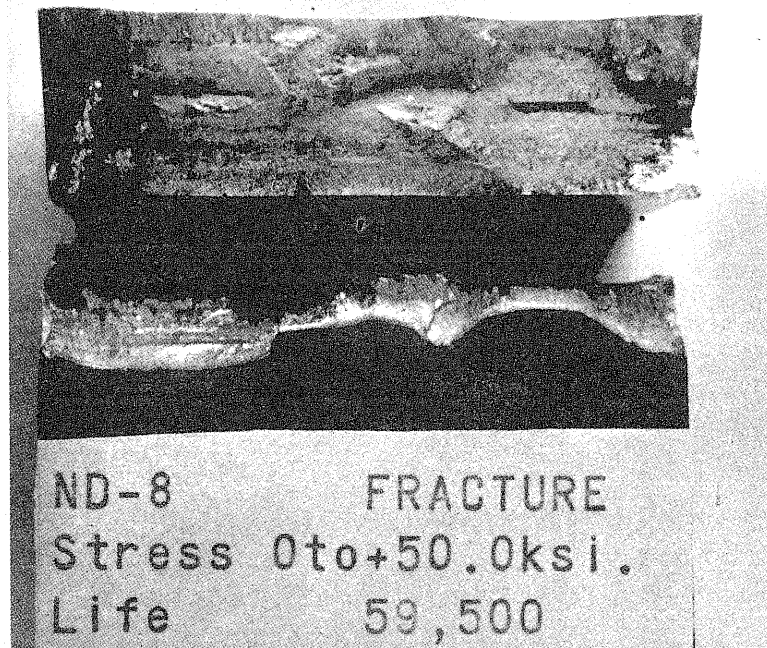


FIG. 3.30 (cont.) FRACTURE SURFACE, AND ULTRASONIC INDICATIONS RECORDED FOR SPECIMEN ND-8

SPECIMEN ND-8 (Cont.)



(d) Radiograph of Specimen Before Test



(e) Fracture Surface After Test

FIG. 3.30 (Cont.) FRACTURE SURFACE, AND ULTRASONIC INDICATIONS RECORDED FOR SPECIMEN ND-8

SPECIMEN ND-21
Stress Cycle: 0 to + 50.0 ksi

Key:

Fracture Surface

- 1) Internal weld flaws visible on fracture surface
- 2) Extent of fatigue crack propagation at intersection with surface

Ultrasonic Readings

- 1) Location and extent of responses as indicated on detector scope
- 2) a. Number designation corresponds to magnitude of peak response as indicated on detector scope
- b. Letter designation corresponds to vertical location on specimen surface

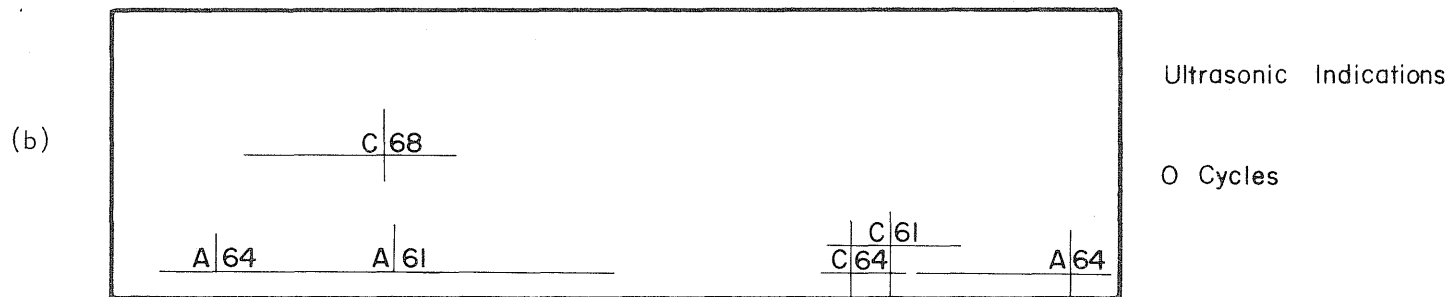
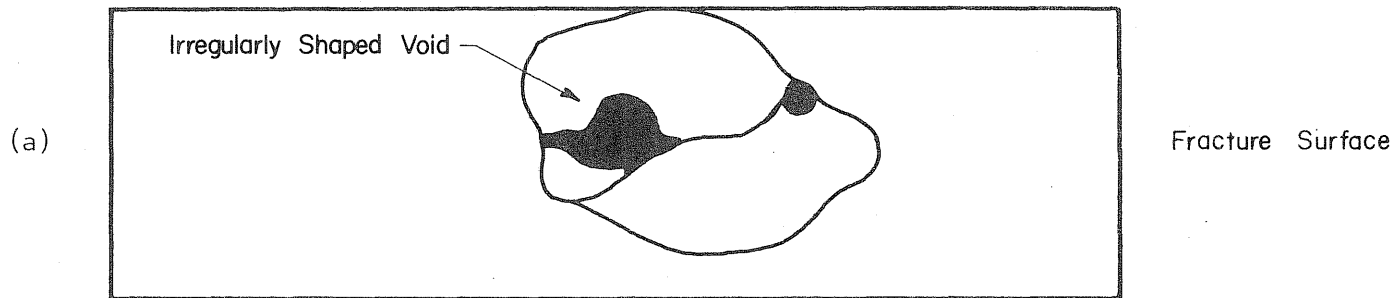
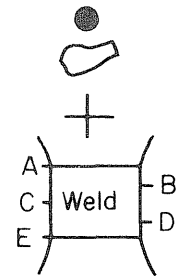
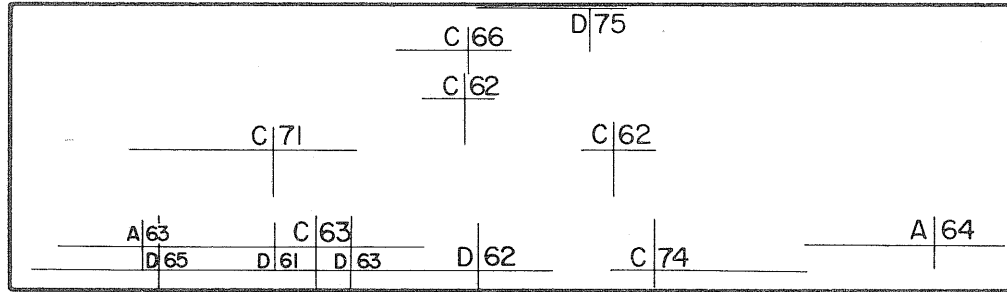


FIG. 3.31 FRACTURE SURFACE, AND ULTRASONIC INDICATIONS RECORDED FOR SPECIMEN ND-21

SPECIMEN ND-21 (Cont.)

(c)



Ultrasonic Indications

30,000 Cycles

(Crack Initiation Estimated at 27,500 Cycles)

FIG. 3.31 (cont.) FRACTURE SURFACE, AND ULTRASONIC INDICATIONS RECORDED FOR SPECIMEN ND-21

SPECIMEN ND-21 (Cont.)



(d) Radiograph of Specimen Before Test



(e) Fracture Surface After Test

FIG. 3.31 (Cont.) FRACTURE SURFACE, AND ULTRASONIC INDICATIONS RECORDED FOR SPECIMEN ND-21

SPECIMEN ND-20
Stress Cycle: 0 to + 50.0 ksi

Key:

Fracture Surface

- 1) Internal weld flaws visible on fracture surface.....
- 2) Extent of fatigue crack propagation at intersection with surface.....

Ultrasonic Readings

- 1) Location and extent of responses as indicated on detector scope.....
- 2) a. Number designation corresponds to magnitude of peak response as indicated on detector scope
- b. Letter designation corresponds to vertical location on specimen surface.....

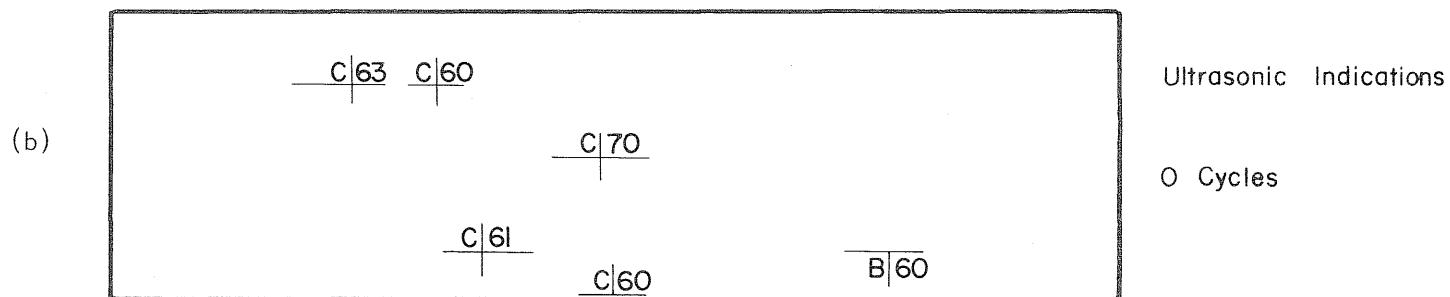
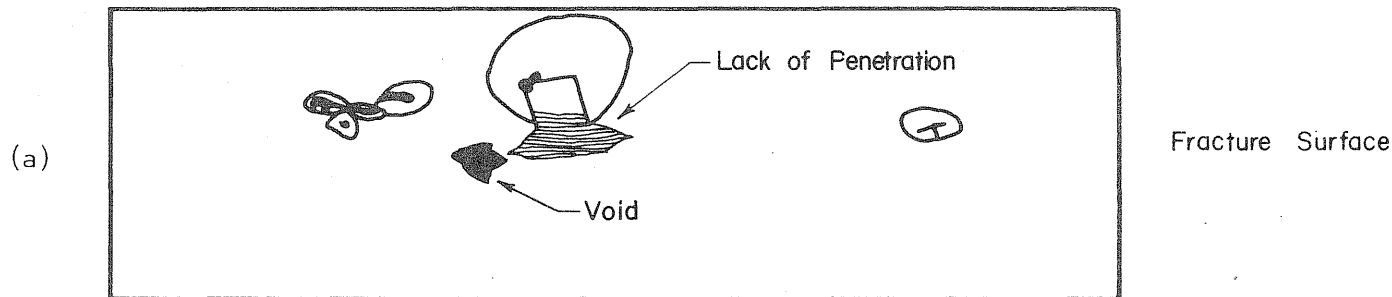
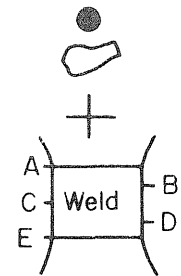


FIG. 3.32 FRACTURE SURFACE, AND ULTRASONIC INDICATIONS RECORDED FOR SPECIMEN ND-20

SPECIMEN ND-20 (Cont.)

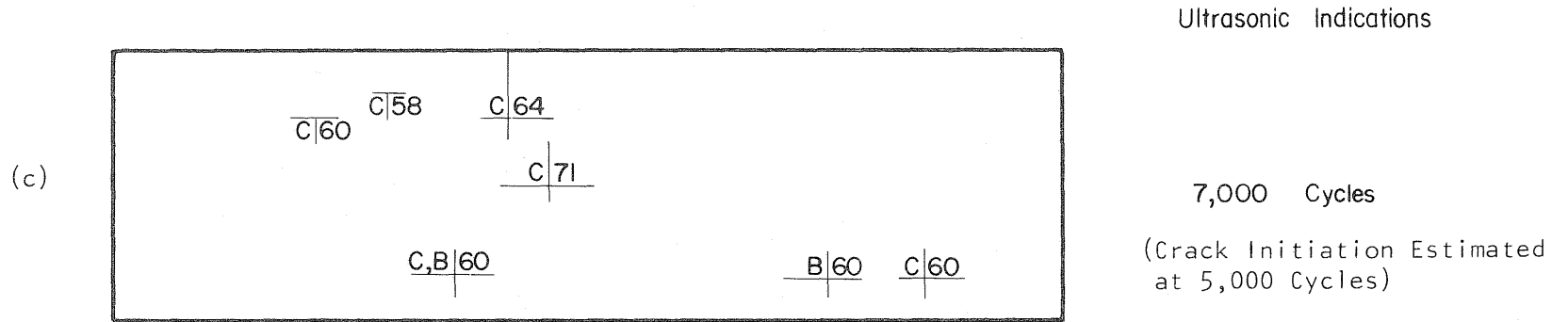
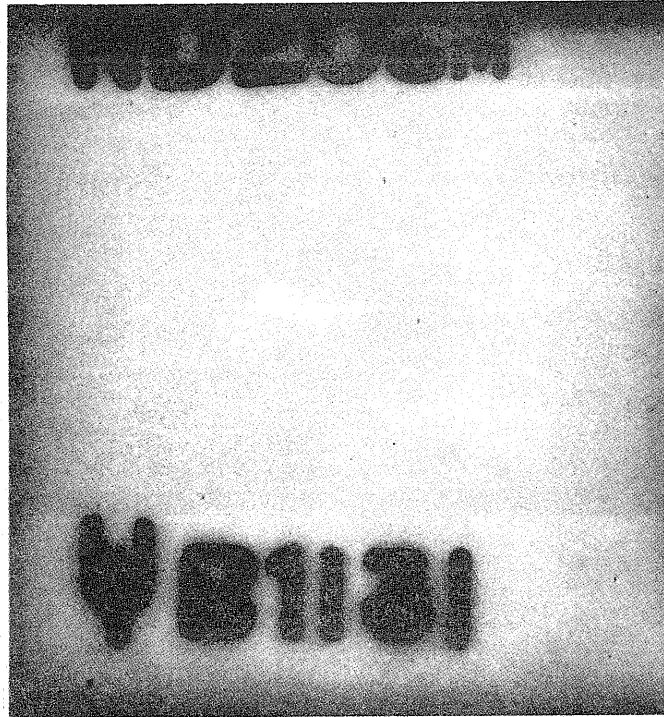
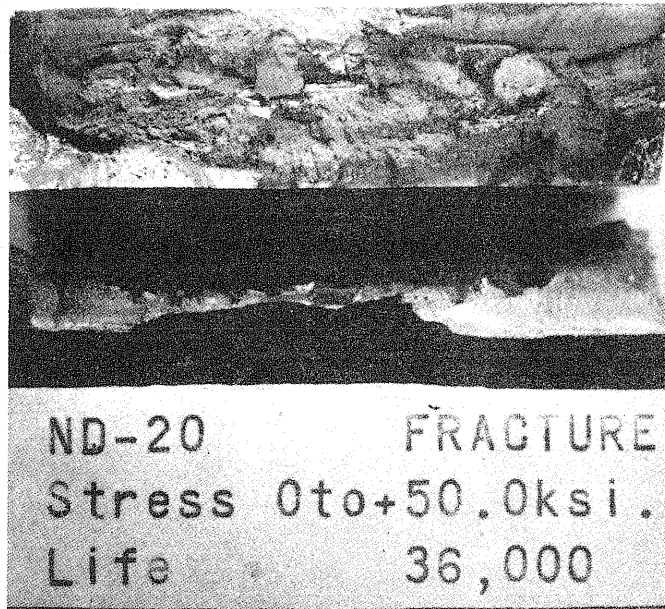


FIG. 3.32 (cont.) FRACTURE SURFACE, AND ULTRASONIC INDICATIONS RECORDED FOR SPECIMEN ND-20

SPECIMEN ND-20 (Cont.)



(d) Radiograph of Specimen Before Test



(e) Fracture Surface After Test

FIG. 3.32 (Cont.) FRACTURE SURFACE, AND ULTRASONIC INDICATIONS RECORDED FOR SPECIMEN ND-20

SPECIMEN ND-10
Stress Cycle: 0 to +50.0 ksi

Key:

Fracture Surface

- 1) Internal weld flaws visible on fracture surface
- 2) Extent of fatigue crack propagation at intersection with surface

Ultrasonic Readings

- 1) Location and extent of responses as indicated on detector scope
- 2) a. Number designation corresponds to magnitude of peak response as indicated on detector scope.
- b. Letter designation corresponds to vertical location on specimen surface

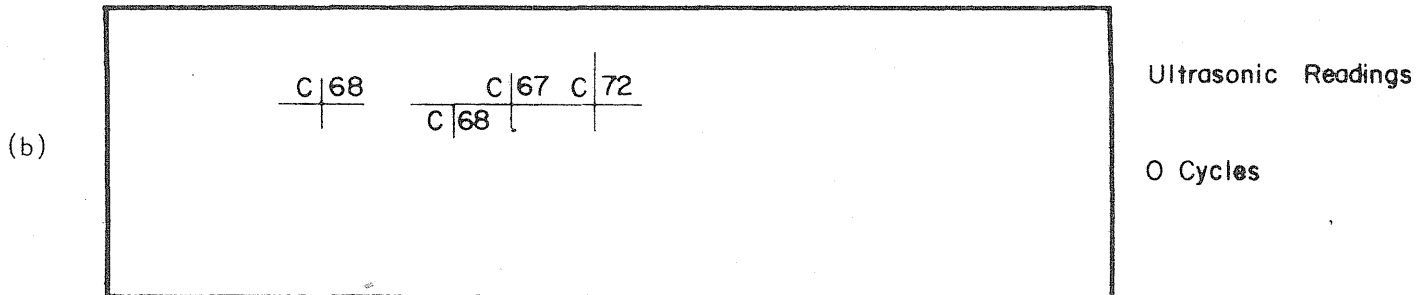
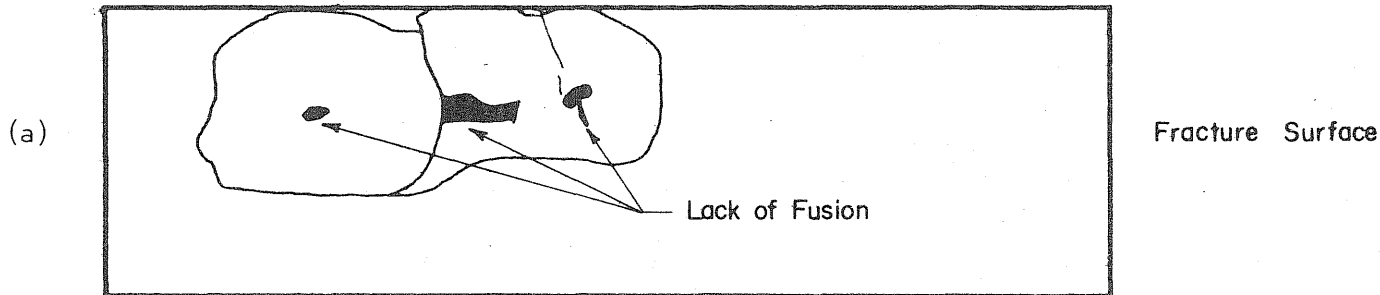
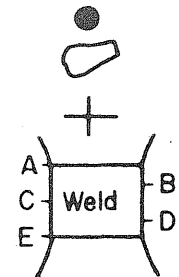


FIG. 3.33 FRACTURE SURFACE, AND ULTRASONIC INDICATIONS RECORDED FOR SPECIMEN ND-10

SPECIMEN ND-10 (Cont.)

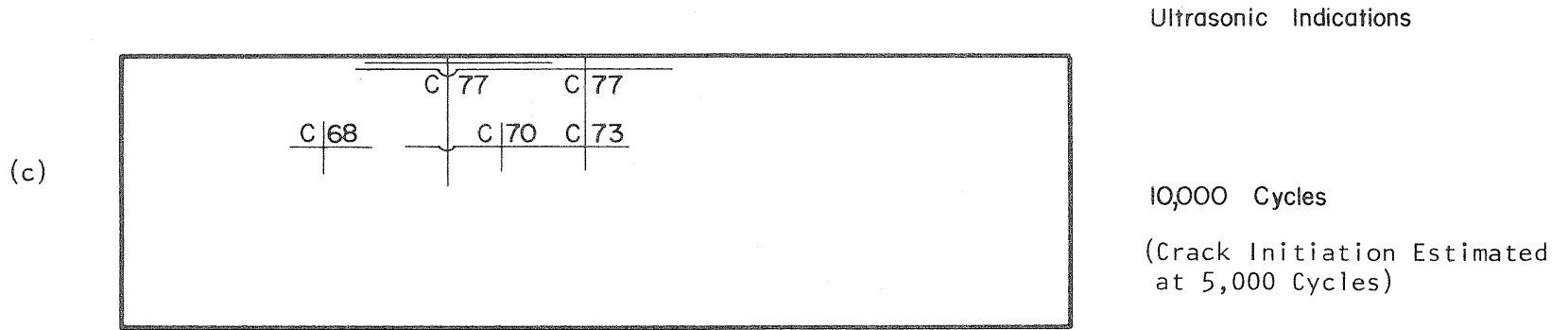
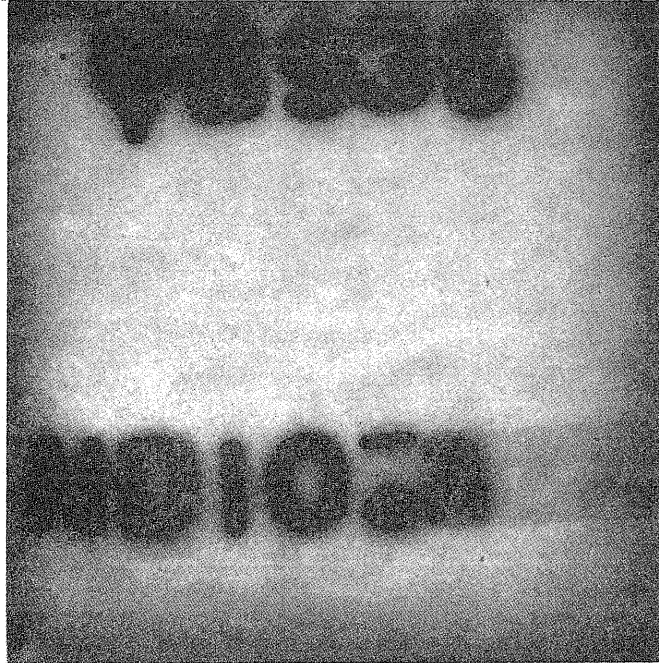
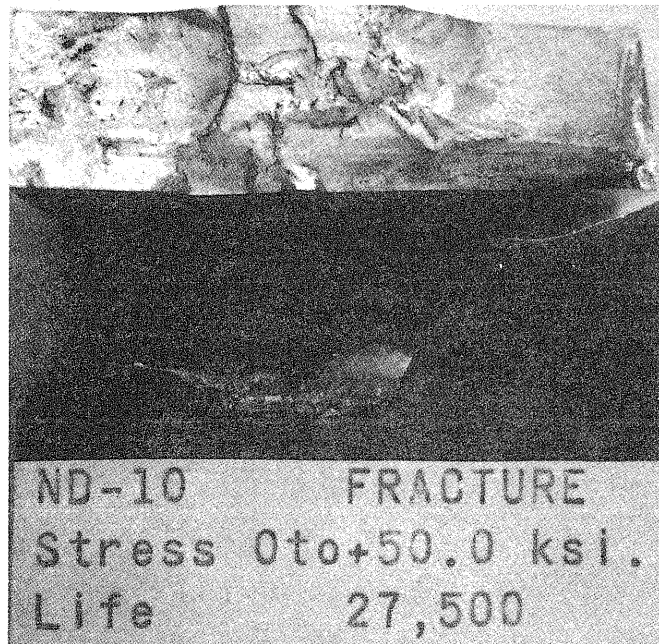


FIG. 3.33 (cont.) FRACTURE SURFACE, AND ULTRASONIC INDICATIONS RECORDED FOR SPECIMEN ND-10

SPECIMEN ND-10 (Cont.)



(d) Radiograph of Specimen Before Test



(e) Fracture Surface After Test

FIG. 3.33 (Cont.) FRACTURE SURFACE, AND ULTRASONIC INDICATIONS RECORDED FOR SPECIMEN ND-10

SPECIMEN ND-18
Stress Cycle: 0 to + 50.0 ksi

Key:

Fracture Surface

- 1) Internal weld flaws visible on fracture surface
- 2) Extent of fatigue crack propagation at intersection with surface

Ultrasonic Readings

- 1) Location and extent of responses as indicated on detector scope
- 2) a. Number designation corresponds to magnitude of peak response as indicated on detector scope
- b. Letter designation corresponds to vertical location on specimen surface

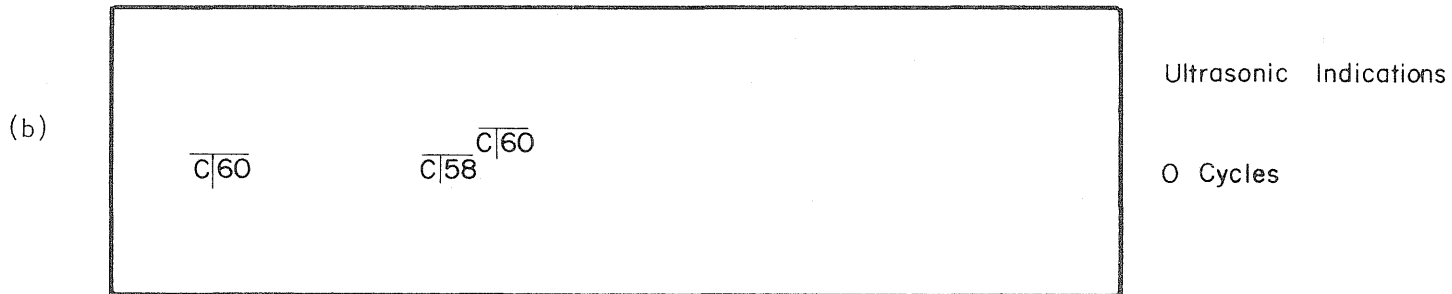
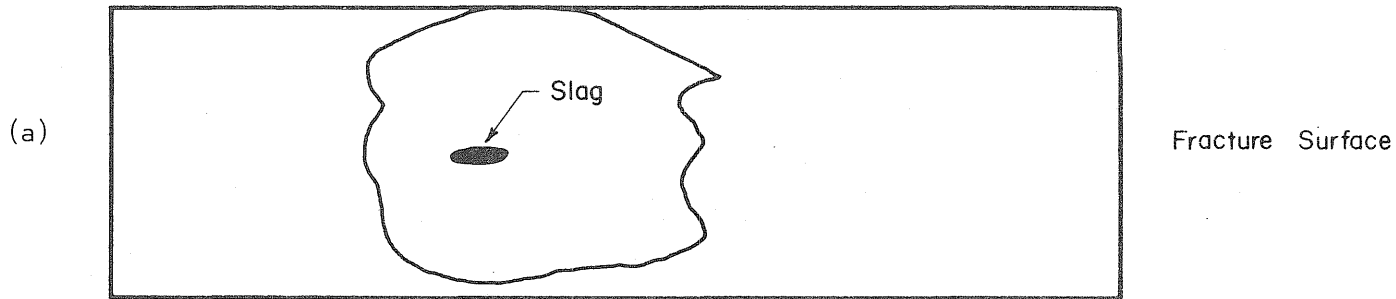
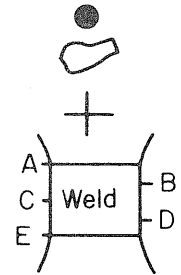


FIG. 3.34 FRACTURE SURFACE, AND ULTRASONIC INDICATIONS RECORDED FOR SPECIMEN ND-18

SPECIMEN ND-18 (Cont.)

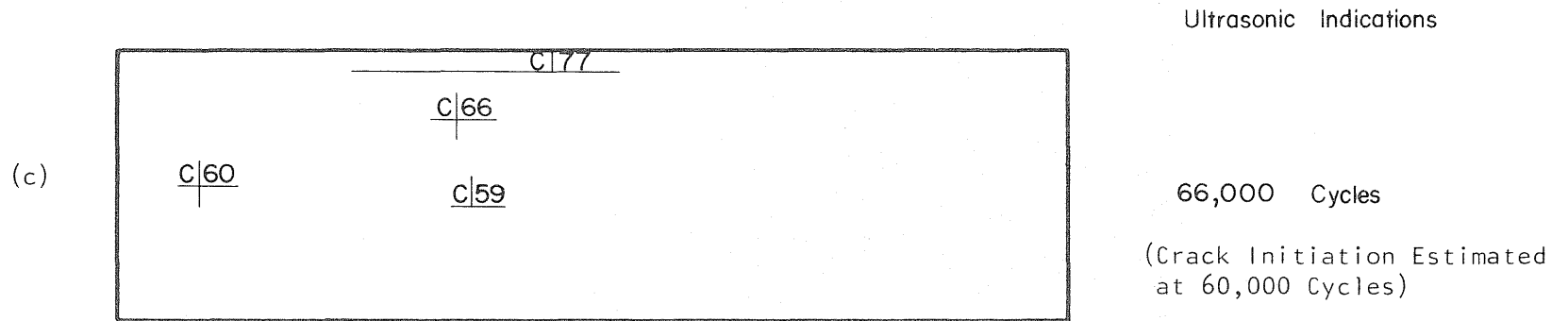
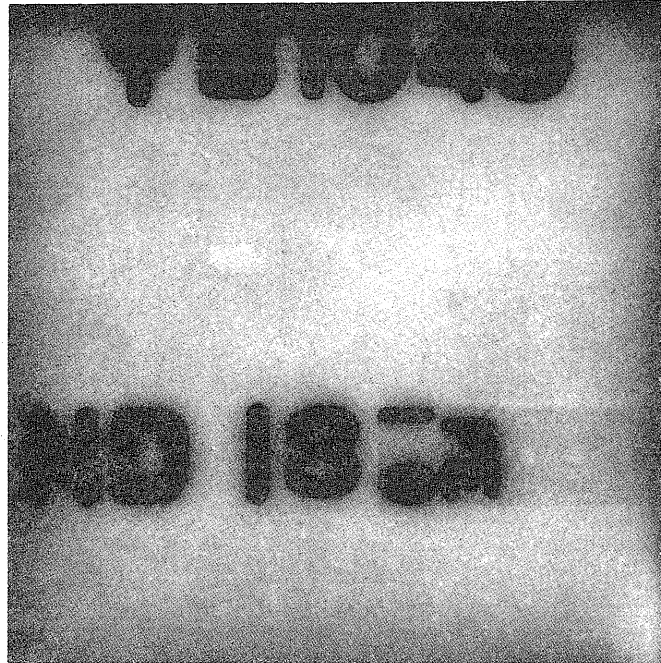
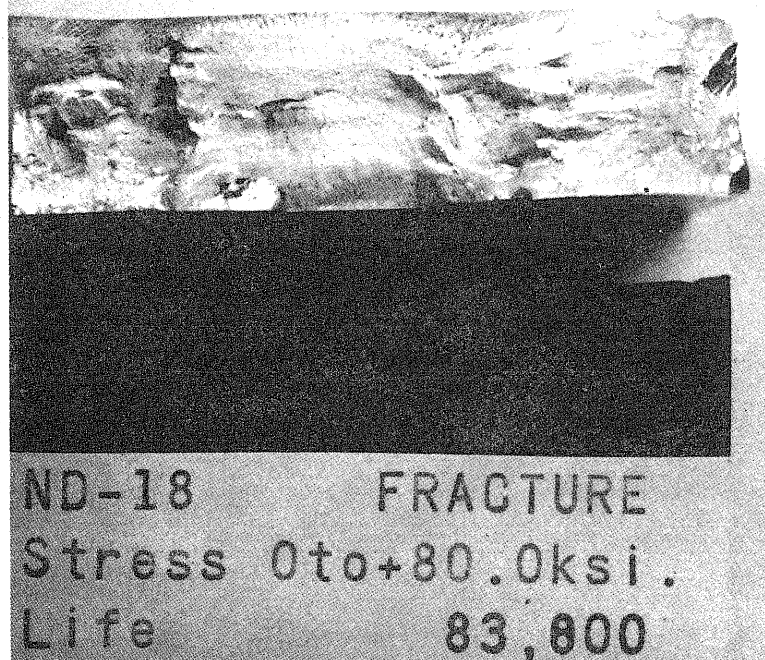


FIG. 3.34 (cont.) FRACTURE SURFACE, AND ULTRASONIC INDICATIONS RECORDED FOR SPECIMEN ND-18

SPECIMEN ND-18 (Cont.)



(d) Radiograph of Specimen Before Test



(e) Fracture Surface After Test

FIG. 3.34 (Cont.) FRACTURE SURFACE, AND ULTRASONIC INDICATIONS RECORDED FOR SPECIMEN ND-18

SPECIMEN ND-17
Stress Cycle: 0 to + 50.0 ksi

Key:

Fracture Surface

- 1) Internal weld flaws visible on fracture surface
- 2) Extent of fatigue crack propagation at intersection with surface

Ultrasonic Readings

- 1) Location and extent of responses as indicated on detector scope
- 2) a. Number designation corresponds to magnitude of peak response as indicated on detector scope
- b. Letter designation corresponds to vertical location on specimen surface

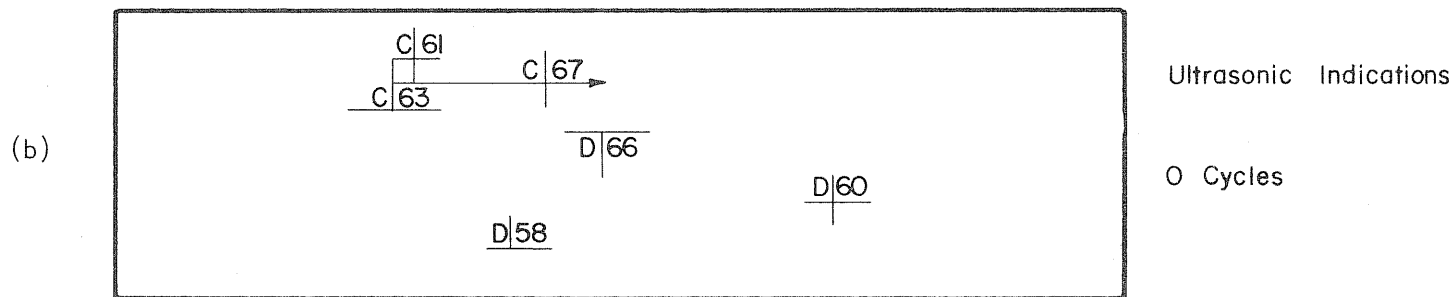
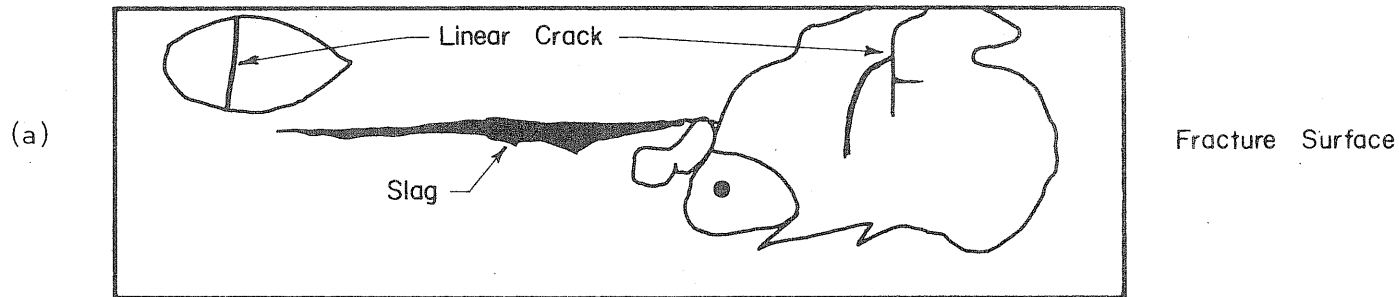
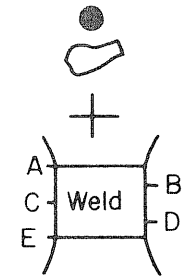
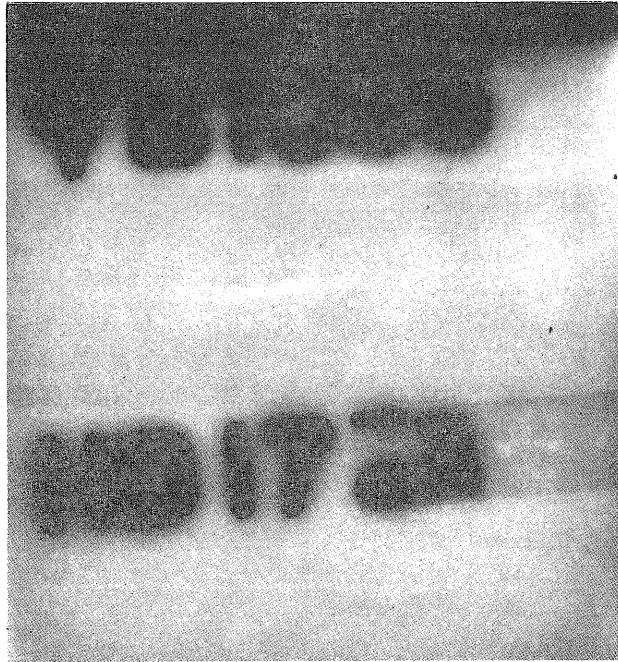
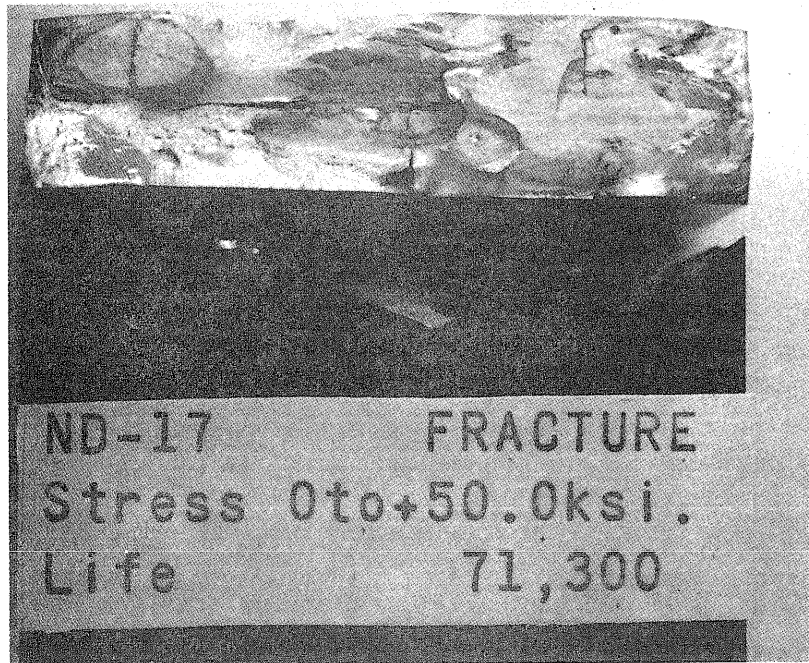


FIG. 3.35 FRACTURE SURFACE, AND ULTRASONIC INDICATIONS RECORDED FOR SPECIMEN ND-17

SPECIMEN ND-17 (Cont.)



(c) Radiograph of Specimen Before Test



(d) Fracture Surface After Test

FIG. 3.35 (Cont.) FRACTURE SURFACE, AND ULTRASONIC INDICATIONS RECORDED FOR SPECIMEN ND-17

SPECIMEN ND-14
Stress Cycle: 0 to + 50.0 ksi

Key:

Fracture Surface

- 1) Internal weld flaws visible on fracture surface
- 2) Extent of fatigue crack propagation at intersection with surface

Ultrasonic Readings

- 1) Location and extent of responses as indicated on detector scope
- 2) a. Number designation corresponds to magnitude of peak response as indicated on detector scope
- b. Letter designation corresponds to vertical location on specimen surface

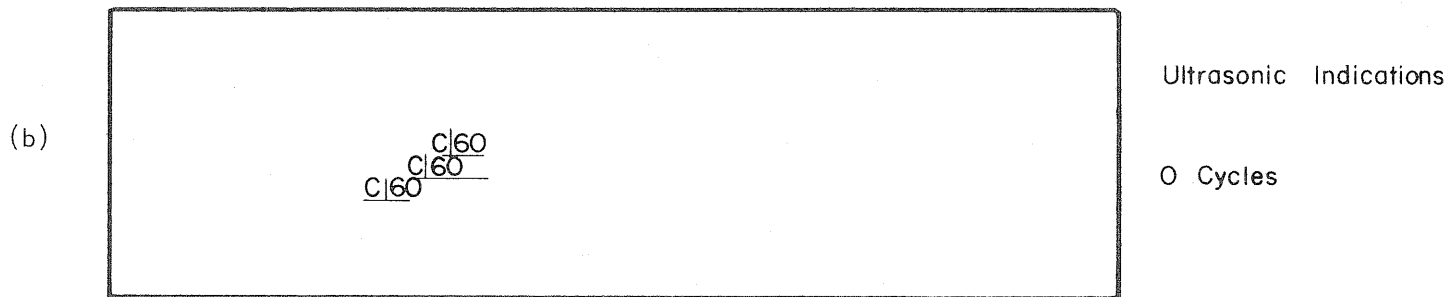
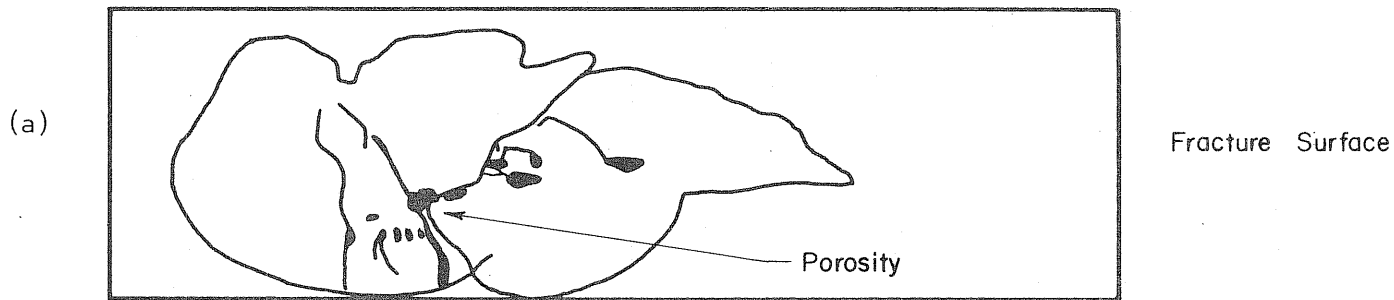
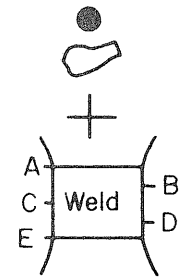


FIG. 3.36 FRACTURE SURFACE, AND ULTRASONIC INDICATIONS RECORDED FOR SPECIMEN ND-14

SPECIMEN ND-14 (Cont.)

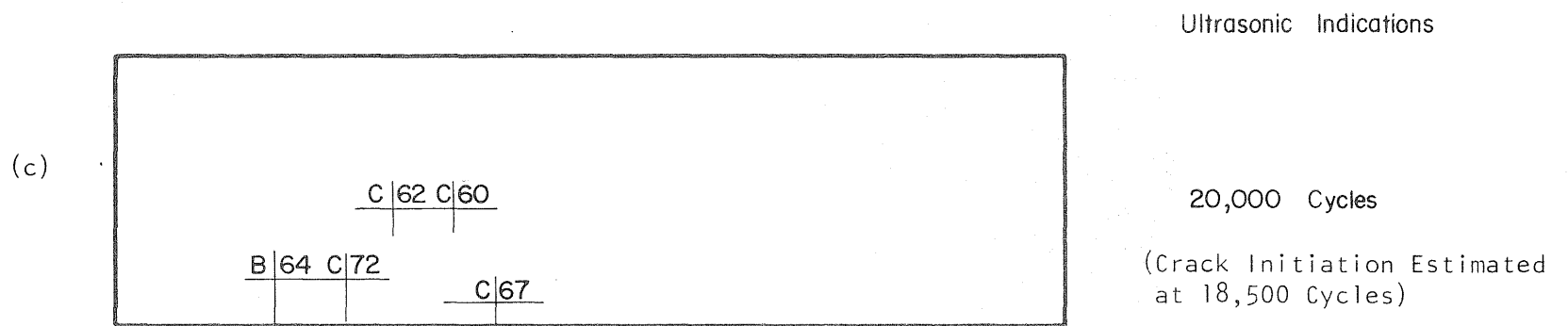
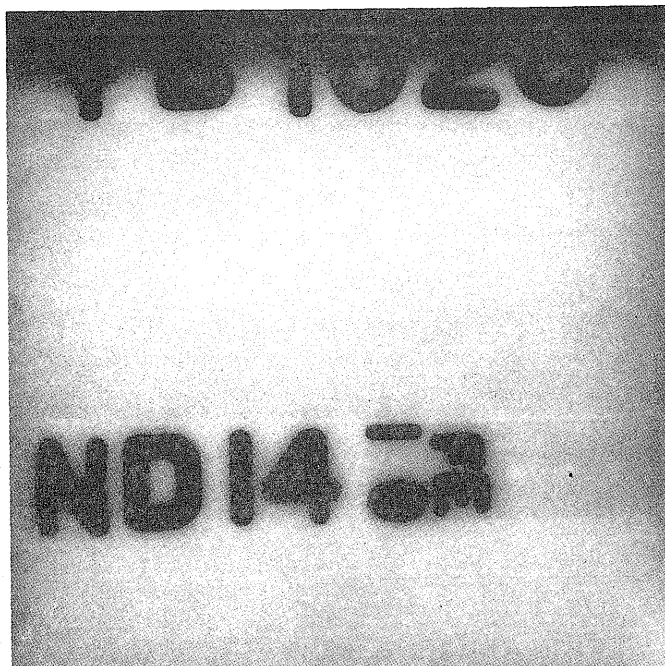
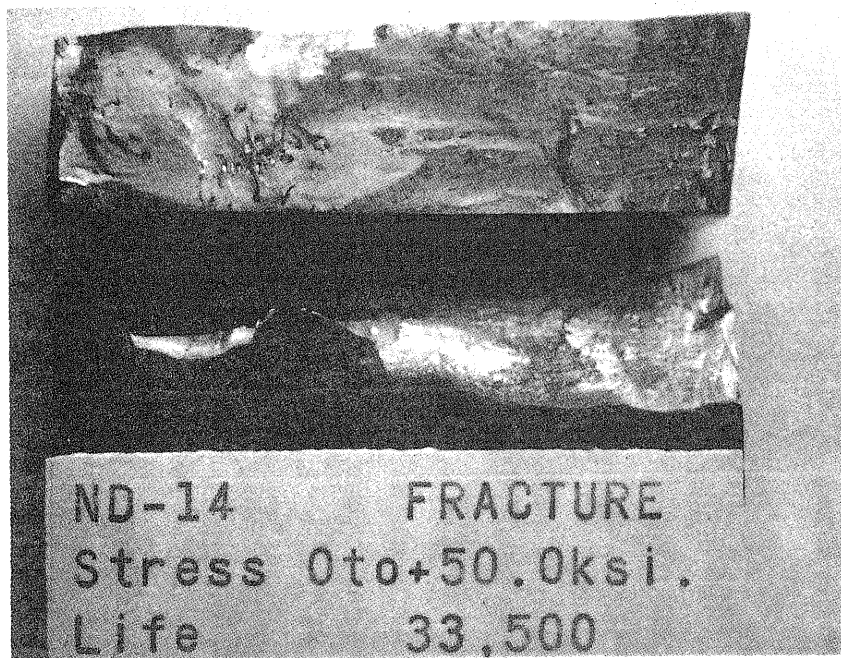


FIG. 3.36 (cont.) FRACTURE SURFACE, AND ULTRASONIC INDICATIONS RECORDED FOR SPECIMEN ND-14

SPECIMEN ND-14 (Cont.)



(d) Radiograph of Specimen Before Test



(e) Fracture Surface After Test

FIG. 3.36 (Cont.) FRACTURE SURFACE, AND ULTRASONIC INDICATIONS RECORDED FOR SPECIMEN ND-14

SPECIMEN ND-15
Stress Cycle: 0 to + 50.0 ksi

Key:

Fracture Surface

- 1) Internal weld flaws visible on fracture surface
- 2) Extent of fatigue crack propagation at intersection with surface

Ultrasonic Readings

- 1) Location and extent of responses as indicated on detector scope
- 2) a. Number designation corresponds to magnitude of peak response as indicated on detector scope
- b. Letter designation corresponds to vertical location on specimen surface

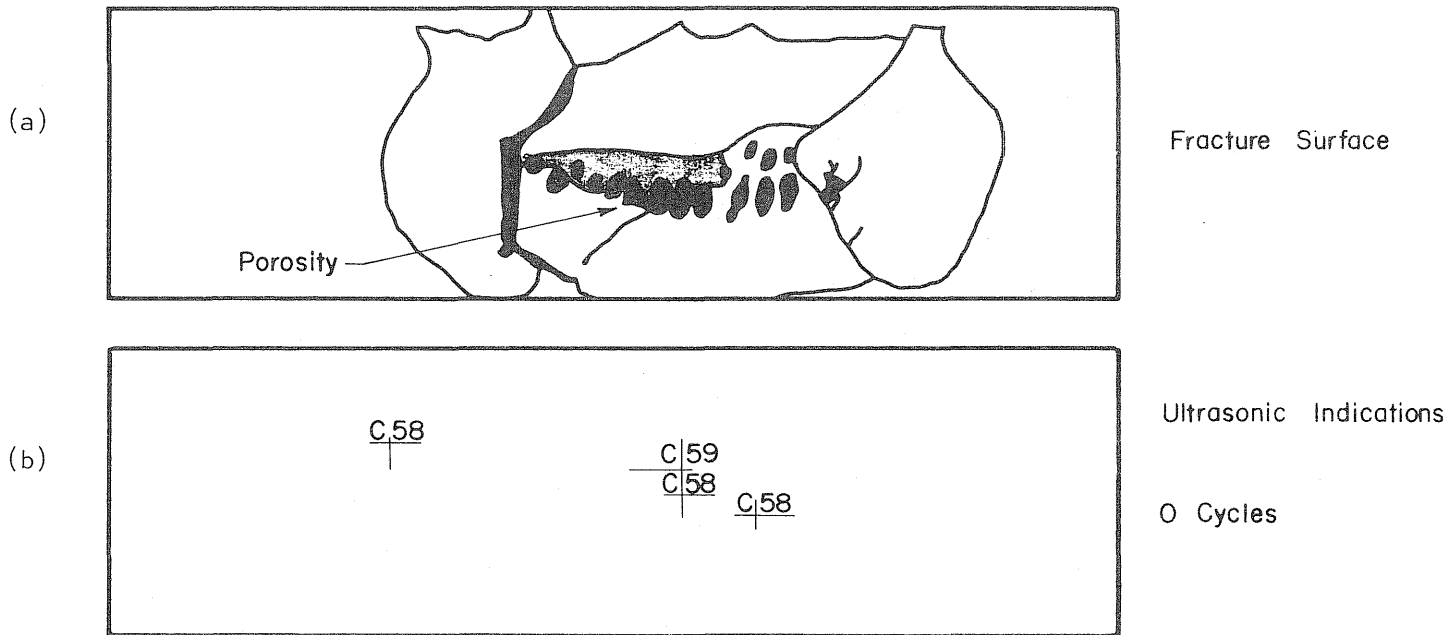
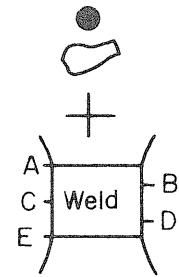


FIG. 3.37 FRACTURE SURFACE, AND ULTRASONIC INDICATIONS RECORDED FOR SPECIMEN ND-15

SPECIMEN ND-15 (Cont.)

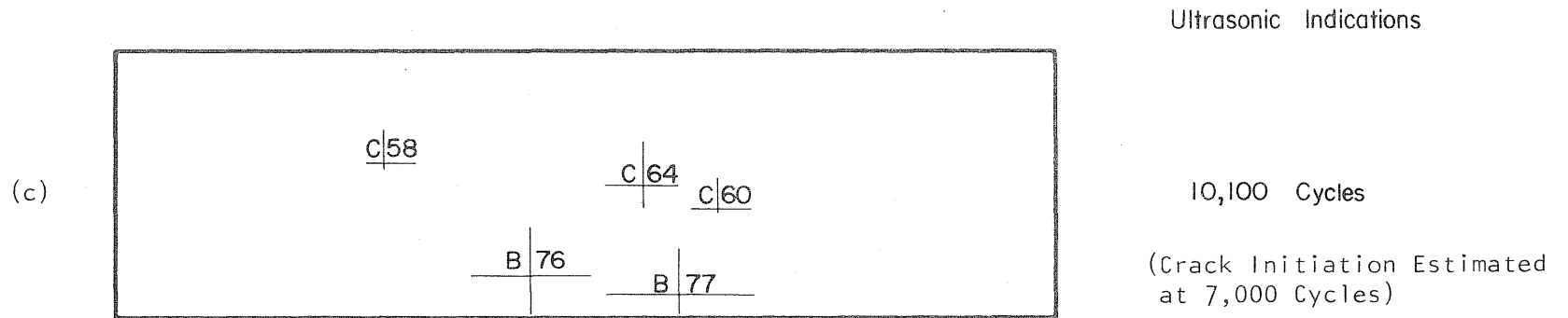
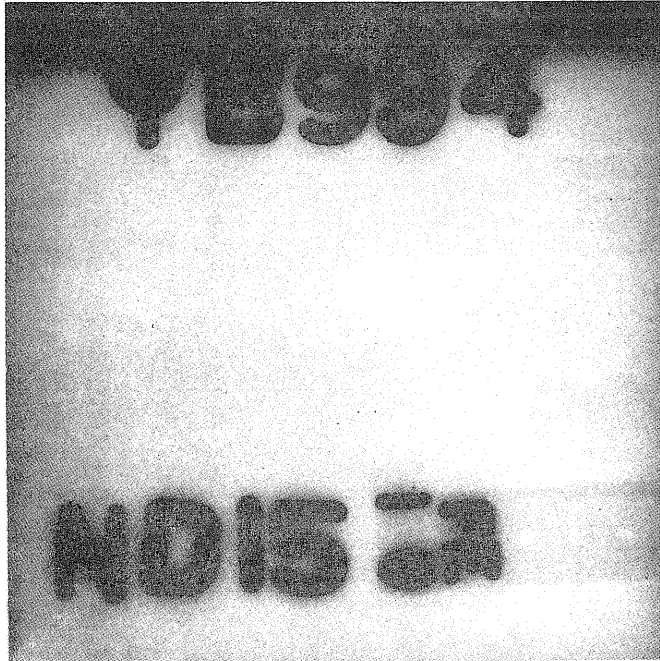
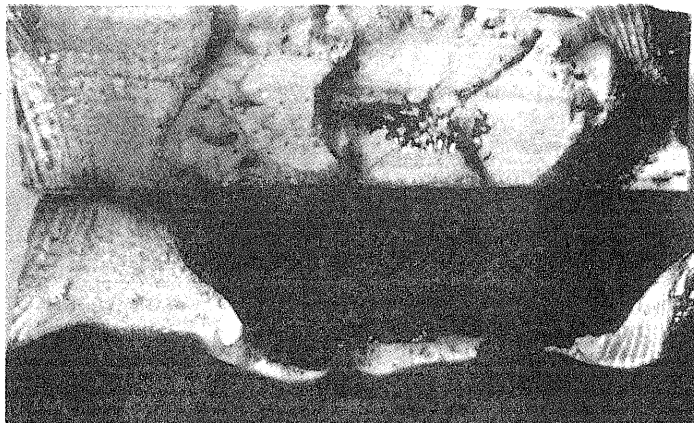


FIG. 3.37 (cont.) FRACTURE SURFACE, AND ULTRASONIC INDICATIONS RECORDED FOR SPECIMEN ND-15

SPECIMEN ND-15 (Cont.)



(d) Radiograph of Specimen Before Test



ND-15	FRACTURE
Stress 0 to +50.0ksi.	
Life	32,400

(e) Fracture Surface After Test

FIG. 3.37 (Cont.) FRACTURE SURFACE, AND ULTRASONIC INDICATIONS RECORDED FOR SPECIMEN ND-15

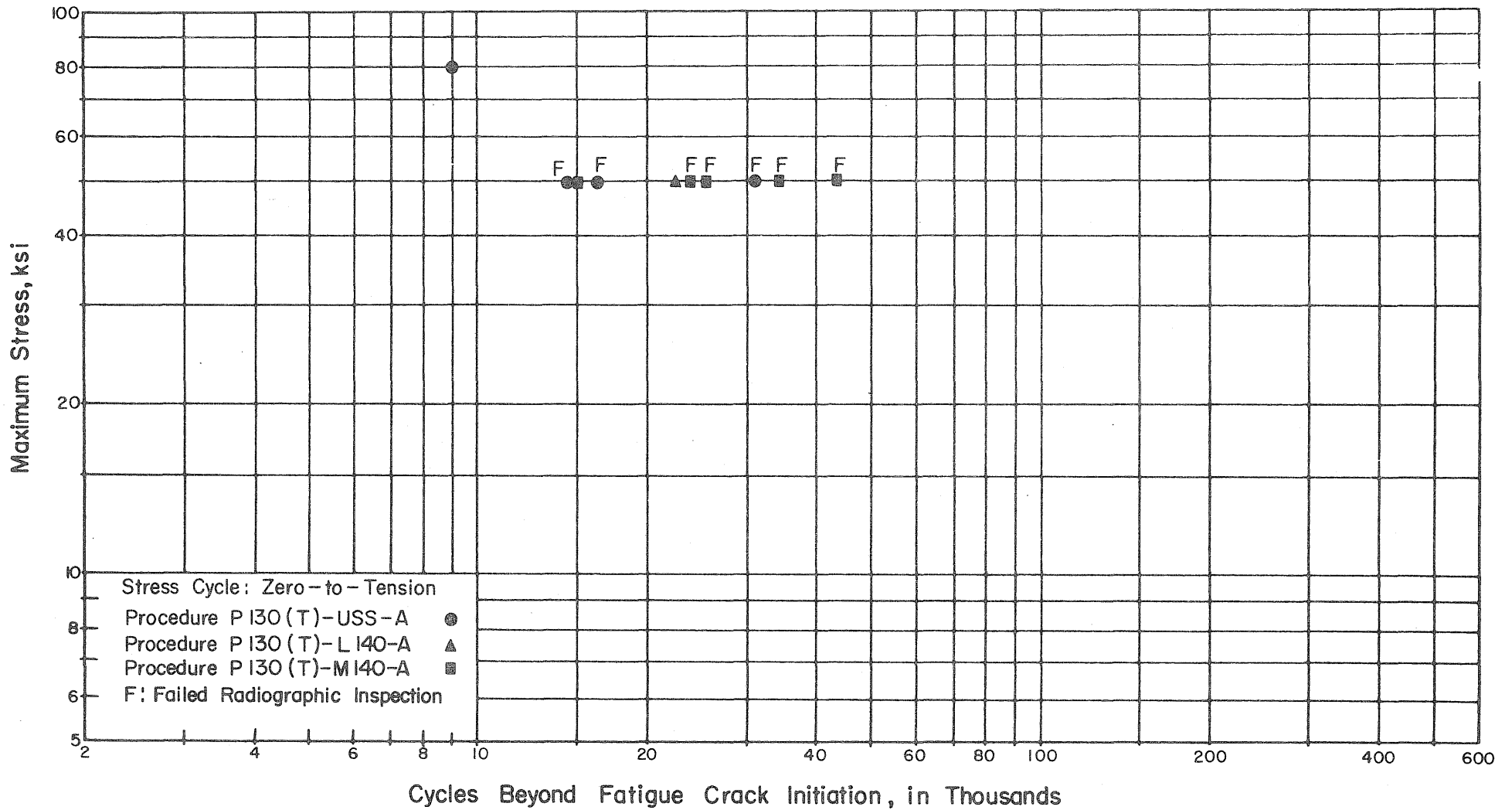


FIG. 3.38 CYCLES TO FAILURE FOLLOWING INTERNAL FATIGUE CRACK INITIATION IN HY-130 (T) TRANSVERSE BUTT WELDS WITH REINFORCEMENT REMOVED

DISTRIBUTION LIST

Administrative Requirements

Naval Ship Engineering Center NAVSEC 6101D Department of the Navy Washington, D. C. (4)	Defense Metals Information Center Battelle Memorial Institute 505 King Avenue Columbus, Ohio 43201
Naval Ship Engineering Center NAVSEC 6120 Department of the Navy Washington, D. C.	Pressure Vessel Research Committee Welding Research Council 345 E. 47th Street New York, New York 10017
Naval Ship Engineering Center NAVSEC 6132 Department of the Navy Washington, D. C.	Weldability Committee Welding Research Council 345 E. 47th Street New York, New York 10017
Naval Ship Systems Command SHIPS 205 Department of the Navy Washington, D. C. (2)	National Academy of Science (Material Advisory Board) 2101 Constitution Avenue Washington, D. C. 20018
Naval Ship Systems Command SHIPS 0342 Department of the Navy Washington, D. C.	Southwest Research Institute 8500 Calebra Road San Antonio, Texas
U. S. Naval Research Laboratory Washington, D. C.	Battelle Memorial Institute 505 King Avenue Columbus, Ohio 43201
U. S. Naval Applied Science Laboratory Brooklyn, New York	Columbia University Attn: A. M. Freudenthal Columbia Heights New York, New York 10027
Naval Research and Development Center Annapolis Division Annapolis, Maryland (2)	Sheffield Division Armco Steel Corporation Attn: V. W. Butler P. O. Box 1367 Houston, Texas
Defense Documentation Center Cameron Station Alexandria, Virginia 22314 (22)	Electric Boat Division General Dynamics Corporation Attn: Mr. E. Franks Via: Naval Ship Systems Command, Connecticut Groton, Connecticut
United States Steel Corporation ATTN: Mr. S. L. Magee 1625 "K" Street, N.W. Washington, D. C. 20005	
Lukens Steel Company Coatesville, Pennsylvania	Newport News Shipbuilding and Drydock Company Attn: Mr. F. Daly Via: Naval Ship Systems Command, NPTNWS Newport News, Virginia
Babcock and Wilcox Company Barberton, Ohio	

Ingalls Shipbuilding Corp.
Attn: F. G. Ranson
Via: Naval Ship Systems
Command Pascagoula
Pascagoula, Mississippi

Republic Steel Corporation
1625 "K" Street, N. W.
Washington, D. C.

DOCUMENT CONTROL DATA - R & D

(Security classification of title, body of abstract and indexing annotation must be entered when the overall report is classified)

1. ORIGINATING ACTIVITY (Corporate author)		2a. REPORT SECURITY CLASSIFICATION	
University of Illinois, Urbana, Illinois Department of Civil Engineering		Unclassified	
		2b. GROUP	
3. REPORT TITLE			
LOW CYCLE FATIGUE OF HY-130(T) BUTT WELDS			
4. DESCRIPTIVE NOTES (Type of report and, inclusive dates)			
Final Report; November 1967 - October 1968			
5. AUTHOR(S) (First name, middle initial, last name)			
James B. Radziminski		Prem N. Panjwani	William H. Munse
Frederick V. Lawrence		R. Johnson	
S. Mukai		Richard Mah	
6. REPORT DATE		7a. TOTAL NO. OF PAGES	7b. NO. OF REFS
December, 1968		108	20
8a. CONTRACT OR GRANT NO.		9a. ORIGINATOR'S REPORT NUMBER(S)	
N00024-68-C-5125		Structural Research Series	
b. PROJECT NO.		No. SRS 342	
SFO20-01-01; Task 729			
c.		9b. OTHER REPORT NO(S) (Any other numbers that may be assigned this report)	
d.			
10. DISTRIBUTION STATEMENT			
Qualified requesters may obtain copies of this report from DDC			
11. SUPPLEMENTARY NOTES		12. SPONSORING MILITARY ACTIVITY	
		Naval Ship Systems Command, U. S. Navy	
13. ABSTRACT			
<p>A preliminary evaluation of the axial fatigue behavior of plates and transverse butt-welded joints in HY-130(T) steel is presented. The weldments were prepared using each of two experimental "second-generation" GMA welding wires and a coated electrode. Fatigue tests were conducted using both sound weldments and weldments containing various internal defects, including porosity, slag, lack of fusion, and lack of penetration. Radiographic and ultrasonic testing techniques were used to study the initiation and propagation of fatigue cracks originating at internal weld flaws.</p> <p>The fatigue studies have indicated that although the highest standards of quality may be used in the fabrication of HY-130(T) welded joints, it has not been possible to guarantee the elimination of all defects which have proven to be critical sites for internal fatigue crack nucleation under axial loading. Internal failures were as likely to occur in specimens rated as sound weldments under radiographic inspection as in weldments having regions containing readily detected flaws.</p> <p>Fatigue cracks originating at internal defects were found to initiate at approximately twenty to eighty percent of the total cyclic lifetime of a butt-welded joint, for tests conducted at a stress cycle of zero-to-tension. Within the normal limits of scatter for fatigue data, however, the number of cycles of crack propagation to failure beyond the point of internal initiation was found to be reasonably consistent at a specific test stress level, for weldments containing various types and percentages of weld defect area.</p>			